COMPARISON OF GROUND MOVEMENTS DURING TRENCHLESS TECHNOLOGY OPERATIONS FOR PIPE AND BOX INSTALLATIONS BY NUMERICAL ANALYSIS

by

TAHA ASHOORI

Presented to the Faculty of the Graduate School of

The University of Texas at Arlington in Partial Fulfillment

of the Requirements

for the Degree of

DOCTOR OF PHILOSOPHY

THE UNIVERSITY OF TEXAS AT ARLINGTON

May 2018

Dedication

To my family, and to my wife

for their endless support and encouragements

ACKNOWLEDGEMENTS

First and foremost, I would like to express my deepest gratitude to my advisor, Dr. Mohammad Najafi for giving me the opportunity to work on this interesting study and for his guidance and support throughout my Doctoral research. This research study would not have been accomplished without his continuous motivation, patience and immense knowledge. It also was my utmost pleasure to be a Graduate Research and Teaching Assistant at the Center for Underground Research and Education (CUIRE) and at the University of Texas at Arlington. I am particularly grateful to Dr. Yu, Dr. Kermanshachi and Dr. Basu for their helpful comments and advices.

I offer my regards to all colleagues, friends and Civil Engineering Department faculty and staff at the University of Texas at Arlington who supported me throughout my Doctoral studies.

Most importantly, I would like to thank my wife, Saiedeh for her invaluable support, love and caring and to my mom, dad and sisters who taught me love, kindness and patience. To them I dedicate this Dissertation.

ABSTRACT

COMPARISON OF GROUND MOVEMENTS DURING TRENCHLESS TECHNOLOGY OPERATIONS FOR PIPE AND BOX INSTALLATIONS BY NUMERICAL ANALYSIS

Taha Ashoori, Ph.D., E.I.T.

The University of Texas at Arlington, 2018

Supervising Professor: Mohammad Najafi

Trenchless Technologies (TTs) are alternatives or methods of choice for the construction and renewal of buried pipes or boxes with little or no surface disruptions. Specifically, TTs are used when other traditional methods, such as cut-and-cover methods are not physically possible. Other reasons for TT methods to be increasingly adopted by pipeline owners, engineers, and contractors are their low environmental impacts and, based on the project and site conditions, lower costs per foot of installed pipe, making these technologies much more efficient and versatile with results within a shorter time span. Trenchless technology methods are divided into two main categories of Trenchless Construction Methods (TCMs) and Trenchless Renewal Methods (TRMs). TCMs are used to install new utilities and pipes underground while TRMs are used to renew, renovate and replace an existing utility or pipe.

Trenchless construction methods are divided into three categories of Pipe/Box Jacking, Horizontal Earth Boring (HEB) and Tunneling. There are conceptual differences between TCM excavation methods and pipe/liner laying for each method, but all methods have similar ground displacement patterns since an overcut excavation (overcut) is created around pipe or box. In many cases, this overcut excavation is the main source of surface

settlements (volume loss), and specifically in shallow conditions, may cause damage to existing road pavement or railroad bed.

The main objective of this research is to compare box and pipe in terms of surface, subsurface and horizontal soil settlements. Trenchless construction methods for this dissertation include pipe and box jacking and large size manual excavation (hand mining or roadheader) tunnels. To provide necessary data, two box jacking projects in sand, one pipe jacking in clay, two centrifuge tests for tunnels in clayey soils and two tunnel constructions by hand mining and open shield tunneling were considered for analyses and model validations.

Secondary objective of this study is to investigate ground displacement induced by pipe and box in sandy and clayey soil conditions with different construction depths and different pipe and box sizes. Finally, numerical comparison of arching effects over the crown and applicability of empirical methods for predicting surface and subsurface ground settlements for different pipes and box sizes are covered in this research.

Numerical methods using Finite Element Analysis (FEA) was used for model simulations to investigate surface and subsurface settlements, effects of box height, box width and overcut for different soil conditions and box/pipe shapes. Pipe and box models in different soil conditions were validated from real-life case histories.

The results of this dissertation show that, on the average, there is 5 to 25% higher surface and subsurface settlements in box over a pipe with the same cross-sectional area of the box, where pipe diameter is considered equal to box width. It was observed that settlement in box installations is dependent on ratio of soil cover to width of the box. Different pipe settlement predictive models, such as Gaussian and Modified Gaussian curves, fitted well with the numerical results obtained for box installations.

TABLE OF CONTENT

LIST OF FIGURES

LIST OF TABLES

Chapter 1 INTRODUCTION AND BACKGROUND

INTRODUCTION

Underground pipelines are necessary facilities for serving urban and rural areas. They have one of the most important functions to sustain world's economy and growth. Pipelines and conduits are mostly used for water and wastewater, storm water, electricity, gas and oil and telecommunication applications. After construction, they need to be constantly maintained, rehabilitated and renewed to provide basic human needs.

In the congested urban areas, trenching techniques can severely disrupt everyday life and damage surface developments. In these situations, trenchless technology might be the only option for construction of new underground pipelines. Advancement in technology and improvement in obtaining geotechnical data and development of new equipment have led to improvement in trenchless construction installations. These new and advanced means of installing underground pipes facilitate construction and renewal with minimum surface disruption and social costs (Najafi and Gokhale, 2004).

Pipe and box jacking (PBJ) is a trenchless technology method for installing a prefabricated pipe or box through the ground from a drive shaft to a receiving shaft. The most basic approach of box jacking, which is widely used, is where a prefabricated box or pipe is placed in the launch shaft, adjacent to where it is to be installed, and is jacked into the ground with excavation taking place within an open face shield or with mechanical means, such as a tunnel boring machine (TBM). The first use of pipe or box jacking was at the end of the 19th century (Najafi, 2013). In the 1950s and 1960s, new capabilities were added to pipe jacking by U.S., European and Japanese companies, including extended drive lengths, upgraded line and grade accuracy, enhanced pipe-joint mechanism, new pipe materials, and improved excavation techniques. These developments as well as the

improved operator skills and experiences have enabled pipe/box jacking to be common trenchless technology methods (Najafi, 2013).

UNDERGROUND PIPELINES INSTALLATION METHODS

Cut-and-cover Method

The conventional method for construction, replacement and repair of underground pipelines has been trenching or cut- and-cover. Based on the type of work, this method is also called dig-and-install, dig-and-repair, or dig-and-replace. This method includes direct installation of pipe systems into open-cut trenches. Cut-and-cover methods involve digging a trench along the length of proposed pipeline, placing the pipe in the trench on suitable bedding materials and then embedding and backfilling. Most of the time the construction effort is concentrated on such activities as detour roads, managing the traffic flow, trench excavation and shoring, dewatering (if needed), backfilling and compaction operation, bypass pumping systems, and reinstatement of the surface. These results in a small part of the construction efforts actually being spent on the final product, which is pipe installation itself (Najafi and Gokhale, 2004).

In some cases, the backfilling and compaction and reinstatement of the ground and pavement alone amount to 70 percent of the total cost of the project (Najafi and Gokhale, 2004). As such, considering all the project parameters, the cut-and-cover method is more time consuming and does not always yield the most cost-effective method of pipe installation and renewal. In recent times, due to understanding of the various social costs involved with cut-and-cover, this method of installation is being discouraged. Social costs include cost to general public, environmental impacts, and damage to pavement, existing utilities, and structures (Najafi and Gokhale, 2004). Figure 1-1 shows a typical pipeline installation using cut-and-cover construction method.

Figure 1-1 Typical Cut-and-cover Pipeline Installation (Najafi et al., 2016)

Trenchless Technology Methods

Trenchless technology (TT) consists of a variety of methods, materials, and equipment for inspection, stabilization, rehabilitation, renewal, and replacement of existing pipelines and installation of new pipelines with minimum surface and subsurface excavation (Najafi et al., 2016). Environmental concerns, social (indirect) costs, new and more stringent safety regulations, difficult underground conditions (containing natural or artificial obstructions, high water table, etc.) and new developments in equipment have increased demand for trenchless technology. These methods include installing or renewing underground utility systems with minimum surface or subsurface disruptions. Figure 1-2 shows main divisions of trenchless technology methods and their categories.

Trenchless technology for new installations has become popular for urban underground utility construction and road crossings. As stated previously, in recent years, there has been remarkable progress in development of new trenchless technology equipment and methods. These developments have produced improvement in jacking

force capacity and increased drive length, improvements in steering and tracking systems, availability of new and different types of pipes and other advancements. However, preparation of design guidelines, construction specifications, process inspection, material testing, and the training of engineers, construction and permit inspectors in contracts and bid documents, has not kept pace with new developments (Najafi et.al, 2005). Some agencies may not be current with capabilities and limitations of the new methods, materials, and equipment.

In summary, there are several advantages for trenchless construction methods (TCMs) over conventional cut-and-cover methods (Najafi and Gokhale, 2004):

1. Less effort in earthwork as TTs do not require soil backfilling and compaction,
2. They can be implemented in congested areas with minimum disturbance to traffic,
3. They rarely require relocating existing underground utilities,
4. They minimize the need for spoil removal and minimize damage to pavement and other utilities.

As shown in Figure 1-2, TT methods are divided into two main areas as Trenchless Construction Methods (TCM) and Trenchless Renewal Methods (TRM). TCM include all the methods for new utility and pipeline installation, where a new pipeline or utility is installed. TRM include all the methods of renewing, rehabilitating and renovating, an existing, old or host pipeline or utility system (Mamaqani, 2014).

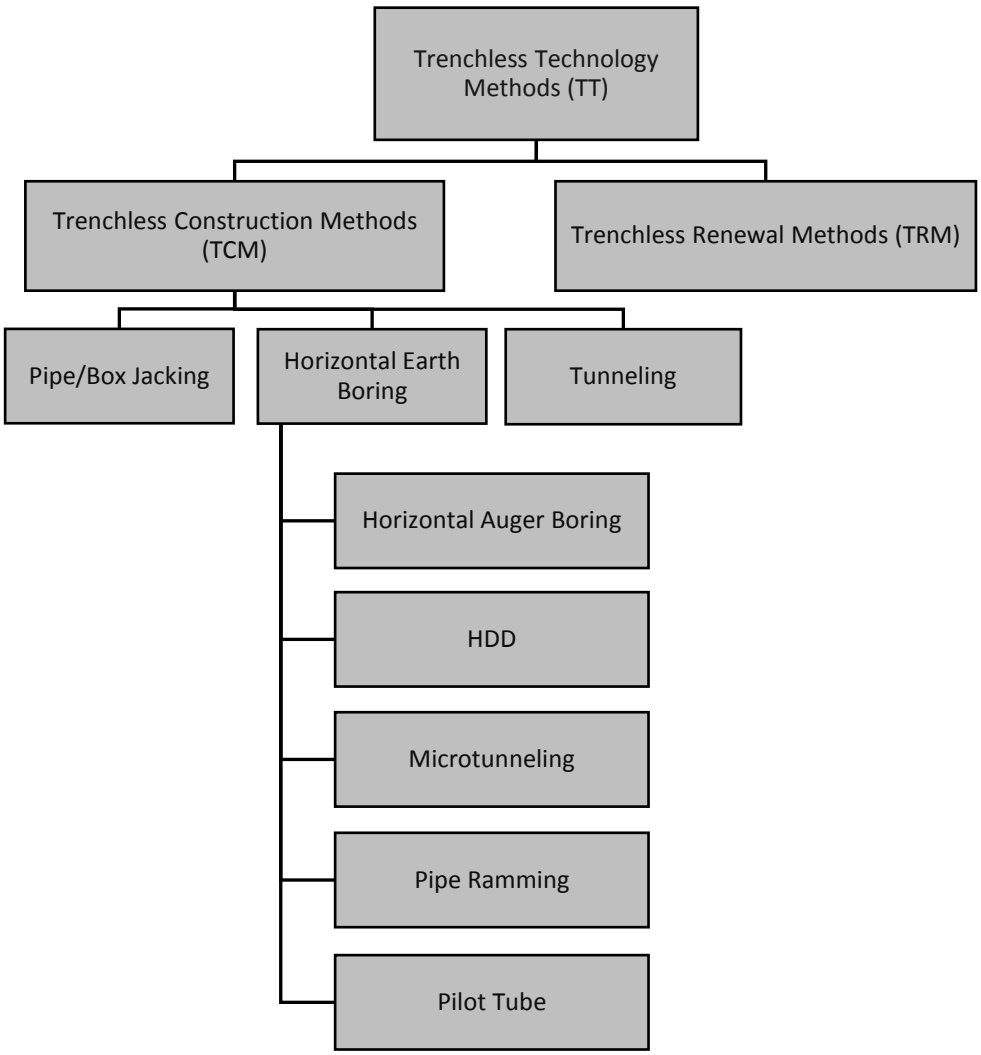

Figure 1-2 Trenchless Technology Methods (Adapted from Najafi & Gokhale, 2004)

TRENCHLESS CONSTRUCTION METHODS (TCM)

Pipe Jacking

Pipe jacking (PJ) is a worker-entry technique, whereas microtunneling (MT) does not require workers to be inside the pipe. Pipe jacking is used for different underground

applications for more than 100 years. However, MT was developed first in 1975 in UK and its first use in the United States was in 1984 (Iseley and Gokhale, 1997).

Except on limitations for jacking forces and logistical factors, there are no theoretical limits to the length of individual pipe jacking projects although practical engineering considerations, such as economics and above-surface conditions (whether in urban or rural area) may impose restrictions (Pipe Jacking Association, 2017). In certain conditions, drives of several hundred meters (feet) either in a straight line or to a radius or a series of radii are achievable with a range of mechanical and remote-controlled excavation systems. Pipes in the range 1,100 mm (42.0 in.) to 3,660 mm (144 in.), can be installed by employing the appropriate system (Najafi, 2010). If properly executed, pipe jacking provides ground support and reduces potential ground settlement. Najafi (2013) summarizes the applicability of pipe jacking methods for different soil conditions as shown in Table 1-1.

To install a pipeline using pipe/box jacking technique, thrust (entry) and reception shafts or pits are constructed, usually at manhole or access point locations. Shaft sizes will vary according to the excavation methods employed, job site location and social impact factors.

A thrust wall is constructed to provide a reaction against jacking thrust. Thrust wall is usually constructed with reinforced concrete. In poor ground, piling or other special arrangements may have to be employed to increase the reaction capability of the thrust wall. Where there is insufficient depth to construct a normal thrust wall, for example jacking through embankments, the jacking reaction has to be resisted by means of a structural framework having adequate restraint provided by means of piles, ground anchors or other methods for transferring horizontal loads (Pipe Jacking Association, 2017). Figure 1-3 illustrates the typical components of pipe jacking operation.

Technical Benefits

Benefits associated with pipe jacking include (Pipe Jacking Association, 2017):

1. Inherent strength of pipe
2. Smooth internal finish giving good flow characteristics compared to rectangular (box) sections
3. No requirement for secondary lining
4. Considerably less joints than a segmental tunnel
5. Prevention of watertable ingress by use of pipes with sealed flexible joints
6. Provision of invert channels in larger pipes to contain
7. Less risk of settlement
8. Minimal surface disruption
9. Minimal reinstatement
10. Reduced requirement for utilities diversions in urban areas

Table 1-1 Applicability of Pipe Jacking Methods for Different Soil Types (Najafi, 2013)

Type of Soil	Applicability
Soft to very soft clays, silt, and organic deposits	Marginal
Medium to very stiff clays and silts	Yes
Hard clays and highly weathered shales	Yes
Very loose to loose sands (above the watertable)	Marginal
Medium to dense sands below the watertable	No
Medium to dense sands above the watertable	Yes
Gravels with less than 50 mm (2 in.) to 100 mm (4 in.) diameter	Yes
Soils with significant cobbles, boulders, and obstructions larger than 100 mm (4 in.) to 150 mm (6 in.) diameter	Marginal
Weathered rocks, marls, chalks, and firmly cemented soils	Marginal
Significantly weathered to unweathered rocks	No

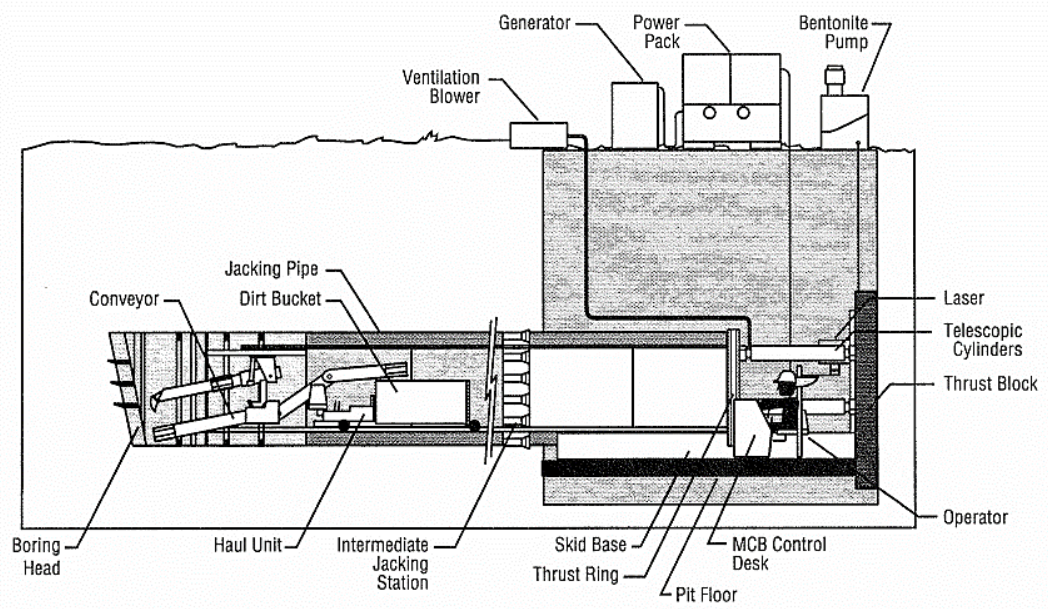

Figure 1-3 Typical Components of Pipe Jacking Operation (Iseley & Gokhale, 1997)

Box Jacking

Box jacking is another form of pipe jacking with origins in the pipe jacking technology of the late 1960s in the U.K. This method has been used to form a variety of passageways under busy railway tracks and to a lesser extent under highways. Initially, a series of small pre-cast box segments were jacked to form pedestrian subways and foundations for under-bridges (Clarkson and Ropkins, 1977).

New development simplifies the jacking process, improves control of box alignment during tunneling and provides low maintenance structure. Large size rectangular tunnels are another form of methods usually used for underground roads with four or six lanes. As a tunneling operation, the method in many instances is much less disruptive to the operation of a railway or highway than traditional cut-and-cover construction methods. A box is structurally efficient, simple to construct. Figure 1-4 shows a typical box cross section (Ropkins, 1998).

Although simple in principle, the basic concept described above could potentially result in unacceptable levels of ground disturbances. As the box moves through the ground, it tends to drag the ground along with it. Drag at the top of the box can cause considerable disturbances to the overlying ground. If the box is wide relative to the depth of cover then potentially most of the ground above the box could be carried forward with it. Drag at the bottom of the box can result in compaction and forward transport of the ground immediately below, with the result that the box dives during installation. Other potential sources of ground disturbance are loss of ground at the tunnel face, overcut of the tunnel perimeter and poor control of box alignment during installation. Measures must be taken in the design of a jacked box tunnel project to effectively control these potential causes of ground disturbance, to limit ground settlements to within acceptable levels (Ropkins, 1998).

Box and pipe jacking have the same operation except difference in pipe geometry and excavation. Hand mining or boring machines perform the soil boring in pipe jacking but box jacking is mostly performed by hand mining or roadheader. However, technology advancement has provided new equipment for rectangular shaped tunnel excavation for large-size rectangular tunnel construction. For example, Rectangular Tunnel Boring Machine (RTBM) is used to construct underground pedestrian and vehicles crossings as shown in Figure 1-5. It features a rectangular shield box jacking technique, which makes use of the principles of an Earth Pressure Balance Machine (EPBM) during excavation. The thrust cylinders in the box jack remains in the shaft to push forward the entire box segments (Figure 1-6). New segments are placed within the shaft as the machine advances. As the RTBM advances and cuts through the soil, it turns the excavated material into a soil paste that is used as pliable, plastic support medium, to balance the pressure conditions at the tunnel face. Figure 1-7 illustrates a large-size rectangular tunnel in China using box jacking machine.

Drive Length

The length of the box jacking drive shaft is determined by the amount of available jacking thrust and the compressive strength of the pipe and workmanship quality (Najafi, 2013). The jacking thrust is managed by appropriate size of overcut, applying sufficient lubrication and/or grouting between the outside surface of the box and excavated ground. Intermediate jacking stations can be used to distribute jacking thrust along the boxes and add maneuverability of system by horizontal and vertical curves along the jacking operation. Pipe jacking operations have relatively longer drive lengths when compared with box jacking operations due to the shape of the pipe segments (Chaurasia, 2012).

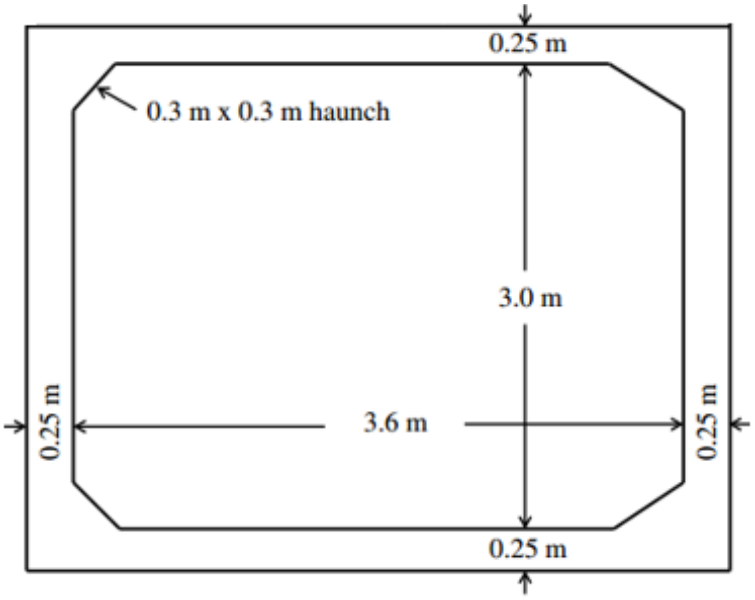

Figure 1-4 A Typical Box Cross Section (Adapted from Acharya et al., 2014)

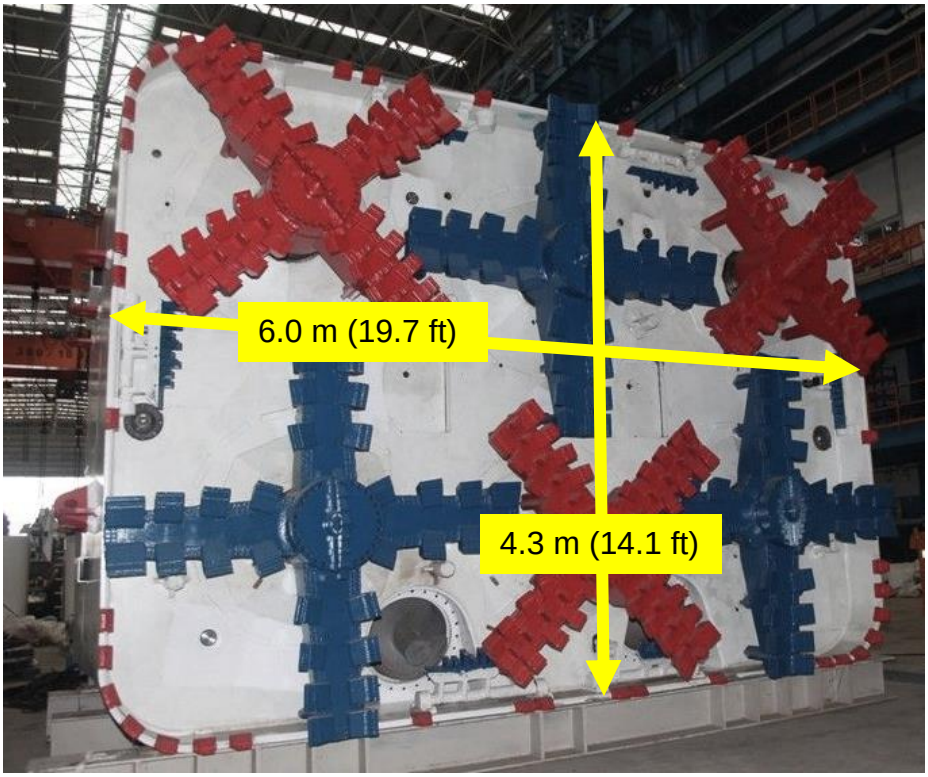

Figure 1-5 Rectangle Pipe Jacking EPBM (www.drillcuttingbit.com)

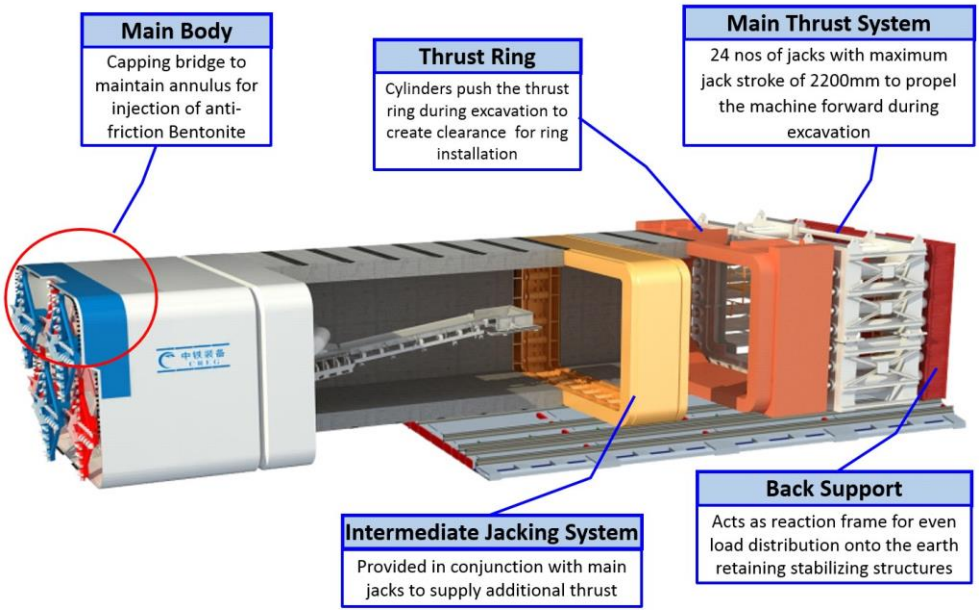

Figure 1-6 Side View of Rectangular Pipe Jacking Machine (www.drillcuttingbit.com)

However, boxes do possess some advantages. For example, they can cope with large flow situation where headroom (soil cover) is limited because the height of box can be reduced while the size of pipe with the same hydraulic capacity is fixed. Secondly, for some difficult site conditions, e.g., excavation of structure in rock, for the same equivalent cross-sectional area, the width of box can be designed to be smaller than that of pipe and this enhances smaller amount of excavation and backfilling (Chu, 2010). Mamaqani, 2014 has provided a side-by-side comparison between pipe and box jacking methods. A summary of this comparison is presented in Table 1-2.

Figure 1-7 Box Installation in a Tunnel Project in China (Curtesy of Dr. Najafi, 2017)

Table 1-2 Comparison of Pipe Jacking and Box Jacking (Mamaqani, 2014)

Criteria	Pipe Jacking (PJ)	Box Jacking (BJ)
Shape	Circular	Rectangular
Jacking Frame Shape	Circular	Rectangular
Weight	Relatively Low	Relatively High
Dimensions	1.2 m (48 in.) to 1.8 m (72 in.)	1.2 m (4 ft) x 1.2 m to 24 m (80 ft) x 12.2 m (40 ft)
Jacking Load	Relatively Low	Relatively High
Favorable Soil	Cohesive	Cohesive
Ground Settlement	Relatively Low	Relatively High
Excavation Method	TBM, EBPM, Hand Mining	Hand Mining, Roadheader

Horizontal Earth Boring (HEB)

In the horizontal earth-boring methods (HEBs), workers may work in the shaft or pit, but usually do not enter the borehole or enter the installed pipe. Therefore, these methods can be used for small diameter pipe installations (less than 1,000 mm (42 in.)). The horizontal earth boring method is further divided into a number of methods including Horizontal Auger Boring (HAB), Horizontal Directional Drilling (HDD), Microtunneling, Pilot-Tube (also called Pilot Tube Microtunneling) and Pipe Ramming (Najafi, 2010). Since microtunneling is more related to the scope of this research, it will be described in the next section.

Microtunneling Methods (MTM)

Microtunneling can be described as a remotely-controlled, guided, pipe-jacking process that provides continuous support to the excavation face. The microtunneling process does not require worker entry into the tunnel. The cutterhead and pipes are jacked

into the ground from a shaft by placing sections of pipe onto the jacking frame behind the shield in the shaft. Jacks push the pipe into the bore behind the shield and cutterhead. After each pipe is pushed into the ground, the jacks are retracted to provide space for another pipe to be placed ahead of hydraulic jack and then connections are made, and the process is repeated until the reception shaft is reached. The guidance system usually consists of a laser mounted in the jacking pit as a reference with a target mounted inside the microtunneling machine's articulated steering head. The ability to control the stability of the excavation face by applying mechanical or fluid pressure to the face to balance ground water and earth pressures is a key element of microtunneling (Bennett, 1998).

The total jacking force required to propel the tunneling machine and pipe sections forward must overcome forces associated with face pressure on the machine and friction on the machine and pipeline. As stated above, the face pressure force acts at the front of the machine and originates from ground water and earth pressures. The frictional force develops between the surrounding soil and the exposed outer surface area of the microtunneling machine and installed pipe sections. The face pressure component relates to the depth of burial and is estimated based on the soil and watertable conditions at the site. The face pressure component of the jacking force remains theoretically constant if the depth of soil over the pipeline is constant. However, the frictional force increases as the drive length increases. As a result, longer drives require greater jacking forces.

Microtunneling is a method of pipe jacking and is not limited by size. Typical microtunneling diameters range from 0.6 m (24 in.) to 3.7 m (144 in.) (Staheli, 2006). To reduce frictional resistance, the microtunnel machine excavates a slightly larger diameter hole than the diameter of the installed pipe sections. The distance between the maximum excavated diameter and the outer diameter of the installed pipe sections is referred to as the overcut or annular space. Overcuts of between 19 mm (0.75 in.) and 50 mm (2.0 in.)

on the diameter (i.e., 9.5 mm (0.375 in.) and 35.4 mm (1.0 in.) on the radius) are typical. In addition to reducing frictional forces, overcut is necessary to facilitate steering of the microtunneling machine, and to allow injection of lubrication into the annular space (Staheli, 2006).

Tunneling Method

Tunnel Boring Machines (TBM) have similar excavation method to micro TBMs but instead of pipe, usually segmental linings are joined together by bolts to form a circular supporting structure as shown in Figure 1-8. In comparison, the microtunnel boring machine (MTBM) is operated from a control panel, normally located on the surface and personnel entry is not required for routine operation but TBMs are usually of worker-entry diameter and guided from the inside of the TBM.

Figure 1-8 Closed View of Segmental Linings (www.p3planningengineer.com)

There are two major TBM classifications: (1) earth pressure balanced (EPB) and (2) slurry type shield machine. Selection of shield method depends on ground conditions, surface conditions and congestions, dimensions of the tunnel section, boring distance, tunnel alignment and construction period. Both methods are closed-face type shield machines, meaning the "head" part of machine is "closed" and separated from the rear part of machine. In the slurry machine, the "head" has a working chamber filled with soil or slurry between the cutting face and bulkhead to stabilize the cutting face under soil pressure.

An open face shield is a type of tunnel boring machine (TBM) that has no face support. It is used in trenchless tunnel excavation with either manual or machine digging. Its use is limited and is dependent on the ground being tunneled and the objectives of the project. A TBM with an open face shield has lateral support only and does not provide full protection for internal machinery (www.trenchlesspedia.com). Figure 1-9 illustrates open face TBM used for the São Paulo Metro Line 1.

Figure 1-9 Single-track Open Face TBM (www.tunnel-online.info)

The EPB type shield machine turns the excavated soil into mud pressure and holds it under soil pressure to stabilize the cutting face. It has excavation system to cut the soil, mixing system to mix the excavated soil into mud pressure, soil discharge system to discharge the soil and control system to keep the soil pressure uniform. Therefore, EPB may not be applicable for the rocky soil that is difficult to turn the excavated soil into mud. It can be used at ground predominated by clayey soil. The slurry type shield machine, on the other hand, uses the external pressurized slurry to stabilize the cutting face, similar to bored piles or diaphragm walls using bentonite to contain the trench wall. The slurry is circulated to transport the excavated soil by fluid conveyance. Besides having excavation system, the slurry type shield machine has slurry feed and discharge equipment to circulate and pressurize slurry and slurry processing equipment on the ground to adjust the slurry properties. Figure 1-10 presents an EPB machine.

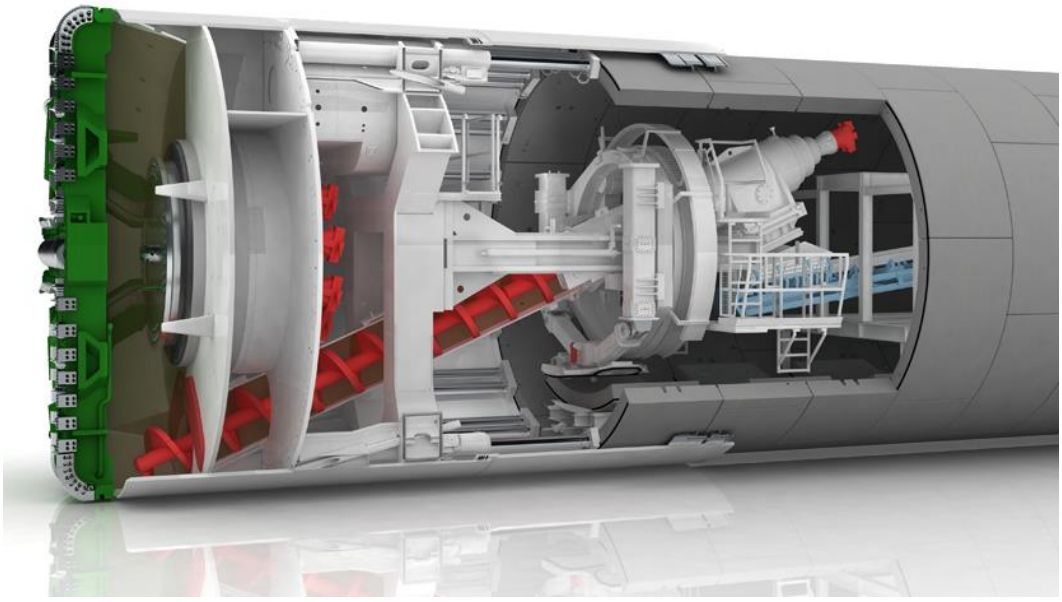

Figure 1-10 EPB Tunnel Boring Machine (www.herrenknecht.com)

RESEARCH NEEDS

Methods to install pipes and boxes are almost the same but the difference between these two methods are the time that needs to be taken to excavate and install pipe or box. Since rectangular shapes have higher spans, they release more stresses in the soil and might cause more settlement trough in box than pipes. However, the geometry of pipe and box, depth of cover and geotechnical properties of the soil are also other important factors influencing the settlement trough especially in shallower depths. It is shown that at the same cross-sectional area at shallow depth conditions, boxes are preferred over round shape pipes as they allow for more depth of cover (Mamaqani, 2014).

These differences together with cost of construction also make a difficult decision for the designers to appropriately choose between pipe and box. As a result, the need to better understand settlement trough induced by pipe and box installation is very important to complete projects with no structural damages to the adjacent infrastructures and facilities.

Several studies were conducted to investigate ground settlement induced by pipe installation by using empirical and experimental methods such as Bennett (1998), Atkinson & Potts (1979), Mair (1979), and by using analytical and numerical methods such as Verrujit and Booker (1996), Loganathan and Poulos (1998), Lim (2003) and Möller (2006) and Liu and Lu (2012). However, there is a gap in knowledge for a comprehensive study of settlement trough (surface settlement) for boxes and differences between box and pipe installation with regards to vertical and horizontal ground settlements.

There are few studies on settlement induced by box installations such as Mamaqani (2014) who studied the settlement trough in sandy soil conditions. That research study was based on 2-D Finite Element Analysis of ground settlements associated with box jacking (BJ) and validated the results by observed field data with the intention of

training an Artificial Neural Network (ANN) model for surface settlement prediction. However, subsurface settlement and horizontal displacement were not covered in that study. Mamaqani (2014) based his results on sandy condition and no comparison of surface settlement in pipe and box was conducted.

Empirical methods such as Gaussian normal distribution curves used to predict deep and surface ground settlements have been just modified for round shape pipes and have not been tested for boxes (Mamaqani, 2014). In addition, no previous studies are found on box induced surface and subsurface settlement in fine soil conditions. Therefore, there is a need to study the differences between pipe and box in various sizes and depths and compare the surface settlement results with existing analytical and empirical models.

OBJECTIVES

The main objective of this research is to compare box and pipe in terms of surface, subsurface and horizontal soil settlement. Trenchless construction methods for this research study include pipe jacking, box jacking and large size manual excavation (hand mining or roadheader) tunnels. Two box jacking projects in sand, one pipe jacking in clay, two centrifuge tests for tunnels in clayey soils and two tunnel constructions by hand mining and open shield tunneling were considered for model validations.

Secondary objective of this study is to investigate ground displacement induced by pipe and box in sandy and clayey soil conditions, different construction depths and different pipe and box sizes. Finally, numerical comparison of arching effects over the crown and applicability of empirical methods for predicting surface and subsurface ground settlement for different pipe and box sizes are included in this research study.

CONTRIBUTIONS TO THE BODY OF KNOWLEDGE

The followings are the main contributions of this research:

1. First study to compare surface and subsurface ground settlement, volume loss, and horizontal soil displacements in pipe and box in sand and clay.
2. There are no previous studies on the effects of large size box installation, so this study will consider settlement induced by large size rectangular tunnel construction.
3. The results of this study show surface settlement induced by box installation predicted by the existing empirical methods such as Gaussian curves or Modified Gaussian curves.

SCOPE AND LIMITATIONS

This research is focused on settlement induced by overcut excavation, depth of installation, shape of structure and soil conditions for pipe and box jacking. It excludes settlement induced by face (advanced) excavation due to lack of collected data for advanced settlement from case studies or using open face excavation. To consider a complete soil settlement, it is required to generate a 3-D model. However, there are some methods to transform the effects of the 3-D soil settlement into the 2-D settlements such as Gap Method, which are explained in Chapter 3. Nevertheless, it was assumed that face settlement can be controlled using available techniques such as freezing, grouting, and chemical stabilization for non-cohesive soils (Mamaqani, 2014), and can be assumed to be negligible because the excavation is in stable clayey conditions (Marshall, 1998). This research study is focused on Load Reduction Method ($\beta - method$) as will be explained in Chapters 3 and 4. In addition to ground loss at the face, below parameters were excluded from this study:

1. Effect of pressurized lubrication and grouting for ground settlement,

2. Structural differences between pipe (box) and segmental linings. Box span depth is designed to limit deflection as per AASHTO LRFD Bridge Design Specifications,
3. Watertable,
4. Permanent loads (i.e., dead loads such as buildings) above surface,
5. Live loads (i.e., traffic loads) above surface,
6. Long term ground settlement, and
7. Jacking loads (only open face excavation is considered for this research study).

HYPOTHESIS

It is assumed that axis depth to diameter ratio (H/D) for pipe installation and axis depth to box width ratio (H/W) for box installation have major impacts on surface ground settlement. It is also expected that the settlement trough for box is greater than pipe with the same cross-sectional area.

The empirical settlement prediction methods such as Gaussian Distribution Curves have been mostly developed for pipes. Therefore, these predictive models are not fitted well for boxes (Mamaqani, 2014).

Volume of settlement trough is typically equal or less than the volume of the over excavation (overcut). It is assumed that volume of settlement trough increases with increase in overcut and decreases with increase in depth to axis. It is also assumed that soil stress redistribution due to the particles dilation will reduce soil settlement to reach perfectly to the surface in sand. Vertical surface settlement occurs due to stress redistribution (Mamaqani, 2014), and reduces by time (Marshall, 1998).

METHODOLOGY

This dissertation reviews pipe and box jacking methods, microtunneling method and tunneling and the conventional soil-structure interactions on pipes and boxes including arching effects. A full review of soil displacement induced by pipe installations are reviewed based on the empirical, analytical and numerical methods.

There are differences between pipe jacking, microtunneling and tunneling but they have similar ground displacement pattern because of ground loss (see Chapters 1 and 3). The ground settlement can be predicted by empirical, simulation by numerical methods and calculated by analytical methods. Case histories collected for this research study covers medium size pipe/box jacking, which in clay by hand excavation (Marshall, 1998), box jacking in sand by hand excavation (Mamaqani, 2014), and large size tunneling method by hand excavation and open face shield tunneling method in stiff clay (Su, 2015). Centrifuge tests by Ong (2007), and Loganathan et al., (2000) also simulate tunnel construction in stiff clay conditions. For convenience, all circular structures are called pipe and all rectangular structures are called box.

A sensitivity analysis is performed to validate simulated model from Abaqus/CAE and then results are compared with data obtained from Mamaqani (2014), for boxes. For comparison of pipes, field data are collected from Marshall (1998), Loganathan and Poulos (1998) and Su (2015).

New models of pipe and box are generated at different depth of installations and soil conditions. Surface and subsurface settlements are compared to existing results obtained from FEA, empirical methods and analytical methods. Figure 1-11 presents the research methodology.

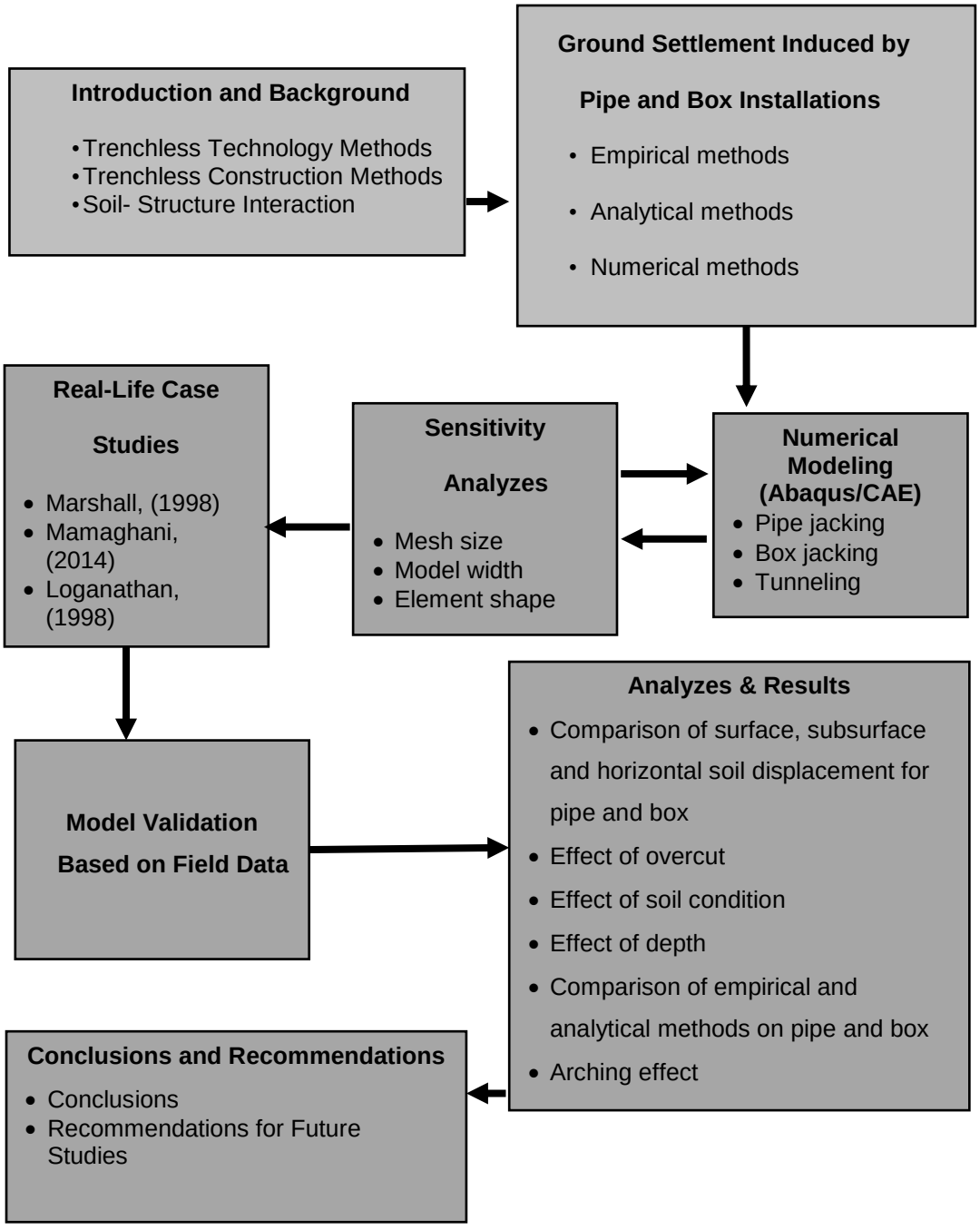

Figure 1-11 Research Methodology

STRUCTURE OF THIS DISSERTATION

Chapter 1 presents the background study on different trenchless construction methods with an emphasis on pipe and box installations. This chapter also provides research needs, objectives, scope, methodology, and contributions to the technical knowledge.

Fundamentals of soil-structure interactions is discussed in Chapter 2. This chapter presents a general overview on stress distribution over a buried structure.

Chapter 3 provides a comprehensive review on analytical, experimental and two-dimensional numerical methods of ground settlement predictions in tunnel.

Chapter 4 presents methodology and includes case studies considered in this research. The results for model validations for each case study is provided in this chapter.

Chapter 5 covers the scenarios for each case study and results and comparison of results in terms of surface vertical settlement.

Finally, in Chapter 6, summary and conclusions are presented followed by explanation for the limitations of the current study and recommendations for future research.

CHAPTER SUMMARY

This chapter presented an overview of trenchless construction methods with an emphasis on pipe jacking, box jacking, microtunneling and tunneling with their range of applications and capabilities. Research needs, objectives, scope and limitations and methodology were also presented in this chapter.

Chapter 2 FUNDAMENTALS OF SOIL-STRUCTURE INTERACTIONS

RIGID PIPES AND FLEXIBLE PIPES

Chapter 1 presented an overview of trenchless construction methods. In this chapter, soil-pipe/box interactions are discussed. Rigid pipes sustain applied loads by means of resistance against longitudinal and circumferential (ring) bending. Under maximum loading conditions, rigid pipes do not deform sufficiently enough to produce horizontal passive resistance from the soil surrounding the pipe. Typical examples of rigid pipes are clay pipes and concrete pipes. On the other hand, flexible pipes are capable of deforming (without damage to the pipe) to the extent that the passive resistance of soils on the sides is mobilized providing additional support. ASTM standards define flexible pipes as pipes that deflect more than 2 percent of their diameter without any sign of structural failure (Najafi, 2010). Typical examples include ductile iron, high-density polyethylene pipe (HDPE), steel pipes, and polyvinyl chloride (PVC) pipes. Table 2-1 presents examples of different types of rigid and flexible pipes.

Table 2-1 Examples of Rigid and Flexible Pipes (Najafi, 2010)

Rigid	**Flexible**
Concrete pipe	Steel pipe
Vitrified clay pipe	Ductile iron pipe
Prestressed concrete cylinder pipe	Polyvinyl chloride pipe
Reinforced concrete pipe	Polyethylene pipe
Bar-wrapped concrete cylinder pipe	Fiberglass reinforced plastic pipe
Asbestos-cement pipe	Acrylonitrile-butadiene styrene pipe
Fiber-cement pipe	Steel pipe

Rigid and flexible pipes differ in the way they transfer the applied loads to the surrounding soil structure. Figure 2-1 gives a simplified illustration of the load transfer mechanism for both types of pipes due to the vertical soil pressures (Najafi, 2010). This dissertation is focused on rigid reinforced concrete pipes and boxes.

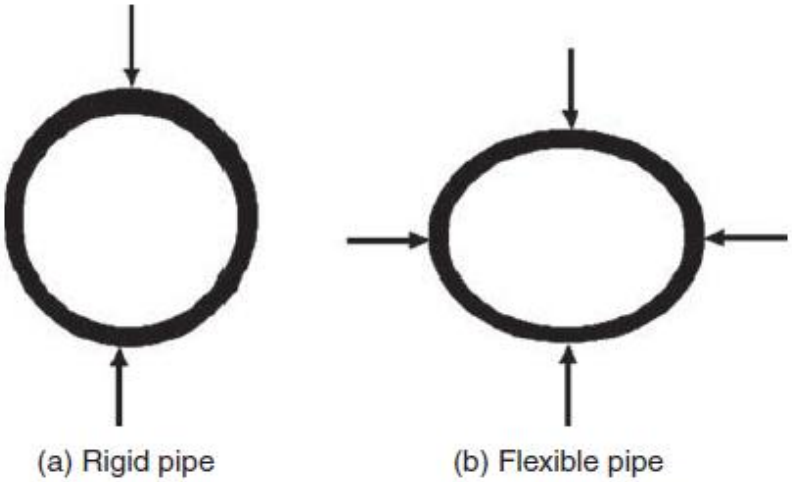

Figure 2-1 Load Transfer Mechanisms for Rigid and Flexible Pipes (Najafi, 2010)

As said earlier, whether a pipe is rigid or flexible has considerable effect on the way in which it interacts with the surrounding soil. The interaction between structure and soil influences the magnitude of loads applied on the pipe and the manner in which the pipe transfers these loads to the surrounding soils. Calculation of loads exerted on underground pipelines can be traced back to the studies carried out by Anson Marston during the early part of the twentieth century (Moser and Folkman, 2008). A model later was developed by Spangler and Watkins and is still in use (Moser and Folkman, 2008). Figure 2-2 provides an illustration of the soil load distribution on rigid and flexible pipes. In the case of rigid pipes, the theory proposes that the soil in the side prism tends to settle relative to the central prism. This causes the pipe to assume full load of the central prism

and a portion of the load from the side prisms. In contrast, a flexible pipe tends to deflect, which result in a lowering of the pressure from the central prism.

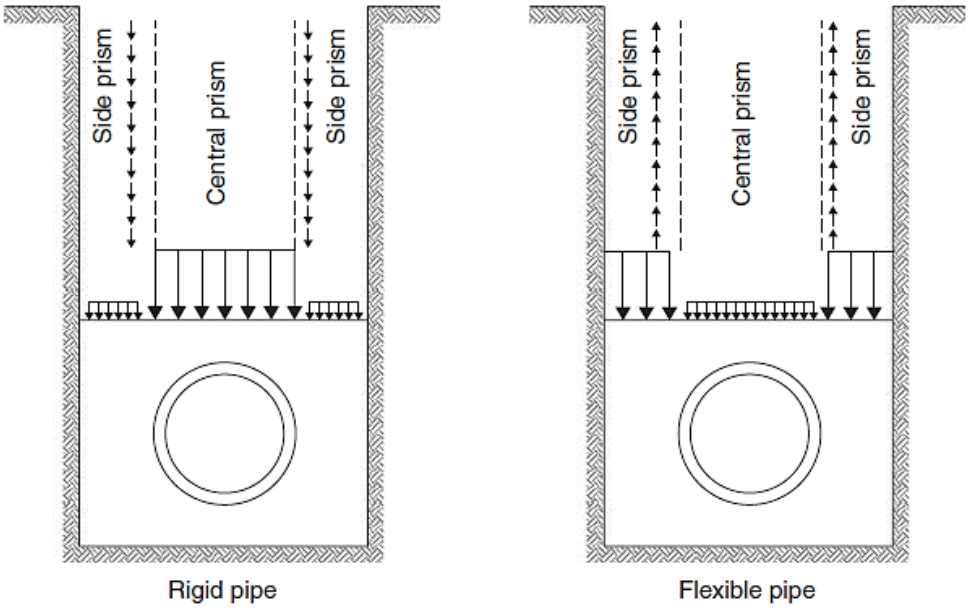

Figure 2-2 Load Comparisons for Rigid and Flexible Pipes (Najafi and Gokhale, 2004)

ARCHING EFFECT

Shear stress occurs while part of a soil mass yields adjacent to the part that remains stationary. This shear stress opposes the relative settlement of soil masses. Since the shearing resistance tends to keep the yielding mass in its original position, the pressure on the yielding part is decreased and stress on the adjoining stationary part is increased. Arching effect can be described as a transfer of forces between a yielding zone and adjoining stationary members. The shear resistance tends to keep the yielding mass in its original position resulting in a change in the pressure on both of the yielding part's support and the adjoining part of soil. If the yielding part moves downward, the shear resistance will act upward and reduce the stress at the base of the yielding mass. On the contrary, if the yielding part moves upward, the shear resistance will act downward to impede its

settlement and causes an increase in stress at the support of the yielding part (Moradi and Abbasnejad, 2013).

Depending upon relative stiffness in the groundmass, arching can be either active or passive. Active arching occurs when the structure is more compressible than the surrounding soil, and the stresses on the structure are less than those on the adjacent ground. Figure 2-3 shows active arching decreases stress on top of a buried structure compared to adjacent soil.

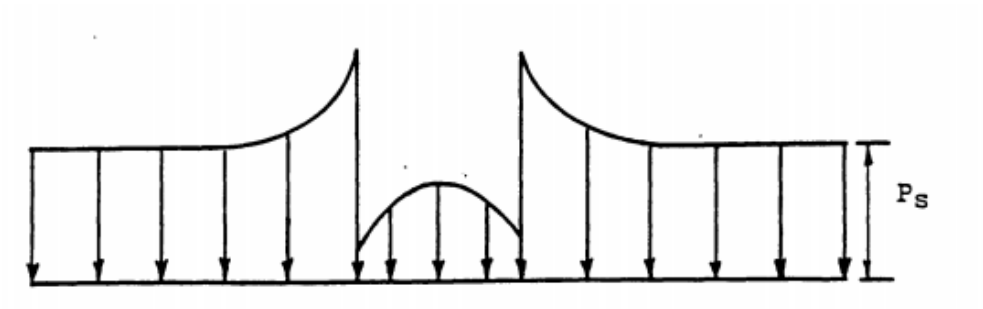

Figure 2-3 Stress Distribution on Top of Structure in Active Arching (Evans, 1983)

In passive arching, the soil is more compressible than the structure. Figure 2-4 shows passive arching increases stress on top of a buried structure compared to adjacent soil.

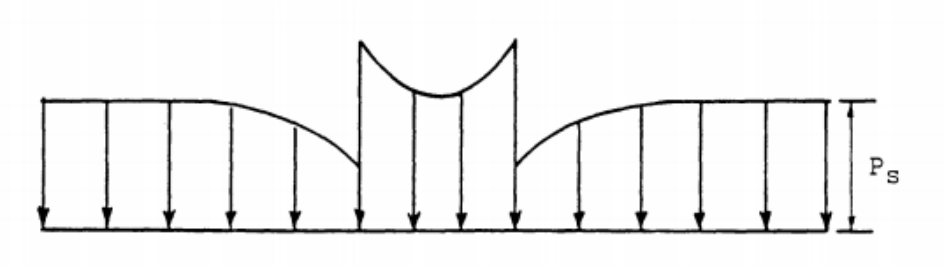

Figure 2-4 Stress Distribution on Top of Structure in Passive Arching (Evans, 1983)

As a result, the soil undergoes large settlements, mobilizing shear stresses, which increase the total pressure on the structure while decreasing the pressure in the adjacent ground. The stress along a plane will be uniform when the adjoining ground and the

structure have the same properties. The stress along the vertical direction will be linear and increases with depth as no arching would be presented in this case. This condition is highly unlikely to be found in natural or man-made environments due to the differences in the mechanical properties of geomaterials (like soils or rocks) and structure components (like steel or concrete) (Moradi and Abbasnejad, 2013).

Terzaghi's Trap Door Experiment

In Terzaghi's experiment, a trap door, which was mounted flush with the base of a box containing sand, was translated downward while the total load on the trapdoor and its settlement were monitored (Terzaghi, 1943). Horizontal and vertical stresses at various heights above the door were indirectly measured using the friction tape method. Terzaghi noted that arching does not necessitate the crushing of soil particles to support the arch formation. It is a temporary circumstance dependent on the shear stresses in the soil. Terzaghi proposed a theoretical approach for the arching problems in sand under plane strain condition. He defined the arching effects as the pressure transfer between a yielding mass of soil and adjoining stationary parts (Terzaghi, 1943). A shearing resistance within the contact zone of the yielding and stationary masses opposes the relative settlement in the soil. Hence, the pressure transfer is possible through the shearing resistance, which plays an important role in the arching theory (Terzaghi, 1943).

The real surfaces of sliding, as observed by Terzaghi in 1936, are curved and at the soil surface, their spacing is greater than the width of the yielding strip. The yielding strip (ab) at the solid base is presented in Figure 2-5, and the real sliding surfaces are curve (ac) and curve (db) in Figure 2-5. Several assumptions are used in the arching theories based on the experimental observations.

The sliding surfaces are assumed vertical. The vertical sections ae and bf through the outer edges of the yielding strip in Figure 2-5 represent surfaces of sliding. The

pressure on the yielding strip is thus equal to the difference between the weight of the sand located above the strip (ab) and the shear resistance along the vertical sections. The free body diagram for a slice of soil in the yielding zone above the strip ab can be seen in Figure 2-6. In addition to the vertical sliding surface assumption, Terzaghi also assumed that the normal stress is uniform across horizontal sections and the coefficient of lateral stress (K) is a constant. Cohesion (c) was assumed to exist along the sliding surfaces. Figure 2-6 shows the vertical equilibrium for the free body.

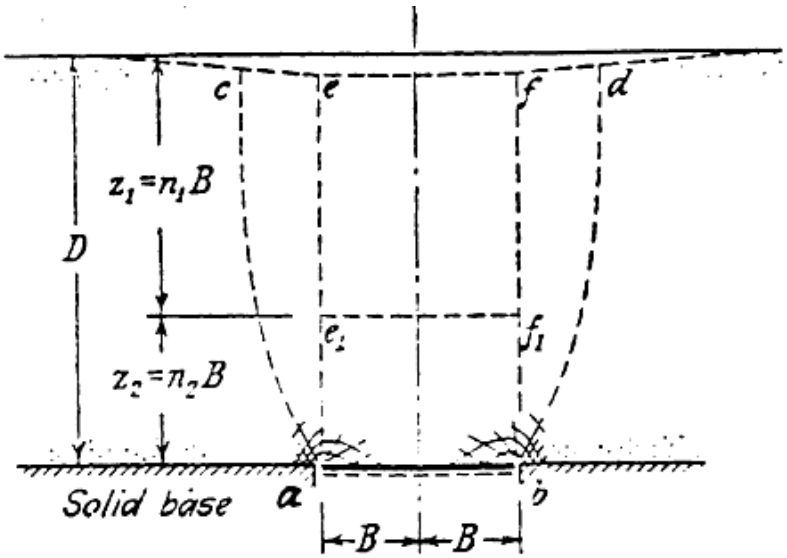

Figure 2-5 Yielding in Soil Caused by Downward Settlement of a Long Narrow Section (Terzaghi, 1943)

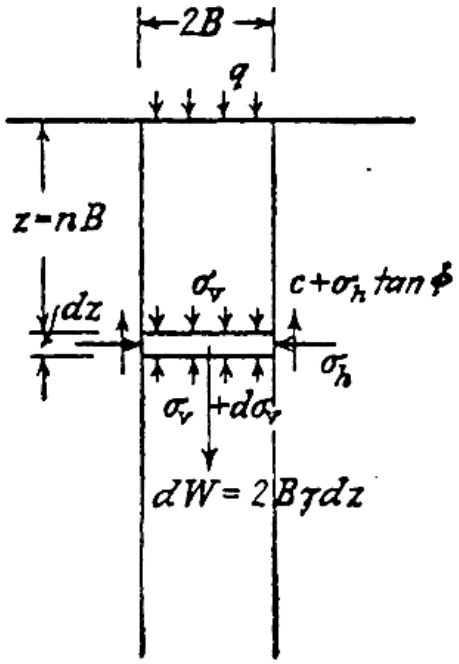

Figure 2-6 Free Body Diagram for a Slice of Soil in the Yielding Zone (Terzaghi, 1943)

$$2B\gamma dz = 2B(\sigma_v + d\sigma_v) - 2B\sigma_v + 2cdz + 2\sigma_v dz \tan\phi \quad \text{(Eq. 2-1)}$$

Where:

2B = width of the yielding strip (ab), [m, (ft)],

z = depth [m, (ft)],

γ = unit weight of soil [kN/m^3 (lb/ft^3)],

σ_v = vertical stress [kPa (psi)],

σ_h = horizontal stress = Kσv [kPa (psi)],

K = the coefficient of lateral stress,

c = cohesion [kPa (psi)], and

ϕ= friction angle.

The boundary conditions are σ_v = q (surcharge) at z =0. By solving Equation 2-1 we have:

$$\sigma_v = \frac{B\left(\gamma - C/B\right)}{K \tan\phi}\left(1 - e^{-K \tan\phi .z/B}\right) + q.e^{-K \tan\phi .z/B} \quad \text{(Eq. 2-2)}$$

The experimental investigations regarding the state of stress in the sand located above a yielding strip have shown that the arching effect only extends to a height of 5B. In other words, at elevations of more than 5B above the centerline due to lowering of the strip has no effect on the state of stress in the sand (Terzaghi, 1942). Terzaghi assumed that the shear resistance of the sand was active only on the lower part of the vertical boundaries (ae) and (bf) in Figure 2-7. With this assumption, the upper part of the soil prism (ee_1f_1f) is treated as a surcharge (q) on the lower part (e_1abf_1). If z_1 (= n_1B) is the part of prism, which acts like surcharge, and z_2 (= n_2B) is the part of prism with shear resistance at the vertical boundaries, then Equation 2.2 becomes:

$$\sigma_v = \frac{B\left(\gamma - C/B\right)}{K \tan\phi}\left(1 - e^{-K\, n2.\tan\phi}\right) + q.e^{-K\, n2.\tan\phi} \quad \text{(Eq. 2-3)}$$

Application of Arching Theory in Tunnels

The stress state in the soil above the top of a tunnel is similar to the stress state in the soil above a yielding strip. Terzaghi assumed the soil adjacent to the tunnel yields laterally towards the tunnel during construction. This creates an active earth pressure condition with the boundaries of the yielding zone inclined at about (45 +ϕ/2). The yielding zones at the sides of the tunnel and the assumed yielding prism ($e_1b_1b_1e_1$) are shown in Figure 2-7.

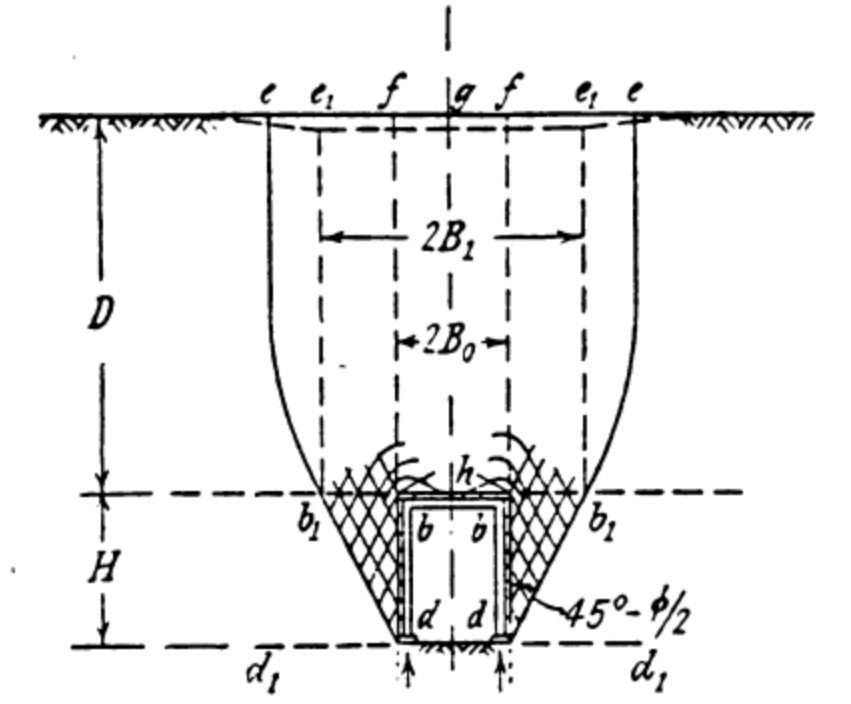

Figure 2-7 Flow of Soil toward Shallow Tunnel When Yielding Happened in the Soil (Terzaghi, 1943)

At the level of the tunnel roof, the width of the yielding strip for a rectangular tunnel is:

$$2B_1 = 2(B_0 + H.\tan(45 - \phi/2)) \quad \text{(Eq. 2-4)}$$

If the tunnel roof is located at a depth D in the ground, the vertical stress on the roof is:

$$\sigma_v = B_1(\gamma - C/B_1)/(K\tan\phi)\left(1 - e^{-K.\tan\phi\, D/B_1}\right) \quad \text{(Eq. 2-5)}$$

If a tunnel is located at a great depth below the surface, the arching effect cannot extend beyond a certain elevation D_1 above the tunnel roof. In addition, the soil located above this elevation has a depth D_2. Figure 2-8 shows the configuration of the tunnel at a great depth. The vertical stress on the roof is then expressed as:

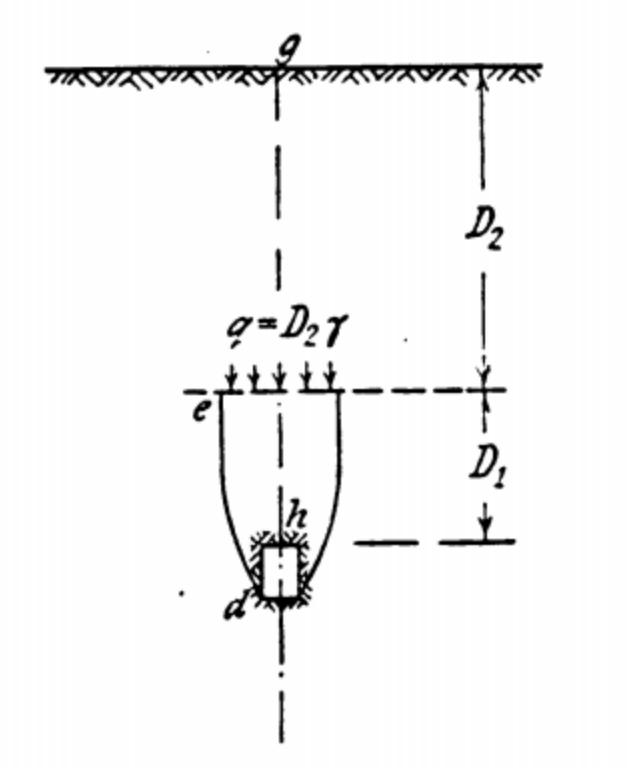

Figure 2-8 Yielding Zone in Soil When Tunnel Located at Great Depth (Terzaghi, 1943)

$$\sigma_v = B_1(\gamma - C/B_1)/(K\tan\phi)\left(1 - e^{-K.\tan\phi.{}^{D_1}/_{B_1}}\right) + \gamma D_2.e^{-K.\tan\phi.{}^{D_1}/_{B_1}} \quad \text{(Eq. 2-6)}$$

When D_1 is very large, the vertical stress will reach a limit value:

$$\sigma_v = B_1(\gamma - C/B_1)/(K\tan\phi) \quad \text{(Eq. 2-7)}$$

If the tunnel is constructed in sand, then cohesion (c) is equal to 0. However, for safety reasons, c = 0 is assumed and Equation 2-7 can be simplified to:

$$\sigma_v = B_1\,\gamma/K\tan\phi \quad \text{(Eq. 2-8)}$$

Loads on Buried Conduits

In 1913, Anson Marston developed a theory to explain the characteristics of a soil column above a buried conduit. Marston found that the load due to the weight of the soil

above a buried conduit does not fully act on the conduit; part of the weight is undertaken by the arching action in which load is transferred to the adjacent side material (e.g., soil). Buried conduits can be grouped according to their installation procedures. The two major categories are those installed in a trench excavated through existing soil, i.e., trench conduit (Figure 2-9 (a)), and those placed at existing ground level above which an embankment is subsequently constructed, i.e., projecting conduit. If the top of the structure projects above the ground surface, it is a "positive" projecting conduit (Figure 2-9 (b)). If it is placed in a shallow trench and the top lies below the ground surface, it is a "negative" projecting conduit (Figure 2.9 (c)). Arching action and the equal and opposite arch support play a tremendously important role in the development of earth load on a structure. In some cases, such as the case of a pipe in a trench (a ditch conduit), its effect is favorable; that is, it reduces the load as compared to the dead weight of the prism of soil lying above the structure.

In other cases, such as some installations under embankments, arching action may be inverted and the load on the structure may be considerably greater than the weight of the overlying prism of soil. The imperfect ditch method utilizes the principles of arch action and arch support to minimize the load on a buried structure. Figure 2-9 (d) shows the layout of an imperfect ditch conduit.

In the development of load on an underground structure, arch action is considered the resultant of lateral thrust and vertical shearing forces, which are mobilized on certain vertically oriented planes in the soil overburden. The magnitude of arch support can be evaluated by means of the Marston Theory. For ditch conduits, this load formula is derived by considering the forces acting on a thin horizontal slice of backfill material. The layout of a ditch conduit is shown in Figure 2-10. Equating the upward and downward vertical forces on the horizontal slice, Equation 2-9 is obtained.

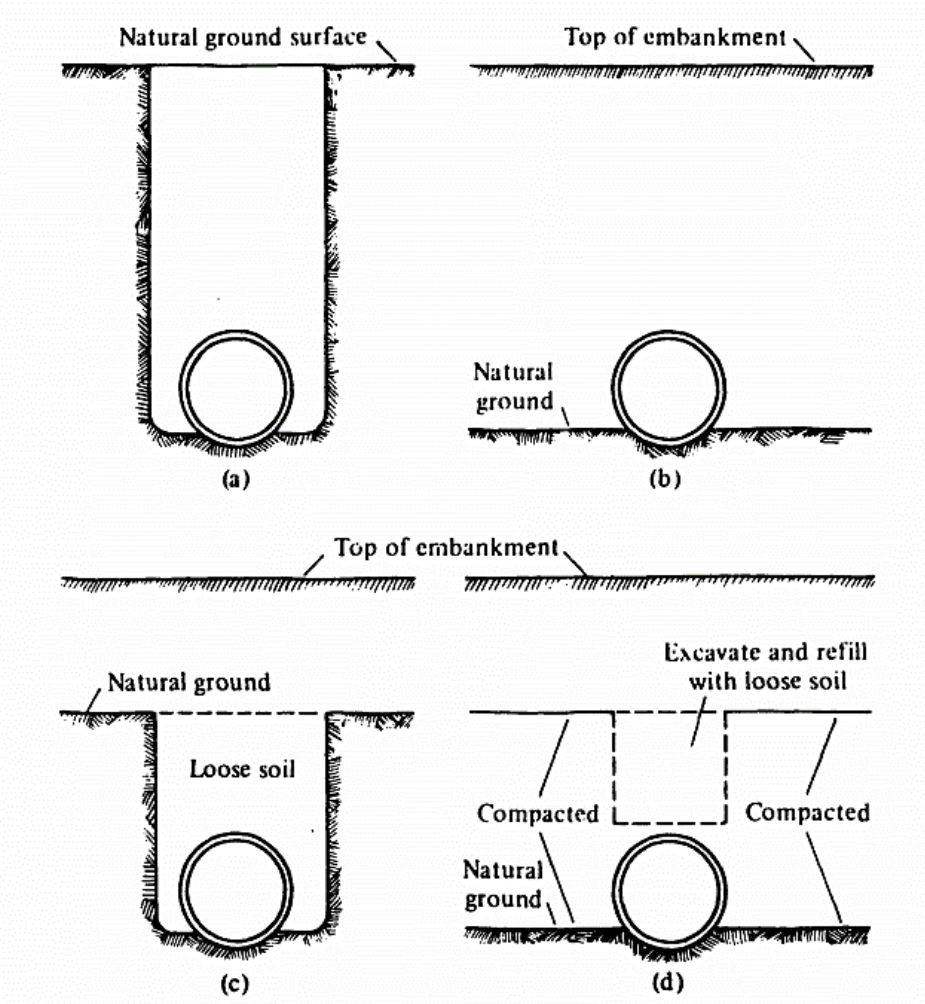

Figure 2-9 Various Classes of Conduit Installations: (a) Ditch Conduit, (b) Positive Projecting Conduit, (c) Negative Projective Conduit, and (d) Imperfect Ditch Conduit (Spangler & Handy, 1973)

$$V + dV + 2K\mu' \frac{V}{B_d} dh = V + \gamma B_d dh \qquad \text{(Eq. 2-9)}$$

Which:

V = vertical pressure on the top of the horizontal slice [kPa (psi)],

dV = vertical pressure increment [kPa (psi)],

γ = unit weight of backfill [kN/m^3 (lb/ft^3)],

K = the coefficient of lateral stress,

$\mu' = \tan\phi'$ = coefficient of friction between fill material and sides of ditch, and

B_d = width of ditch at top of conduit [m, (ft)].

This is a linear differential equation, the solution is:

$$V = C_d \gamma B_d^2$$

Which:

$$C_d = \left(1 - e^{2K\mu' H/B_d}\right)/(2K\mu') \quad \text{(Eq. 2-10)}$$

H = the distance from the ground surface to the top of the conduit, [m, (ft)]

Hence, for the case of a rigid ditch conduit with relatively compressible side fills, the load on the conduit (W_c) will be:

$$W_c = C_d \gamma B_d^2 \quad \text{(Eq. 2-11)}$$

The magnitude of arch support is the algebraic difference between the weight of backfill and the load on the structure. For the case of ditch conduits, this difference is:

$$A_s = B_d \gamma (H - C_d . B_d) \quad \text{(Eq. 2-12)}$$

Which:

A_s = arch support (support derived from both sides of the ditch) [m^2 (ft^2)],

The thin slice of backfill material in the free body diagram of Figure 2-10 will look like an arch shape slice when the arching effect is activated in the backfill over a ditch conduit. This case is when an underground conduit is stiffer relative to the soil medium and the load distribution at the top level of the conduit would be higher just above the pipe. In other words, the stiff conduit takes almost the entire load from overburden soil. When this occurs, Equation 2-10 is valid. However, for the case of a flexible pipe conduit and thoroughly tamped side fills having essentially the same degree of stiffness as the pipe itself, the value of W, given by Equation 2-10 might be multiplied by the ratio B_c/B_d, where

B, is the outside width of the conduit. The load from the overburden is distributed uniformly on the conduit and the soil beside it. Therefore, the load on the flexible pipe would then be:

$$W_c = C_d \gamma B_d . B_c \qquad \text{(Eq. 2-13)}$$

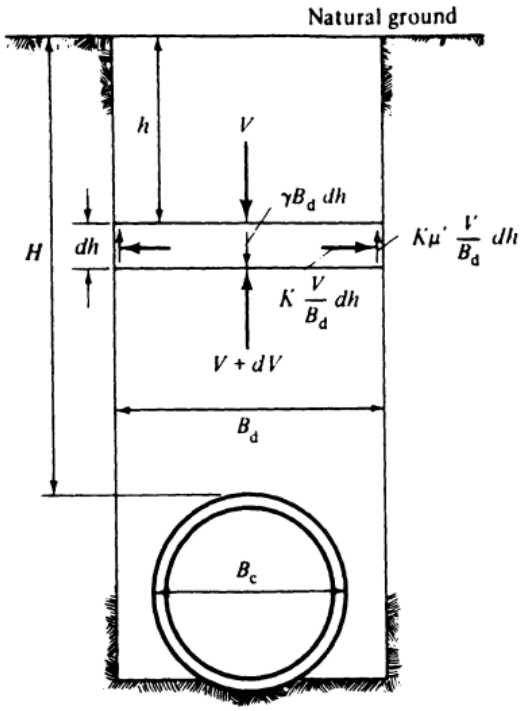

Figure 2-10 Free Body Diagram for Trench Conduit (Spangler & Handy, 1973)

It is emphasized by Spangler & Handy (1973), that for Equation 2-12 to be applicable, the side fills must be compacted sufficiently to have the same resistance to deformation under vertical load as the pipe itself. Equation 2-12 cannot be used merely because the pipe is a flexible type. In the actual conditions, it is probable that the load on a pipe lies somewhere between the results in Equations 2-11 and 2-13, depending upon the relative rigidity of the pipe and the side fill columns of soil.

As to projecting conduits, there are two types of them, the positive projecting conduits and the negative projecting conduit. When a conduit is installed as a positive

projecting conduit, shearing forces also play an important role in the development of arch action and the resultant load on the structure. In this case the planes along which relative settlements are assumed to occur and on which shearing forces are generated, are the imaginary vertical places extending upward form the sides of the conduit as indicated in Figure 2-11 (a) and 2-11 (b). The width factor in the development of an expression for load is the outside width of the conduit, designated as B_c.

The magnitudes and directions of relative settlements between the interior prism ABCD in Figure 2-11 (a) and (b), and the adjacent exterior prisms are influenced by the settlement of certain elements of the conduit and the adjacent soil. Marston combined these settlements into an abstract ratio, called the settlement ratio (Spangler & Handy, 1973),

$$r_{sd} = \frac{(S_m + S_s) - (S_f + d_c)}{S_m} \qquad \text{(Eq. 2-14)}$$

Which:

r_{sd} = settlement ratio,

S_m = compression strain of the side columns of soil of height pB_c,

P = projection ratio,

pB_c = the vertical distance from the natural ground surface to the top of the structure [m, (ft)],

B_c= outside width of the conduit [m, (ft)],

S_s= settlement of the natural ground surface and adjacent to the conduit [m, (ft)],

S_f = settlement of the conduit into its foundation [m, (ft)], and

d_c= shortening of the vertical height of the conduit [m, (ft)].

Marston also defined a critical plane, which is the horizontal plane through the top of the conduit when the fill is level with its top, i.e., when H = 0. During and after construction

of the embankment, this plane settles downward. If it settles more than the top of the pipe, as illustrated in Figure 2-11 (a), r_d is positive; the shearing forces on the exterior prisms move downward with respect to the interior prism.

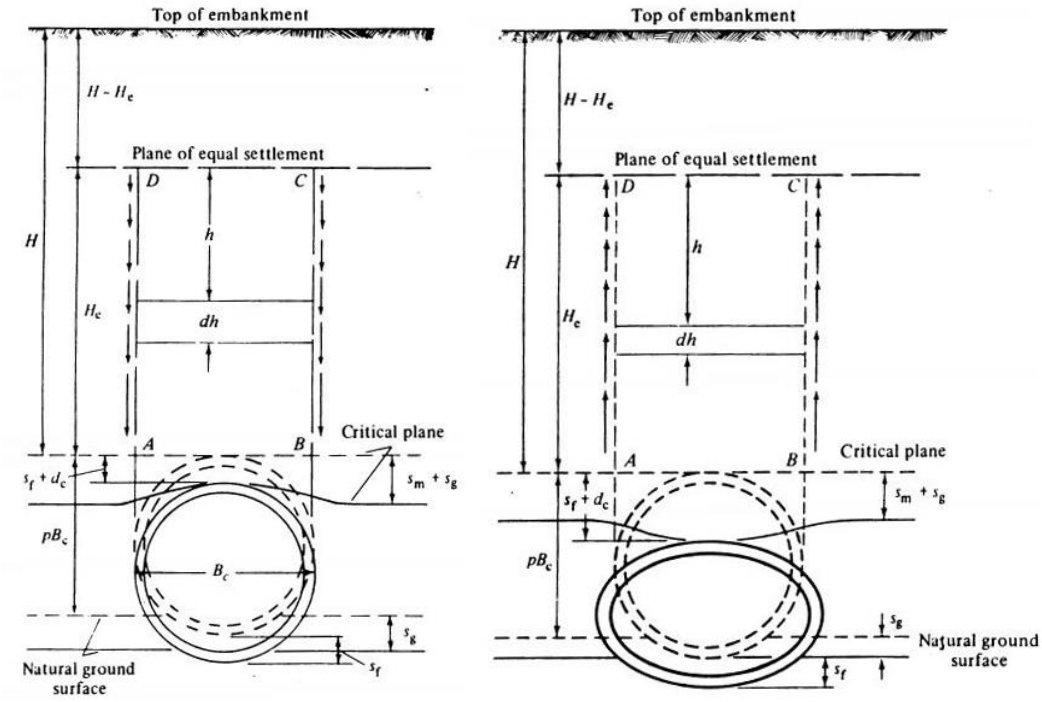

(a) Rigid Conduit/ Projection Condition (b) Flexible Conduit/ Ditch Condition

Figure 2-11 Settlement in Positive Projection Conduits

As stated above, if the shearing forces on the interior prism are directed downward, the resultant load on the structure is greater than the weight of the prism of soil directly above it. This case is called "projection condition" and the arching effect increases the load on the conduit. If the critical plane settles less than the top of the conduit, like the one shown in Figure 2-11 (b), the interior prism moves downward with respect to the exterior prisms. The shearing forces on the interior prism are directed upward, and the resultant load on the structure is less than the weight of the soil above the structure. This case is called the "ditch condition" and the arching effect decreases the load on the conduit. Using

the aforementioned parameters, if the shear stresses at the sides of the interior prism are developed to the top of the embankment, which is called the "complete condition," the load on the positive projecting conduits derived by Marston is:

$$r_{sd} = \frac{(S_m + S_s) - (S_f + d_c)}{S_m} \quad \text{(Eq. 2-15)}$$

Which:

$$C_c = \left(e^{\pm 2K\mu\, H/B_c} - 1\right)/(\pm 2K\mu) \quad \text{(Eq. 2-16)}$$

$$\mu = \tan\phi$$

The plus signs are used for the projection condition and the minus signs are used for the ditch condition. Two different results in analyzes of positive projecting conduits are caused by the stiffness of the buried conduit. If the conduit is rigid relative to the refilled soil, projection condition exists like Figure 2-11 (a). If the conduit is flexible relative to the refill soil, the ditch condition exists like Figure 2-11 (b).

In order to reduce the load on the conduit under the projection condition. Marston proposed the idea of the imperfect ditch conduits in 1920. Spangler provided the analysis of loads on imperfect ditch conduits later in 1950. In the imperfect ditch conduit construction procedure, illustrated in Figure 2-9 (d), the conduit is first installed as a positive projecting conduit. Then the soil backfill at the sides and over the conduit is compacted up to some specified elevation above its top. Next, a trench of the same width as the outside horizontal dimension of the pipe is excavated down to the structure and refilled with very loose, compressible material, e.g., loosened soil, straw, or hay. The purpose of this method is to ensure that the interior prism of soil will settle more than the exterior prisms, thereby generating friction forces, which are directed upward on the sides of the interior prisms. The resultant load on the conduit is then reduced. The load formula for an imperfect ditch conduit is:

$$W_c = C_n \gamma B_c^2 \quad \text{(Eq. 2-17)}$$

Where C_n is a load coefficient, which is a function of the ratio of the height of fill to the width of ditch, H/B, the projection ratio p', and the settlement ratio r_{sd}. Spangler and Handy provided several sets of C_n, diagrams with different parameter values (Spangler & Handy, 1973 & 1982). The settlement ratio, r_{sd}, is always a negative quantity in the imperfect ditch conduit case, which means the arching effect will always transmit the load at the top of conduit to the side soil media (the direction of shear forces at the sides of the interior prism is always upward). The negative projecting conduit has the same function as the imperfect ditch conduit. The analysis of loads on negative projecting conduits follows the same procedures as that for imperfect ditch conduits, but uses a different width factor, B_d, instead of the width of the imperfect ditch; B. B_d is the width of the shallow ditch in which the pipe is installed (see the layout at Figure 2-9 (c)). The same load coefficient diagrams are applicable to both cases.

CHAPTER SUMMARY

This chapter presented an overview of arching theory and its effect on soil settlement over pipe and box. Effects of rigid or flexible pipes on adjacent soil were also explained in this chapter. Soil settlement over pipe or box is affected by soil conditions, pipe or box shape and burial depth to the surface ground.

Chapter 3 LITERATURE REVIEW

INTRODUCTION

There have been several research studies carried out to understand the effect of induced ground settlements by pipe/box installation. This chapter will cover the review of some the past researches to predict the ground response associated with tunneling in different soil conditions. Most of the past studies were carried out by empirical, analytical, experimental, numerical methods and by back analysis from the field monitoring data. In this chapter, the current understanding on the tunneling effects observed from various studies using different methods is discussed and the discrepancies between different research outcomes are highlighted.

GROUND SETTLEMENTS AND VOLUME LOSS

Ground settlements are an inevitable consequence of tunnel construction and pipe/box jacking operations. It is not possible to create a void instantaneously and provide an infinitely stiff lining to fill it exactly. In the time taken to excavate, the ground around the tunnel is able to displace inwards as the stress relief is taking place. Thus, it will always be necessary to remove a larger volume of ground than the volume of the finished void. This extra volume excavated is termed the volume loss (Peck, 1969).

The lining, pipe or box, which are of slightly smaller diameter (size) than the shield size, are erected immediately behind it. The annulus between the structure and ground is normally filled with cementitious materials. Thus, there is a further opportunity for the ground to displace radially onto the lining, pipe or box, until the filling material has hardened sufficiently to resist the earth pressures. The sum of the two radial settlements is termed ‘radial’ ground loss as illustrated in Figure 3-1. The face loss and radial loss total to give the overall volume loss, V_L, for the construction of the tunnel, measured in cubic meters

(cubic feet) per meter (per ft) advance of the tunnel drive. V_L is normally expressed as a percentage of the gross area of the finished tunnel and can be expressed as (Peck, 1969):

$$A = \frac{\pi\ (D_S^2 - D_R^2)}{4} \qquad \text{Eq. 3-1}$$

Where:

D_S= Outside diameter of the jacking, shield machine or EPBM [m, (ft)], and

D_R= Outside diameter of the jacked pipe, box or segmental linings [m, (ft)].

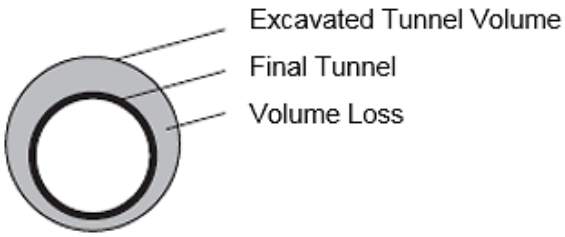

Figure 3-1 Volume Loss in Tunnel Construction (Möller, 2006)

The choice of tunneling construction whether shield machine or hand excavation with shield, usually depends on its ability to excavate ground and remove the spoil in a safe and controlled manner. Some tunneling machines may also control volume loss to within tight limits. In particular, face loss may be reduced or even eliminated by applying pressure to the face equal to the mean in-situ horizontal stress. In earth pressure balance machines (EPBM), the compartment at the face is maintained at a pressure above atmospheric by controlling the rate at which spoil is removed by a screw conveyor. This machine is used in softer soils or permeable soils where water inflow into the face may be a problem and relies upon the spoil behaving as a plastic continuum under pressure. The addition of bentonite slurry (a slurry machine) may assist this process in sands and gravels. However, in harder impermeable materials, such as over consolidated clays, the spoil may not break down enough at the heading for either method to be practicable. In these

circumstances, an open-faced machine is used, relying on the strength, stand-up time and low permeability of the clay for face stability.

It is much harder to control the radial loss (Bloodworth, 2002). One option is to inject slurry into the annulus around the shield. However, because the shield is moving forward, and the erection of the lining or pipe must necessarily be carried out at atmospheric pressure, prevention or even control of radial settlements is not practicable. It can be the most significant cause of settlement, especially if grouting of the annulus is not carried out immediately. The best approach is to keep a steady fast rate of advance and rely on dealing with the problem by treating its effects (surface settlements) rather than at source. The use of compressed air to maintain pressure in the tunnel during the entire excavation and lining cycle has safety implications and is usually too expensive (Bloodworth, 2002).

Prediction of the total amount of volume loss would be useful for tunnel designers but is difficult because volume loss apparently depends on a number of factors that are not known at the design stage. These include the tunneling machine type, the construction sequence and the effectiveness of the grouting behind the lining, the latter being a 'workmanship' factor. The designer ideally knows the soil properties and in-situ stress state. It is also known that volume loss does not necessarily increase with stress (Bloodworth, 2002).

STUDY OF GROUND SETTLEMENTS DUE TO PIPE INSTALLATION

Various methods are available to predict soil deformation due to tunnel excavation. These methods can be generally categorized as below:

1. Empirical methods,
2. Analytical methods, and
3. Numerical methods.

Empirical Methods

The most common empirical method to predict ground settlements is based on a Gaussian Distribution Curve, which is often referred to as the empirical method. Peck (1969) showed that the transverse (vertical) settlement trough, taking place immediately after construction of a tunnel, is well fitted by the Gaussian Curve as shown in Figure 3-2 and is obtained by using the Equation 3-2;

$$S(x) = S_{max}.\exp(-\frac{x^2}{2i^2}) \quad \text{Eq. 3-2}$$

Where:

$S_y(x)$= Vertical settlement as a function of x [m, (ft)],

S_{max}= Maximum settlement (trough) at the tunnel centerline (x=0) [m, (ft)],

x= Horizontal distance from the tunnel vertical axis [m, (ft)], and

i = Settlement trough width (distance from the tunnel vertical axis to the point of inflexion of the settlement trough [m, (ft)].

Volume loss is approximated by the following equation:

$$V_L = \sqrt{2\pi}.i.S_{max} \approx 2.5iS_{max} \quad \text{Eq. 3-3}$$

Schmidt (1969) also reported that maximum settlement occurs directly above the tunnel axis and the settlement becomes negligible after the distance of 3i from tunnel vertical axis. Unlike volume loss, the trough width parameter is relatively easier to quantify as it is largely independent of construction method and operator experience and can be shown as (Fujita, 1981; O'Reilly and New, 1982):

$$i = \mathrm{K}Z_0 \quad \text{Eq. 3-4}$$

Where:

K= Trough width parameter, and

Z_0= Tunnel depth below ground level to tunnel horizontal axis [m, (ft)].

The settlement trough agrees well with K values in the range of 0.4 to 0.6 for clay and 0.25 to 0.45 for sand.

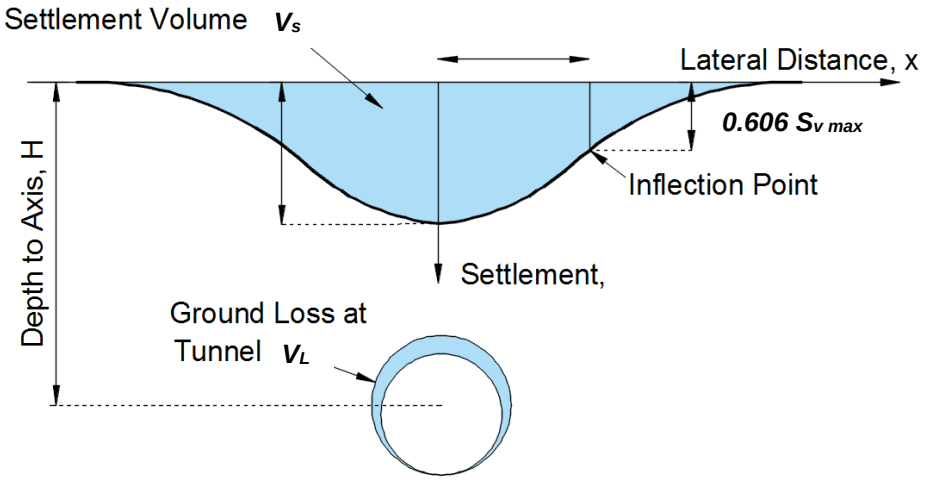

Figure 3-2 Gaussian Curve Used to Approximate Vertical Surface Settlement Trough (Adapted from O'Reilly & New, 1982)

To obtain S_{max}, it is first required to make an estimation on the volume loss, which is usually expressed as the percentage of the ratio of the volume of the surface settlement trough, V_S to the excavated volume per unit length of the tunnel, A.

Cording and Hansmire (1975) summarized the field observation data from the Washington, D.C., Metro line construction and showed that the volume of surface settlement trough is equal to the volume of ground loss for tunneling in clays under undrained conditions. For tunneling in dense sands, which is in drained condition, the volume of the settlement trough is less than that of the ground loss due to dilation effect (Su, 2015). Depending on equipment, control procedures and experience of the crew, ground loss values between 0.5% and 2% are realistic in homogeneous ground. In sands, a loss of only 0.5% can be achieved, whereas soft clays involve the range from 1% to 2%, as reported by Mair (1996). Considering data for mixed ground profiles with sands or fills

overlaying tertiary clays, Mair and Taylor (1997) reported ground loss values between 2% and 4%.

In open face tunneling, the ground loss is largely controlled by the round length and the size of the (partial) excavations, whilst ground stiffness and initial stresses also have a significant influence. Mair (1996) concluded that ground loss ratios in stiff clays are between 1% and 2%, whilst conventional tunneling in London clay has resulted in even smaller losses varying between 0.5% and 1.5%. Many authors have proposed various different relationships for ground loss ratios.

Several researchers (Jacobsz et al., (2004), Celestino et al., (2000) and Vorster et al., (2005)) suggested different curves for different soil types to better fit the empirical ground surface prediction to the real case studies. For example, Modified Gaussian model was developed to cover the lack of fit in Gaussian curve for the results of soil settlements in some centrifuge experiments conducted by Vorster et al., (2005). Parameter “n” in Modified Gaussian is shape function parameter controlling the width of the profile and “α” is parameter to ensure that i remains the distance to the inflection point. The Modified Gaussian Curve becomes Gaussian Curve when shape function (n) is equal to 0.5 (Vorster et al., 2005). Yield Density was developed to better predict ground distortion since Gaussian curves tend to predict lower ground distortions than the real values (Celestino et al., 2000). Ground distortion is a parameter used to predict the building damage due to settlement as shown in Equation 3-5 (Celestino et al., 2000). In Yield Density Method, parameter “a” strongly influences the trough width, whereas “b” influences the shape of the curve where was found to vary in the ranges 2-3 for porous clay, and 2-2.8 for stiff clay (Celestino et al., 2000). Table 3-1 summarizes different curves used to fit settlement trough data above tunnels.

$$\gamma_{max} = \frac{S_{max}\ b\ B^{b-1}}{a(1+B^b)^2} \quad \text{(Eq. 3-5)}$$

Atkinson and Potts (1979), O'Reilly and New (1982), Lake et al., (1992) and many other researchers derived the correlation between trough width and tunnel depth (D) based on different case histories for different soil types as summarized in Table 3-2.

Table 3-1 Curves Used to Fit Settlement Trough above Tunnels

Reference	Equation of Curve
Gaussian Curve (Peck, 1969)	$S(x) = S_{max}.\exp(-\frac{x^2}{2i^2})$ $S(i) = 0.606S_{max}$
Jacobsz (Jacobsz et al., 2004)	$S(x) = S_{max}.exp\left[-0.334\left(\frac{\lvert x\rvert}{i}\right)^{1.5}\right]$ $S(i) = 0.717S_{max}$
Yield Density (YD) (Celestino et al., 2000)	$S(x) = \frac{S_{max}}{1+\ (\lvert x\rvert/a)^b}$ $i = aB;\ B = \left(\frac{b-1}{b+1}\right)^{1/b}$
Modified Gaussian (Vorster et al., 2005)	$S(x) = \frac{nS_{max}}{n-1+\ exp\left[a(\frac{x^2}{i^2})\right]}$ $n = \exp(a)\,.(2a-1)/(2a+1)+1$

Table 3-2 Settlement Trough Width for Different Soil Types

Reference	Soil Type	Settlement Trough Width m, (ft)
Atkinson and Potts (1979)	Loose Sand	$i = 0.25(Z_0 + 0.5D)$
	Dense sand, Overconsolidated soil	$i = 0.25(1.5Z_0 + 0.25D)$
O'Reilly and New (1982),	Cohesive soil	$i = 0.43Z_0 + 1.1$
	Granular soil	$i = 0.28Z_0 - 0.12$
Rankin (1988)	Soft to stiff clay	$i = (0.4 \sim 0.6)Z_0$
	Granular soil	$i = (0.25 \sim 0.45)Z_0$
O'Reilly and New (1991),	Layered sand and clay soil	$i = K_1Z_1 + K_2Z_2$
Lake et al., (1992)	Clay	$i = 0.5Z_0$

When tunneling in urban areas, one may have to consider the interaction with deep foundations or existing tunnels. This leads to the need of having information about the development of subsurface settlement profiles. Mair et al., (1993) analyzed subsurface deformations from tunnels in clays as well as centrifuge tests in clay and suggested the empirical method to estimate subsurface settlement as shown in Equations 3-6 and 3-7. Their studies showed that the value of *i* for subsurface settlement profiles is significantly larger than would be predicted with a constant K (Figure 3-3). Studies also showed that subsurface deformations could also be reasonably approximated by a Gaussian Distribution Curve. As shown in Figure 3-4, the trough width parameter increases as moving toward the ground surface. Table 3-3 presents different subsurface trough with values different soil types.

Table 3-3 Subsurface Trough Width Parameter for Different Soil Types

Reference	Soil Type	Settlement Trough Width, m, (ft)
Mair et al., (1993)	Clay	$i = \mathrm{K}(Z_0 - \mathrm{Z})$ $K = [0.175 + 0.325(1 - Z/Z_0)]/(1 - Z/Z_0)$
Moh et al., (1996)	Silty sand	$i = \left(\frac{D}{2}\right)\left(\frac{Z_0}{D}\right)^{0.8}\left(\frac{Z_0 - Z}{Z_0}\right)^{0.4}$
	Silty clay	$i = \left(\frac{D}{2}\right)\left(\frac{Z_0}{D}\right)^{0.8}\left(\frac{Z_0 - Z}{Z_0}\right)^{0.8}$
Dyer et al., (1996)	Firm to stiff clay over loose sand layers	$i = \mathrm{K}(Z_0 - \mathrm{Z})$

$$S_z = S_{z,max}\exp\left(-\frac{x^2}{2K^2(Z_0 - \mathrm{Z})^2}\right) \quad \text{(Eq. 3-6)}$$

$$S_{z,max} = \frac{1.25V_L}{0.175 + 0.325(1 - Z/Z_0)}\frac{R^2}{Z_0} \quad \text{(Eq. 3-7)}$$

Where:

Z_0= Tunnel depth below ground level to tunnel horizontal axis [m, (ft)],

$S_{z,max}$= Maximum subsurface settlement at depth Z [m, (ft)],

V_L= Volume loss (%), and

R= Tunnel radius.

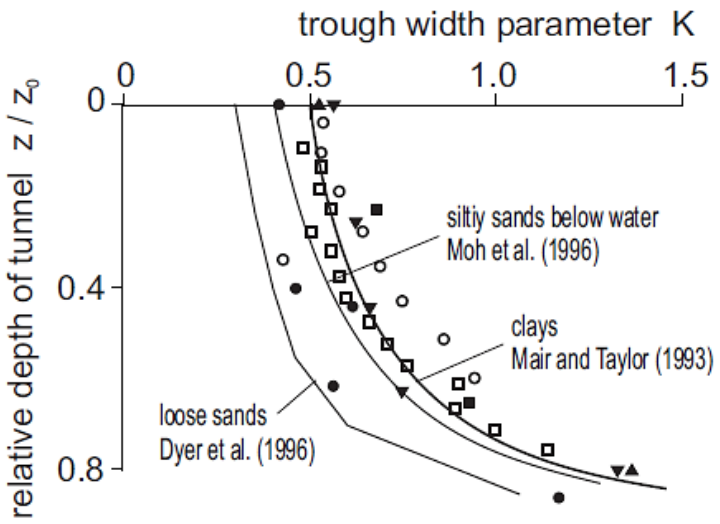

Figure 3-3 Relationship between Trough Width Parameter and Depth for Subsurface Settlement (Mair & Taylor, 1997)

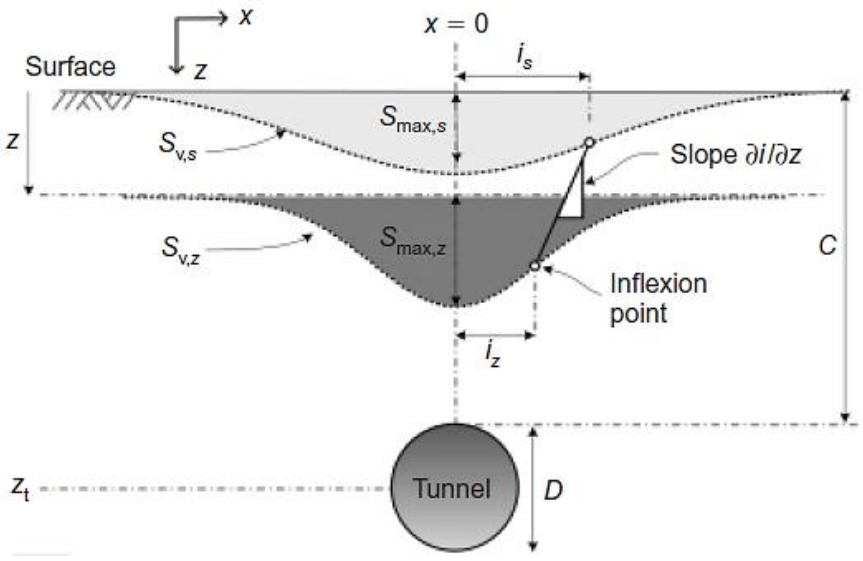

Figure 3-4 Surface and Subsurface Settlement Trough (Marshall, 2012)

Analytical Methods

Sagaseta (1987) introduced the first analytical methods for the prediction of trenchless tunnel induced ground displacement. Sagaseta (1987) developed an analytical closed form solution for ground settlement by simulating the uniform ground loss around a tunnel in the form of a point sink as shown in Figure 3-5. Sagaseta' analytical method is summarized in Equations 3-8 through 3-11. The volume per unit length of point sink is equal to πa^2, which is equal to ground displacement around the tunnel (volume loss). Soil was considered as homogeneous, isotropic elastic and incompressible medium. Vertical and horizontal ground deformation are identical because radial ground deformation was considered to be equal in vertical and horizontal, which resulting in a shallower and wider surface settlement compared to Gaussian Distribution Curve.

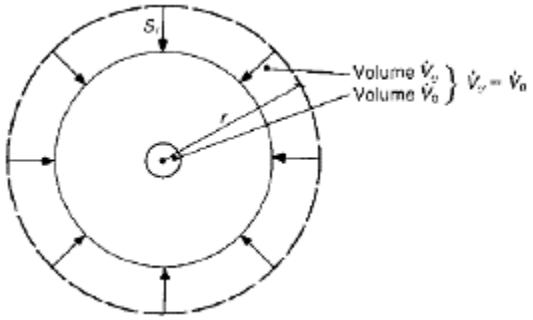

Figure 3-5 Uniform Ground Loss toward a Point Sink (Sagaseta, 1987)

$$S_{Z_0} = \frac{\nu}{\pi}\frac{H}{X^2 + H^2} \qquad \text{Eq. 3-8}$$

$$S_X = -\frac{(X - X_0)}{2}\left(\frac{a}{r}\right)^2 \qquad \text{Eq. 3-9}$$

$$S_{X_0} = -\frac{\nu}{\pi}\frac{X}{X^2 + H^2} \qquad \text{Eq. 3-10}$$

$$S_y = -\frac{(Z - Z_0)}{2}\left(\frac{a}{r}\right)^2 \qquad \text{Eq. 3-11}$$

Where;

$r = [(X - X_0)^2 + (Z - Z_0)^2]$,

ν= Poisson's ratio of soil,

X= Distance from tunnel centerline [m, (ft)],

H= Depth to axis [m, (ft)],

r= Tunnel radius [m, (ft)],

a= Point sink radius [m, (ft)],

S_{Z_0}= Surface ground settlement [m, (ft)],

S_y= Subsurface ground settlement [m, (ft)], and

S_X= Horizontal ground settlement at a distance *x* from tunnel centerline [m, (ft)].

Verrujit and Booker (1996) developed Sagaseta's method by considering more realistic parameters such as compressible soil and the effects of non-uniform ground deformation in the tunnel periphery. This resulted in unequal vertical and horizontal ground deformation around the tunnel. The long-term tunnel deformation was considered in Verrujit and Booker's solution but the effect of tunnel ovalization (Figure 3-6) in association with ground movement in short term ground deformation was not clearly described. Verrujit and Bookers' analytical method is summarized in Equations 3-12 through 3-14.

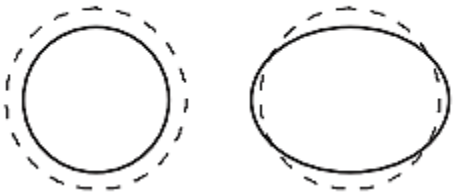

Figure 3-6 Ground Loss and Ovalization of Tunnel (Verrujit and Booker, 1996)

$$U_0 = 2\varepsilon R^2 \left[\left(\frac{m+1}{m}\right)\left(\frac{h}{x^2+h^2}\right)\right] - 2\delta h R^2 \left[\frac{x^2-h^2}{(x^2+h^2)^2}\right] \quad \text{Eq. 3-12}$$

$$U_z = -\varepsilon R^2\left(\frac{z_1}{r_1^2}+\frac{z_2}{r_2^2}\right)+\delta R^2\left(\frac{z_1(kx^2-z_2^2)}{r_1^4}+\frac{z_2(kx^2-z_2^2)}{r_2^4}\right) \quad \text{Eq. 3-13}$$

$$+\frac{2\varepsilon R^2}{m}\left(\frac{(m+1)z_2}{r_2^2}-\frac{mz(x^2-z_2^2)}{r_2^4}\right)$$

$$-2\delta hR^2\left(\frac{(x^2-z_2^2)}{r_2^4}+\left(\frac{m}{m+1}\right)\frac{2zz_2(3x^2-z_2^2)}{r_2^6}\right)$$

$$U_x = -\varepsilon R^2\left(\frac{x}{r_1^2}+\frac{x}{r_2^2}\right)+\delta R^2\left(\frac{z_1(x^2-kz_1^2)}{r_1^4}+\frac{x(x^2-kz_2^2)}{r_2^4}\right) \quad \text{Eq. 3-14}$$

$$-\frac{2xR^2}{m}\left(\frac{1}{r_2^2}-\frac{2mzz_2}{r_2^4}\right)$$

$$-\frac{-4\delta xhR^2}{m+1}\left(\frac{z_2}{r_2^4}+\frac{mz(x^2-3z_2^2)}{r_2^6}\right)$$

Where;

$R^2 = x^2 + z^2$

$r_1^2 = x^2 + z_1^2$

$r_2^2 = x^2 + z_2^2$

$z_1 = z - h$

$z_2 = x + h$

$m = \frac{1}{(1-2\nu)} k = \frac{\nu}{(1-\nu)}$

ε= Uniform radial ground loss (%),

δ= Long term ground deformation as a result of liner ovalization [m, (ft)],

r= Tunnel radius [m, (ft)],

x= Distance from tunnel centerline [m, (ft)],

z= Depth below ground surface [m, (ft)],

h=Tunnel depth [m, (ft)],

ν= Poisson's ratio of soil,

m= Auxiliary elastic constant,

U_0= Surface ground settlement [m, (ft)],

U_z= Subsurface ground settlement [m, (ft)], and

U_x= Horizontal ground settlement at a distance *x* from tunnel centerline [m, (ft)].

Loganathan and Poulos (1998) presented a quasi-analytical method to predict tunneling induced ground settlements based on solutions presented by Sagaseta (1987), and Verrujit and Booker (1996). Although the method has been successfully used to back analysis of numerous case histories in clay, calculated results, have to be treated with caution, as the method does not satisfy volumetric constancy for undrained conditions (Yih, 2003). The method was developed based on the modified Gap parameter, which was initially introduced by Rowe et al., (1983). The gap method was based on the gap zone over the tunnel crown equal to ground loss to consider the effect of construction method, face loss and equipment accuracy. The method consistently yields smaller settlement trough volumes than the prescribed input tunnel face loss. This is due to the assumed empirical distribution of ground loss with horizontal and vertical distance from tunnel centerline as presented in Equations 3-15 through 3-17. Figure 3-7 shows the nonuniform soil convergence and assumed boundary conditions around a tunnel.

$$U_{z=0} = -\varepsilon_0 R^2 \left(\frac{4H(1-\nu)}{H^2+x^2}\right) exp\left(-\frac{1.38x^2}{(Hcot\beta+R)^2}\right) \quad \text{Eq. 3-15}$$

$$U_z = \varepsilon_0 R^2 \left[-\frac{z-H}{(z-H)^2+x^2} + (3-4\nu)\frac{z+H}{(z+H)^2+x^2} - \frac{2z(x^2-(z+H)^2)}{((z+H)^2+x^2)^2}\right] \times exp\left[-\frac{1.38x^2}{(H+R)^2} - \frac{0.69z^2}{H^2}\right] \quad \text{Eq. 3-16}$$

$$U_x = \varepsilon_0 x R^2 \left[\frac{1}{(z-H)^2+x^2} + \frac{3-4\nu}{(z+H)^2+x^2} - \frac{4z(z+H)}{((z+H)^2+x^2)^2}\right] \quad \text{Eq. 3-17}$$

$$\times exp\left[-\frac{1.38x^2}{(H+R)^2} - \frac{0.69z^2}{H^2}\right]$$

Where;

ε_0= Ground loss ratio (%),

H= Tunnel depth [m, (ft)],

R= Tunnel radius [m, (ft)],

z= Depth below ground surface [m, (ft)],

x= Distance from tunnel centerline [m, (ft)],

ν= Poisson's ratio of soil,

$U_{z=0}$= Surface ground settlement [m, (ft)],

U_z= Subsurface ground settlement [m, (ft)], and

U_x= Horizontal ground settlement at a distance *x* from tunnel centerline [m, (ft)].

Although the method proposed by Loganathan and Poulos (1998) incorporated important factors such as various construction methods, tunneling equipment configurations and elastoplastic behavior of the soil, the validation with case studies only covered for soft to stiff clay conditions. Therefore, estimation of the soil response in sand or more complicated layered soil conditions was still left open for further investigation.

Numerical Methods

With the development of sophisticated computer software, numerical methods become an alternative approach to analyze soil-structure interaction problems. In the earlier days, most finite element analyzes on tunneling related problems involved a two-dimensional (2-D) plane-strain approximation in which a section perpendicular to the tunnel axis was considered. The approaches are convenient enough to assess the ground response in terms of efficiency and solving time. Numerous simulation methods were

developed by various researchers for tunnel excavation process such as progressive softening method by Swoboda (1979), the convergence-confinement method by Panet and Guenot (1982), the gap method by Rowe et al., (1983) and the volume loss control method by Potts & Addenbrooke (1997).

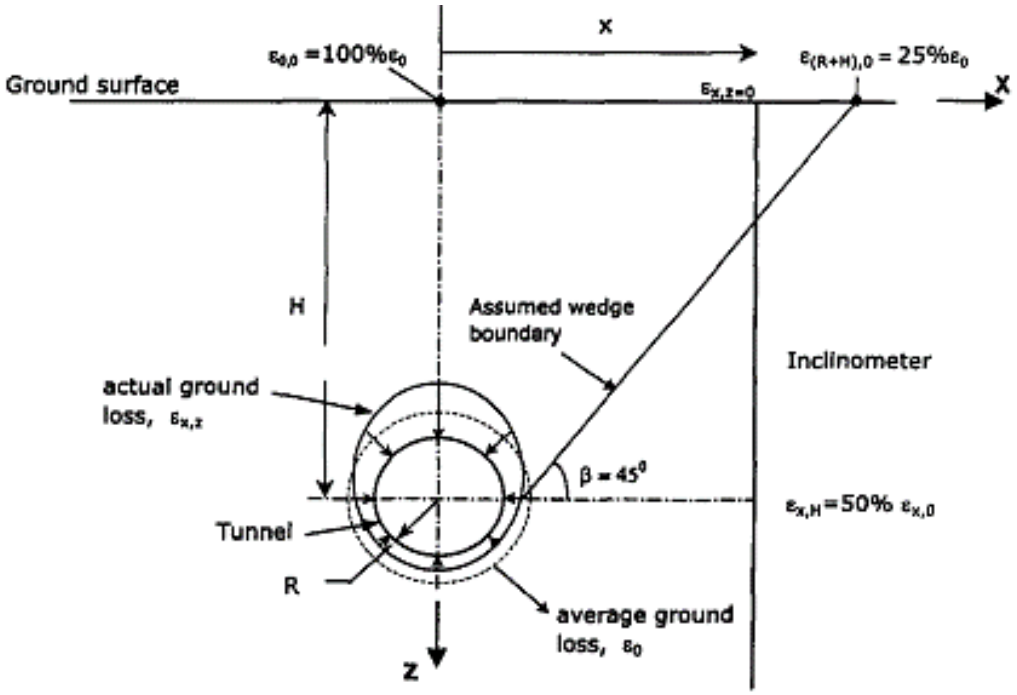

Figure 3-7 Ground Deformation Patterns and Ground Loss Boundary Conditions (Loganathan & Poulos, 1998)

In the convergence-confinement method and volume loss control a proportion of the initial equilibrium radial stress around the tunnel boundary is reduced to match maximum surface settlements or ground loss. The amount of reduction is usually between 20%-40% and can be calibrated to give measured volume loss. These methods have been applied to predict ground settlements due to tunneling (Addenbrooke et al., 1997).

Gap Method

The 'GAP' method was developed by Rowe et al., (1983), in order to predict the settlement using gap parameter in conjunction with FE analysis. The combined effects of

3-D elastoplastic ground deformation at the tunnel face, over excavation around the periphery of the tunnel shield and physical gap related to the tunnel machine, shield, and lining geometry were all considered as equivalent 2-D, non-uniform oval-shaped void (Figure 2.14). For FE simulation, the soil inside the tunnel was excavated and the surrounding soil was allowed to deform into the tunnel under self-weight. The settlements of the nodes on tunnel boundary were monitored during excavation. Once the nodes touched the final tunnel position, the lining element was activated. The GAP represents maximum vertical void between excavated soil (tunnel periphery) and tunnel lining (Figure 3-8). In this method, the difference between the initial and final positions prescribes a value of volume loss. Gap parameters in the method are described as:

$$GAP = G_P + U_{3D}^{*} + \bar{\omega} \qquad \text{Eq. 3-18}$$

Term G_P represents the difference between cutter head and outer lining diameter while U_{3D}^{*} and $\bar{\omega}$ accounts for 3-D heading effects and workmanship quality. The method is originally restricted to analyzes of tunneling in soft ground as it assumes complete tail void closure (Rowe and Lee, 1983) and but was later modified (Lee et al., 1992) to account for grouting by setting G_P to zero. However, the use of Gap Parameter method in FE analysis appears to be unclear due to inconsistencies between the theoretical and FE applied definition of the parameter.

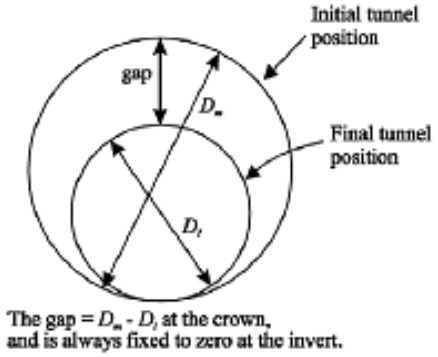

Figure 3-8 Gap Method (Rowe et al., 1983)

The volume loss control method

Addenbrooke et al., (1997) introduced the volume loss control method. This approach is similar to the convergence-confinement method except in the proportion of stress reduction. The tunnel excavation was simulated by applying equivalent nodal forces T over a number of increments in the opposite direction. After each increment, the volume loss V_L was calculated. Once the prescribed V_L was reached, the lining was activated.

The main advantage of using 2-D finite element analysis is that various factors such as tunnel diameter, tunnel depth, soil type, can be considered and incorporated together in one model simulation. Although each 2-D method is useful and convenient, each analysis also has its own shortcomings and limitations. The method requires some empirical input parameters such as volume loss, stress or stiffness reduction parameters, which are determined based on the past experience in relevant soil condition and tunneling methods [Rowe et al., (1983), Panet and Guenot (1982), Swoboda (1979)]. Furthermore, 2-D FE simulation cannot recognize the different tunneling techniques such as NATM, open faced or closed faced shield. Since tunnel simulation is idealized as a plane strain condition, the response of soil in the longitudinal direction cannot be predicted.

GROUND SETTLEMENT IN TRENCHLESS CONSTRUCTION PROJECTS

To evaluate the risks of excessive settlements that could damage roadways, utilities, or other features it is important to conduct a thorough geotechnical investigation and document ground conditions and behavior.it is very important to understand the fundamentals of soil- structure interactions (as discussed in Chapter 2) in trenchless technology. It is also critical to identify any existing surface and subsurface features that could be damaged by settlement. Once the key facilities that must be protected have been identified, the next step is to determine the maximum allowable settlement for each feature. Put simply, the maximum allowable settlement should be below that which would cause

damage to the feature (Wallin, 2008). Suggested Allowable Settlements of Site Features are summarized in Table 3-4.

Table 3-4 Maximum Allowable Settlements for Various Site Features (Wallin et al., 2008)

Site Feature	Allowable Settlement, mm (in.)
Underground Utilities	25.4 (1)
Surface Streets	12.7 (0.5) - 25.4 (1)
State Highways and Interstate Highways	6.4 (0.25) - 12.7 (0.5)
Lined Canal Bottoms	6.4 (0.25) - 12.7 (0.5)
Levee Crests	12.7 (0.5) - 25.4 (1)
Railroads	6.4 (0.25) - 12.7 (0.5)

Settlements in trenchless construction projects can be evaluated using a method developed by Bennett (1998). Bennett's model assumes systematic settlements as an inverted normal probability curve, or settlement trough with maximum settlements occurring directly above the centerline of the bore, and with settlements decreasing with distance from the bore centerline. It was assumed that the unit volume of the settlement trough is equal to volume of soil lost in due to the bore annulus.

Figure 3-9 shows the schematic settlement estimation for microtunneling. Considering Figure 3-9, maximum settlement at the centerline and volume loss around tunnel in trenchless construction projects can be calculated as follows:

$$\Delta h_{max} = \frac{V_s}{W} \qquad \text{Eq. 3-19}$$

$$V_L = \frac{\pi}{4}(d_b^2 - d_p^2) \qquad \text{Eq. 3-20}$$

$$W = \frac{d_b}{2} + \left(h_c + \frac{d_b}{2}\right).\tan(45 - \frac{\varphi}{2}) \qquad \text{Eq. 3-21}$$

Where;

V_s= Volume of settlement per unit length of excavation,

W= Settlement trough half-width,

V_L= Volume loss around tunnel,

h_c= Depth of clearance above crown of bore,

d_b= Diameter of the bore,

d_p= Diameter of the pipe, and

φ= Friction angle of soil.

It was assumed that the volume of annulus is transferred directly to the surface and is equal to the settlement trough volume, (V_L=V_s).

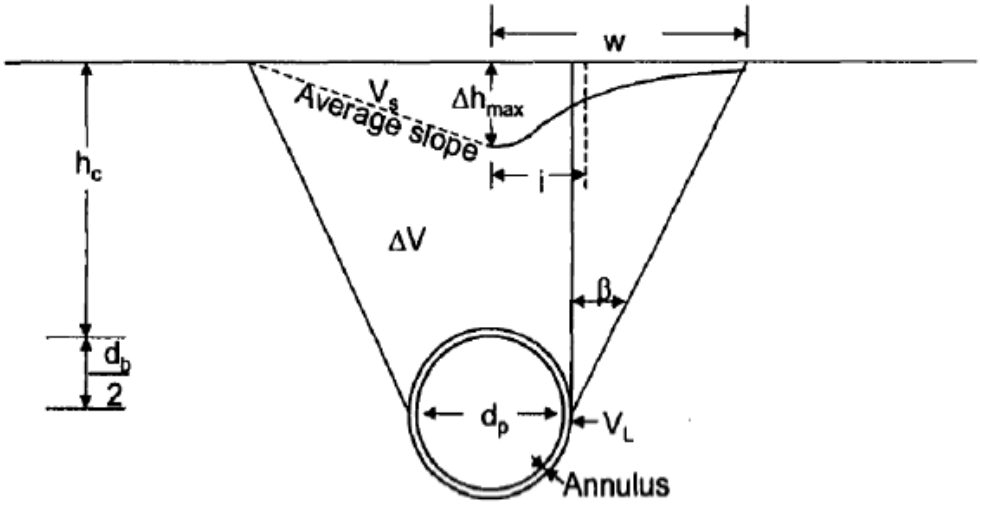

Figure 3-9 Settlements in Trenchless Construction Projects (Bennett, 1998)

Bennett (1998) found that settlements increase with increasing annular volume (e.g., overcut size). On the other hand, settlement decreases with increasing ground clearance from the crown of the pipe. This is because a deeper bore causes the settlement volume to spread out over a larger trough width and decreases the depth of the settlement trough. Figure 3-10 shows the effect of ground clearance on the shape of the settlement

trough and maximum settlement at the centerline of the pipe. However, it should be noted that the enclosed area under both plots are the same.

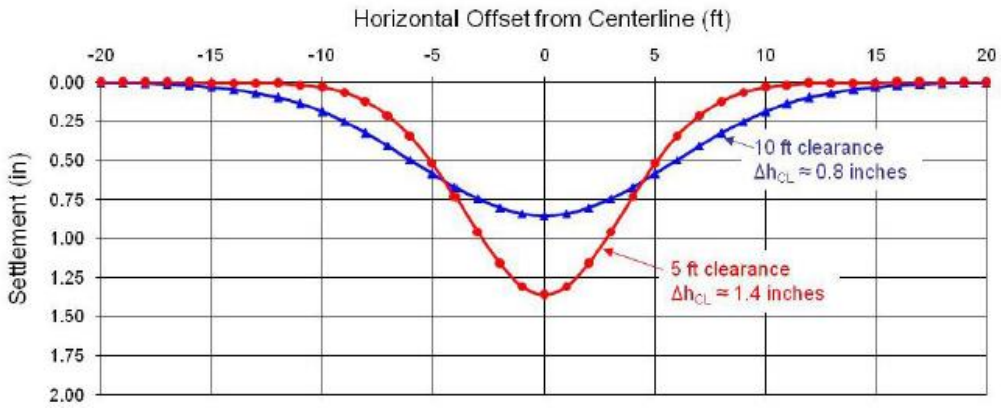

Figure 3-10 Effect of Ground Clearance on Maximum Settlement (Wallin et al., 2008)

As mentioned before, it was assumed that the settlement volume is equal to the annular volume. However, three factors, including soil mass loosening, soil strength (arching), drilling fluid left in the annulus, and cement grouting can affect the percentage of annular volume that contributes to the settlement trough volume. The process of losing soil density and soil dilation is called soil mass loosening, which leads to increased soil volume and, therefore, a decreased volume of the settlement trough at the surface. However, soil mass loosening in very loose soils causes a volume decrease and therefore increases the settlement magnitude at the surface.

Interaction of individual soil particles prevents the soil from collapsing completely onto the pipe and therefore only a percentage of annular space is transferred to the surface. This phenomenon is called soil arching. Arching effect is undermined by seeping ground water toward the bore. In addition, arching effect is reduced as the diameter of the pipe is increased.

Finally, lubrication left inside the annulus and cement grouting can prevent the soil from collapsing onto the pipe and consequently, decrease the maximum surface settlement

(Wallin et al., 2008). Moreover, the proposed equations by Bennett (1998) are for microtunneling only. In addition, other soil properties such as soil unit weight, modulus of elasticity, cohesion were not studied in developing equations.

CHAPTER SUMMARY

This chapter presented a comprehensive literature review on ground settlement induced by underground excavation. Surface, subsurface and horizontal ground settlements are discussed using analytical, empirical and numerical methods. This dissertation uses numerical analysis using FEM and the results are compared with analytical and empirical methods.

Chapter 4 RESEARCH METHODOLOGY AND MODEL VALIDATIONS

INTRODUCTION

This chapter explains the numerical modeling procedure for ground settlement induced by box jacking, pipe jacking and tunneling method.

Chapter 1 discussed the main differences between construction methods. Chapter 2 reviewed the fundamentals of soil structure interaction and the arching effect above different types of the soil and structures. Chapter 3 provided a comprehensive review of ground settlement induced by underground construction. In this chapter, two dimensional (2-D) numerical method is used to analyze ground settlement over a wide variety of projects ranges from medium size to large size for box and pipe installations. In this research, Finite Element Analysis (FEA) using ABAQUS/CAE was used for simulation. This chapter starts with modeling procedure to determine the model size and geometry. A series of sensitivity analysis of models will be carried out to determine exact geometry sizes for different models as well as optimum mesh size and element type. Sensitivity analyzes help reduce the computation cost and time of analyzes Möller (2006).

As discussed in Chapter 3, three calculation methods, namely empirical, analytical, and numerical, are used to analyze settlement associated with underground pipe and box installations. Numerical method is becoming more popular due to its capability to model different types of projects with complicated geometries and conditions. Although tunneling, microtunneling and pipe/box jacking are conceptually different methods of construction, in terms of ground settlements, all methods requires to create an overbreak (overcut) so that pipe is installed safely. This overcut can be the source of ground settlement and calculated from the past case histories. Consequently, construction tolerance and potential ground settlements for these trenchless construction methods are comparable, and in spite of their

major differences, they are able to control ground loss at the face (Pipe Jacking Association, 2017).

Moreover, soil conditions and construction practice are other important parameters affecting the ground settlement. Federal Highway Administration (FHWA, 2009) suggests a relationship between different parameters on ground loss in soft ground tunneling as shown in Table 4-1. Since this research aims to study the effect of ground loss induced by underground construction because of immediate ground settlement, the face loss is assumed to be controlled or soil condition is assumed stable enough to minimize ground loss at the face.

Table 4-1 Relationship between Volumes Loss and Construction Practice and Ground Conditions (FHWA, 2009)

Case	Volume Loss (%)
Good practice in firm ground; tight control of face pressure within closed face machine in slowly raveling or squeezing ground	0.5
Usual practice with closed face machine in slowly raveling or squeezing ground	1
Poor practice with closed face in raveling ground	2
Poor practice with closed face machine in poor (fast raveling) ground	3
Poor practice with little face control in running ground	4 or more

MODELING PROCEDURE AND NUMERICAL ANALYSIS

A lot of numerical methods such as Finite Element Method, Finite Difference Methods, Boundary Element Method and Discrete Element Methods are widely used as the numerical analyzes of tunnels since 1960s (Su, 2015). These methods help engineers to develop a simplified model by generating user-friendly input data and interpreting the

outcome. In the recent years, the rapid developments of the specified software such as ABAQUS and Plaxis have made the numerical analysis easier, faster and more accurate. The real construction stages can be simulated with more realistic and attractive colored results.

However, FEM software have their own shortcomings as well. They still need the user to be well trained and experienced enough to use the software because a simulated model demands a large variety of technical aspects to be applied prior to case history verification. For example, in tunnel design, the basic knowledge of geotechnical and structural engineering might not be enough if one has no or limited software experience. Moreover, the computation cost of the analysis is still high compared to other methods of analysis.

Finite Element Methods are the most applicable numerical method for tunnel design and analysis because a wide range of constitutive models can be applied, and difficult geometry conditions can be drawn. Most commercial and numerical developed software are based on FEA, which makes this method even more attractive.

For modeling purposes, the problem is defined by the domain sketched in Figure 4-1 with a 2-D model in full symmetry with plain strain condition after which a series of sensitivity analyzes were conducted. Soil mass is defined with CPE4I element as a four-node bilinear plane strain quadrilateral, incompatible modes (two Gaussian integration points) and pipe or box (Liner) is defined with B22 element as a 3-node quadratic beam in a plane. CPE4I element avoids shear locking when this element is under bending moment.

Total stress condition using Mohr-Coulomb Constitutive model was selected for the modeling simulation since most of geotechnical spoil properties extracted from case histories were provided in total stress. Mohr-Coulomb criteria is able to model soils with common soil properties such as soil friction angle, cohesion, soil density and modulus of

elasticity. Pipe and box were assumed elastic type material. Since the models are rather small in numbers of elements, it was preferred to use the model in full shape instead of half symmetry for the easier model generation. The full symmetry modeling also removes additional restrained condition applied for liner rotation in the centerline. This condition does not allow the bending moment in the pipe. This sketch is used for a system of reference axes is defined with the origin located at the intersection of the upper line and centerline. The boundary conditions applied to this domain are shown in Figure 4-1.

The vertical and horizontal settlements of the bottom boundary is restricted while only horizontal settlements of the vertical boundaries are restricted. Plain strain is assumed along the Z-plane. It should be noted that this pattern is used for both box and pipe simulation. To optimize the model simulation, a series of sensitivity analyzes were carried out to determine the effects of element shape, mesh size and model dimension as is discussed later in this chapter.

Effect of Model Dimension

The sensitivity analysis was conducted in one of the case studies (Box Jacking Project at Vernon) as an example to determine the model dimension, element type and mesh size. A full project explanation can be found later in this chapter. Meissner (1996), recommended 4-5 times the pipe diameter (D) as the model half width to avoid effect of the vertical boundaries on the surface ground settlement in the shallow tunneling (H/D>1.5) with a depth to axis (H). Möller (2006) recommended Equation 4-1 for the half symmetry model dimension:

$$W = 2D(1 + H/D) \qquad \text{Eq. 4-1}$$

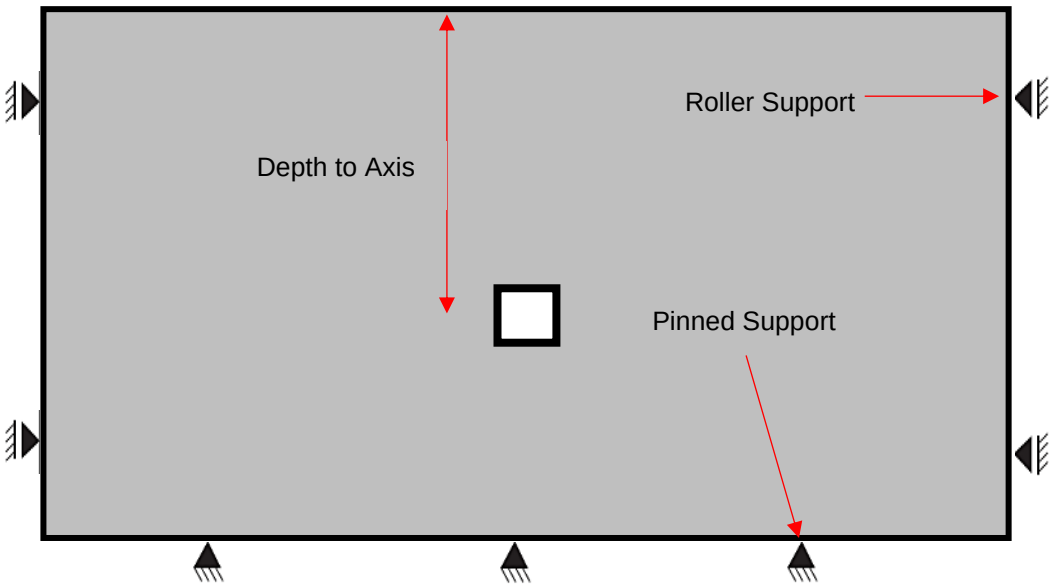

Figure 4-1 General Model Geometry and Boundary Conditions

SENSITIVITY ANALYSIS

Möller (2006) showed that settlement at vertical boundaries should not exceed 1% of the maximum centerline settlement. Mamaqani 2015 showed a relationship between model width (W) and depth to axis (H) in box jacking. He found 7 times the cover depth is the minimum required width in half symmetry models, which had minimum or less effect on the vertical surface settlement. The results shown in Figure 4-2 from sensitivity analysis of Vernon Project have good agreement with the Equation 4-1 as below calculation:

Box Dimension: 1.2×1.8 m

Approximate equivalent pipe dimeter = $2\left(\frac{1.8\times1.2}{\pi}\right)^{0.5}$ = 1.65

W=2×1.65 × (1+7.3/1.65) = 17.9 m

As Figure 4-2 presents, the optimum model dimension for Vernon Project is approximately 20 m, which is close enough to calculation result from Equation 4-1. The

bottom boundary was kept between 2-D and 3-D to reduce the negative effect of boundary condition on results for all models.

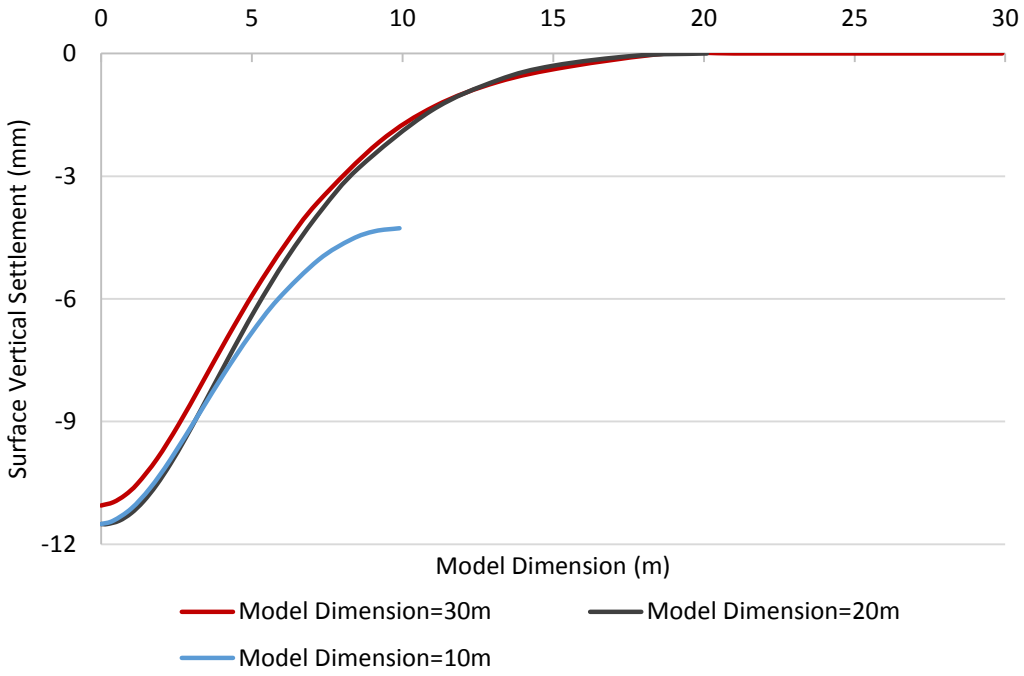

Figure 4-2 Minimum Required Model Dimension

Effect of Mesh Size

A sensitivity analysis was carried out to select the optimum mesh size. Figure 4-3 presents a mesh generation model for box jacking operation. In order to keep the analysis accuracy and reduce the computational cost of the model, mesh sizes gradually doubled from centerline to the boundaries. Different mesh sizes from very coarse to small were tested and the results were compared to the validated results. Figure 4-4 shows comparison of different mesh sizes. It showed medium to small mesh sizes accurately match the ground surface settlement form real life case study. Figure 4-5 also shows the effect of element type on ground surface settlement.

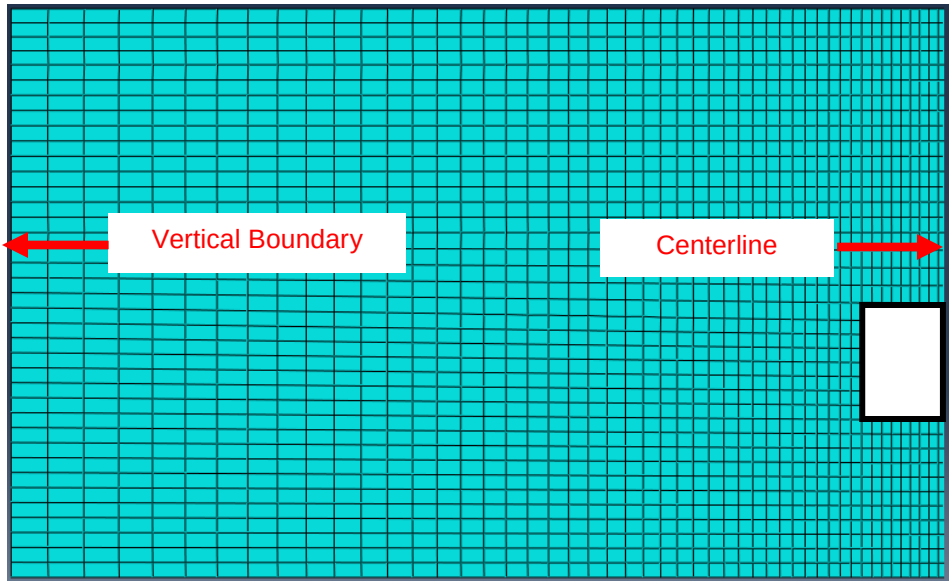

Figure 4-3 Mesh Generation

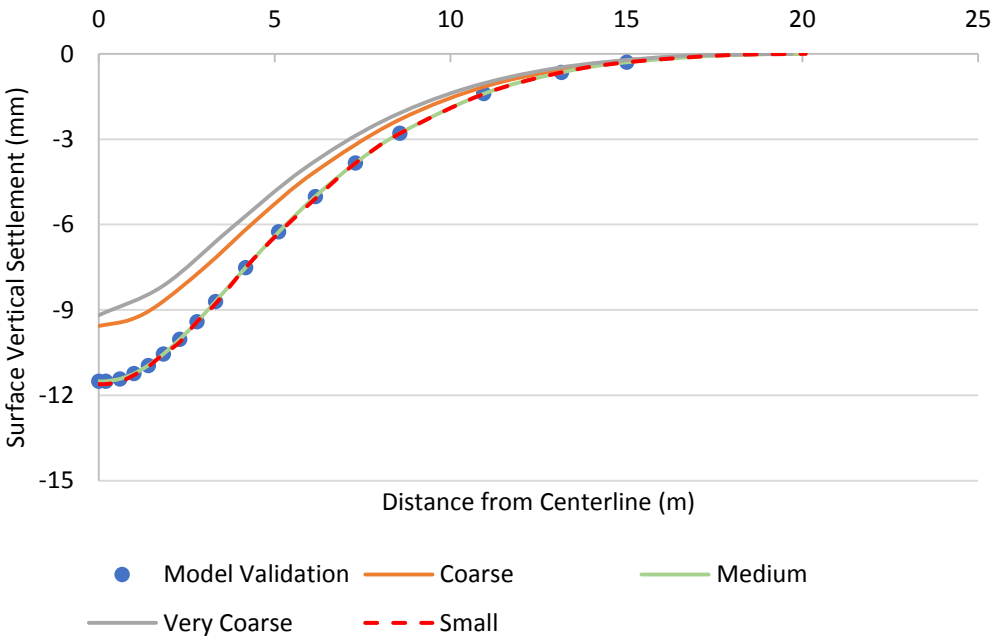

Figure 4-4 Effect of Mesh Size on Vertical Ground Settlement

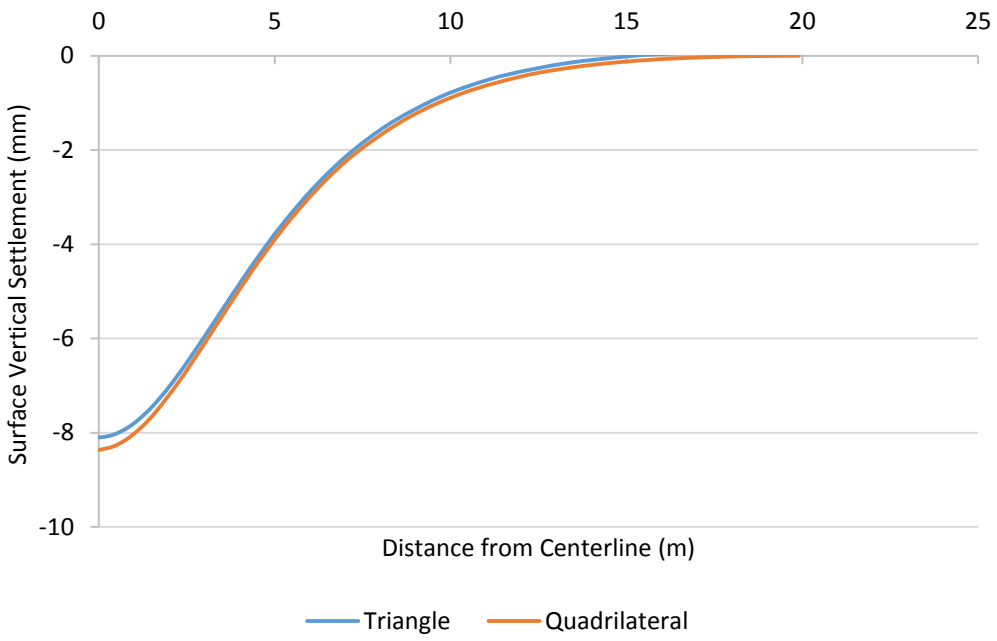

Figure 4-5 Effect of Mesh Size on Vertical Ground Settlement

TWO DIMENSIONAL (2-D) MODELING OF TUNNEL CONSTRUCTION

Construction Methodology and Numerical Modeling Steps

The major ground settlements induced by pipe, box or liner installations are due to soil loss around the installed structure and due to soil deformation at the face. Craig and Muir Wood (1978) showed that the maximum surface ground settlement in the shield tunneling is in association with ground settlement at both face and tail of the shield. The results depending on the ground type is presented in Table 4-2.

In 3-D modeling, the effects of the ground relaxation at the face can be simulated but in 2-D modeling this effect cannot be simulated, which results in inaccurate surface ground settlement prediction. To overcome this deficiency in 2-D modeling, different methods as explained in Chapter 3, such as Progressive Softening Method by Swoboda (1979), Stress Controlled Methods such as Convergence-Confinement Method by Panet

and Guenot (1982), the Gap Method by Rowe et al., (1983), and the Volume Loss Method by Potts & Addenbrooke (1997), are used. Each 2-D method has its own shortcomings and limitations although they are useful and convenient. This is mainly because one parameter needs to be input as a prescribed value in 2-D FE simulation.

Table 4-2 Relationship between Ground Condition and Total Share of Surface Settlement (Craig and Muir Wood, 1978)

Type of Ground	Total share of Surface Settlement at Face of Shield (%)	Total Share of Surface Settlement at Tail of Shield (%)
Stiff Clay	30 – 60	50 – 75
Soft Clay	0 – 25	30 – 55
Saturated Sand	0 – 25	50 – 75
Unsaturated Sand	30 – 50	60 – 80

The method used for this dissertation was load-reduction method or Beta (β) method based on confined-convergence method. A brief description of tunneling process in both pipe (liner) or box installation as shown in Figure 4-6 is as below:

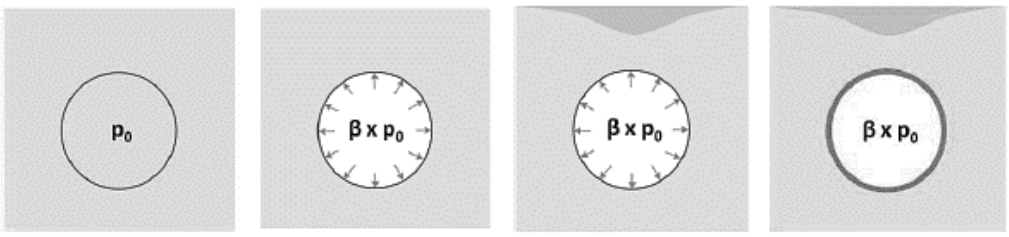

(a) (b) (c) (d)

Figure 4-6 2-D Tunnel Construction Based on Load Reduction Method (Su, 2015)

1. In the first stage, a model was generated considering there is a gap equivalent to volume loss between excavation part and liner (Figure 4-7).

2. In the next stage, the initial stress was generated due to soil weight while the soil was not excavated and the pipe (Liner) was not activated (Figure 4-8 and Figure 4-9).
3. Tunnel excavation was simulated but a boundary condition in X and Y direction was applied around the tunnel periphery to avoid any soil settlement. In this step the loads in each node inside the excavated region was read and then applied to the same node at the opposite direction. This load was the basis for the load reduction analysis. The boundary condition was lifted after the loads were applied in the next steps.

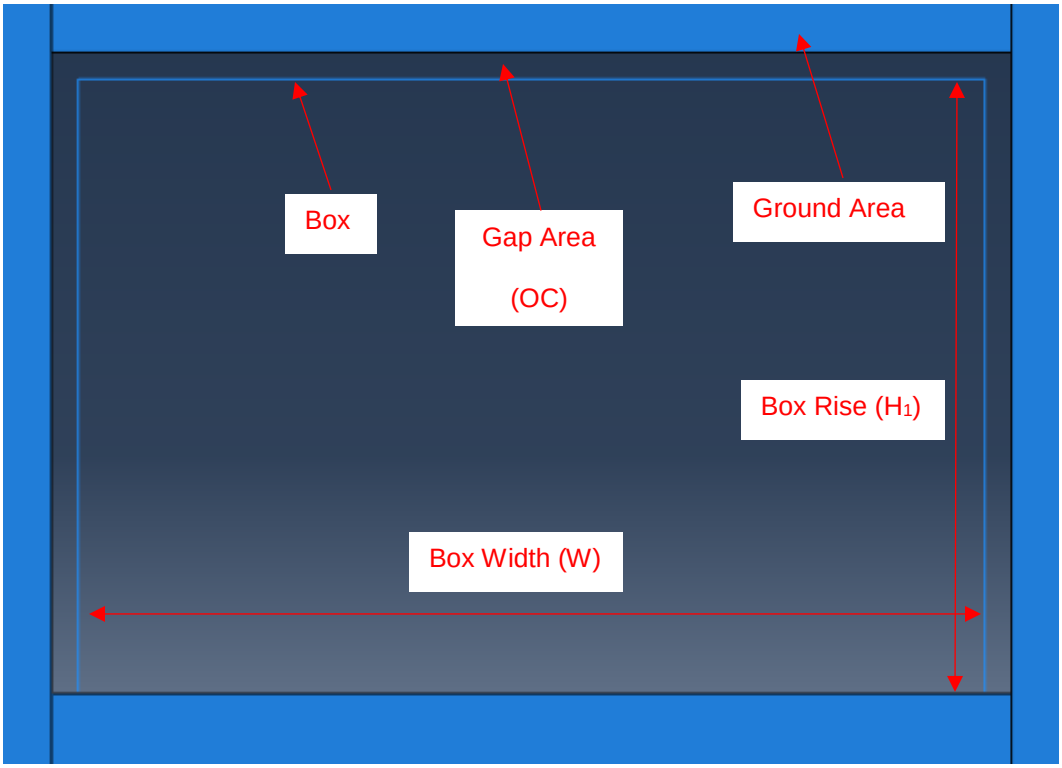

Figure 4-7 Model Generation in the Excavated Area

4. The initial load is reduced by a β factor, which is between 0 and 1. This factor is gradually reduced in two or three steps and the liner is activated when the

predetermined volume loss achieved. The reduction value is based on type of the excavation, ground type and past construction experience. In most box jacking projects, which the hand mining or roadheader are the major excavators, the excavation time is higher than the TBM or Micro TBM excavation, so the soil has more time to be relaxed and the β value is higher than that of pipe installation. In this study, non-uniform load distribution around the pipe or box was used to reflect the real time case histories.

5. The box deflection was controlled to an allowable minimum slab thickness of 1/12 the span as per American Association of State Highway and Transportation (AASHTO) LRFD Bridge Design Specifications.

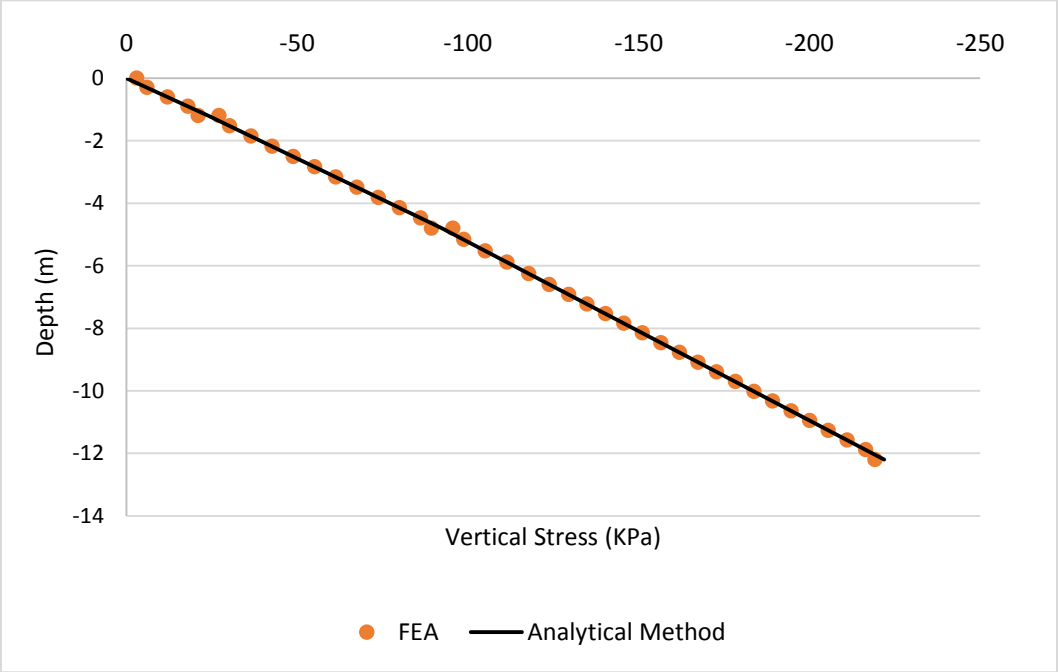

Figure 4-8 Vertical Stress Verification (Vernon Project)

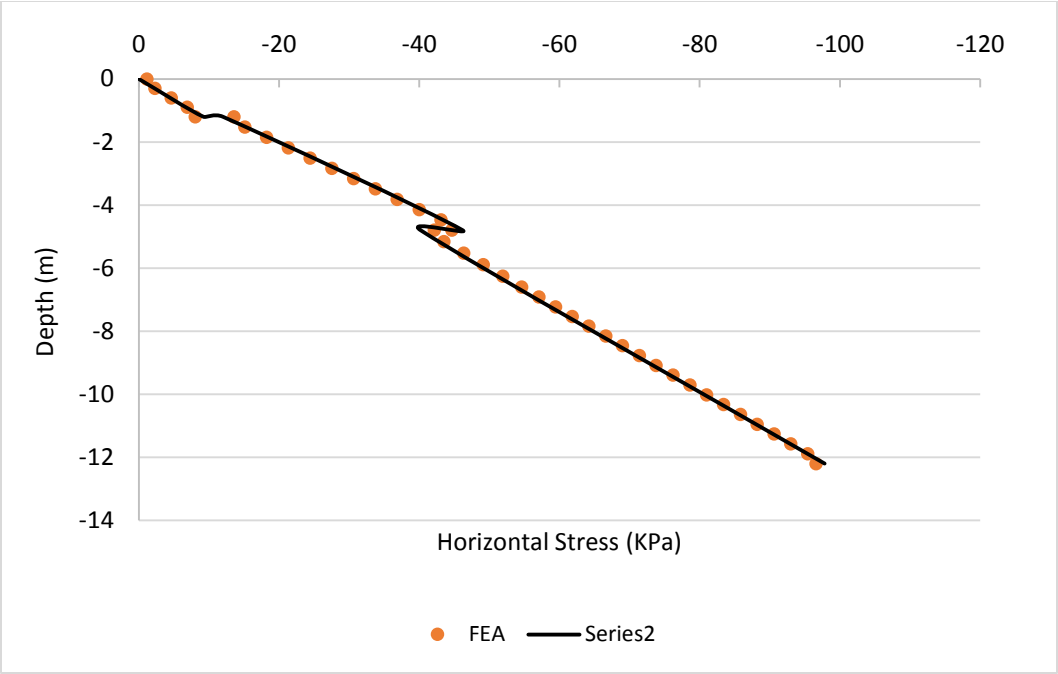

Figure 4-9 Horizontal Stress Verification (Vernon Project)

One of the main problems in 2-D FE modelling of ground settlement induced by tunnel construction is the high invert heave as the soil at the invert of the pipe is deformed vertically as the load is reduced. Past FEM studies used uniform load distribution around the pipe as shown in Figure 4-10. However, this resulted in high invert heave up to 40% of crown settlement and thus less surface ground settlement than expected (Cheng, 2003). To apply the non-uniform load (Stress) around tunnel periphery, Su (2015), suggested keeping the full initial pressure at the tunnel invert to avoid excessive heave settlement. In this research, a portion of initial load at the tunnel invert is kept constant in order to reach the determined volume loss. However, further studies show the amount of pressure to be kept at the tunnel invert depends on soil condition and horizontal soil pressure.

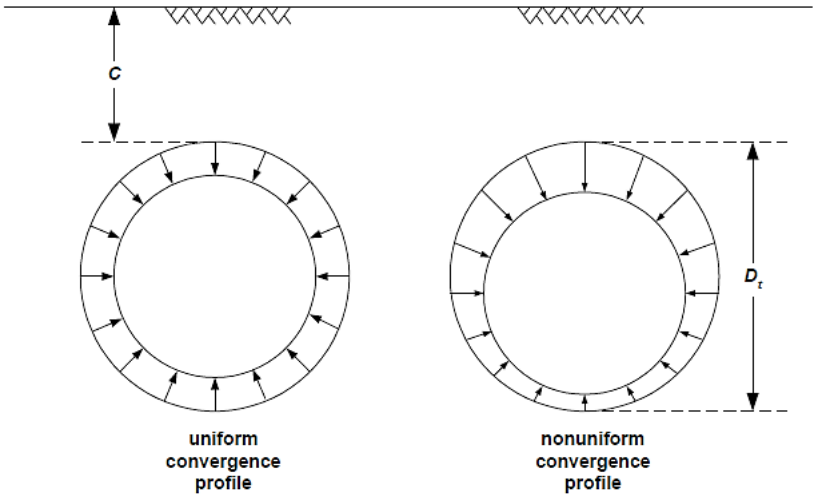

Figure 4-10 Uniform and Nonuniform Convergence around Tunnel (Cheng, 2003)

REAL LIFE CASE HISTORIES

This section introduces two box jacking projects, one pipe jacking project and five tunneling projects as the real-life case histories. The reason for these projects is that they have been implemented in a wide variety of soil conditions, different depths, different soil layers and different sizes. The model for each case study is validated and data is compared to pipe or box at the same geological condition in Chapter 5.

Box Jacking Projects

TxDOT Project at Vernon (Deep Installation)

The location chosen for TxDOT Project was in the City of Vernon, northwest of Wichita Falls, Texas, under US Highway 287 (Figure 4-11). The purpose of this project was to alleviate the flood problem on the upstream side of the highway facility. Prior to construction, there were three rows of 1.83 m (6 ft) wide by 1.22 m (4 ft) high drainage boxes that were undersized and thus provided a reduced capacity to transport the water under the highway due to increased flow from local business and residential improvements.

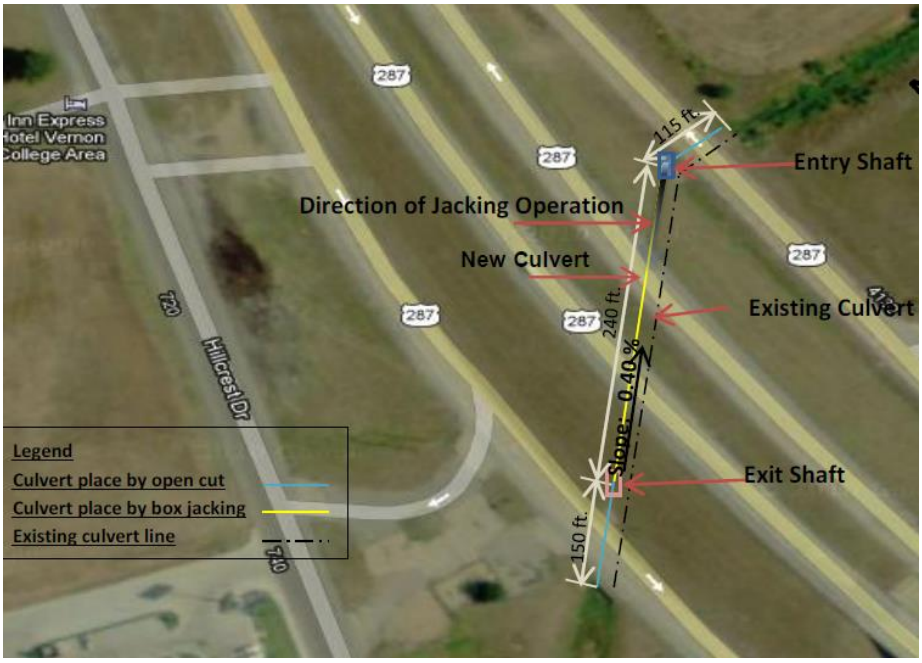

Figure 4-11 Layout of the Vernon Box Jacking Project on US 287 (Najafi, 2013)

TxDOT's Wichita Falls District decided to install a 1.83-m (6-ft) by 1.22-m (4-ft) box by jacking method adjacent to the existing ones to improve the channel capacity. The box jacking alignment traversed under the exiting roadway and embankment of a four-lane highway and two frontage roads. The box was designed to be in accordance with TxDOT's 2004 Standard Specifications Item 476. Prefabricated reinforced concrete box segments were checked for conformance with approved submittal and relevant standards upon arrival to the jobsite (Najafi, 2013). The project was a deep installation as the ratio of the depth to equivalent diameter is greater than 3 as shown in Table 4-3.

Table 4-3 Box Dimension at Vernon Project

Box Dimension (W × H_1) m (ft)	Equivalent Diameter m (ft)	H/D	H/W
1.8 × 1.2 (6×4)	1.65 (5.4)	4.4	4.0

Box Jacking (BJ) Operation

Before starting the jacking operation, the contractor made two reinforced concrete columns and a reinforced concrete wall behind the launch shaft to stabilize the existing soil and prevent soil settlement during the jacking operation. Then the launch shaft was excavated, and jacks were placed. The size of the launch shaft was 5.2 m x 3.96 m (17 ft x 13 ft) with a 3.66 m (12 ft) depth (Mamaqani, 2014). Figures 4-12 and 4-13 show the shaft location before and after construction.

Figure 4-12 Entry Shaft Preparation (Najafi, 2013)

The geotechnical investigation included drilling and sampling three borings (B-1, B-2 and B-3) at distances of 7.62 m, 15.24 m, and 6 m (25 ft, 50 ft and 20 ft) respectively as shown in Figure 4-14. Table 4-4, 4-5 and 4-6 represent the results from soil classification, confined compressive strength and soil properties for each borehole. The result of sieve analysis as shown in Table 4-4 shows the site in a sand-dominant ground with minor mixtures of silt and gravel.

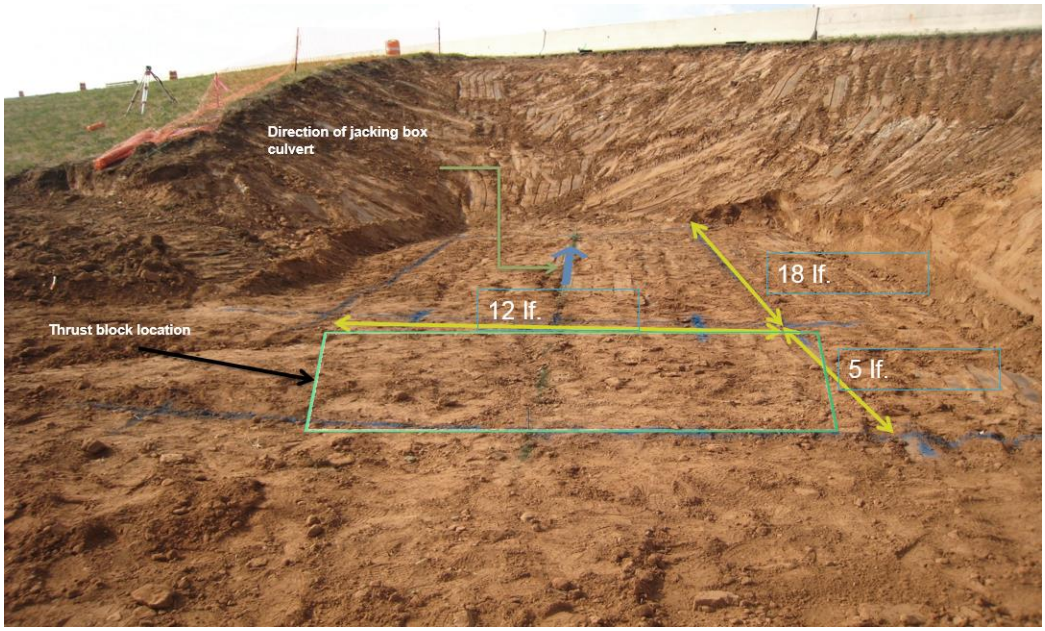

Figure 4-13 Entry Shaft Preparation (Najafi, 2013)

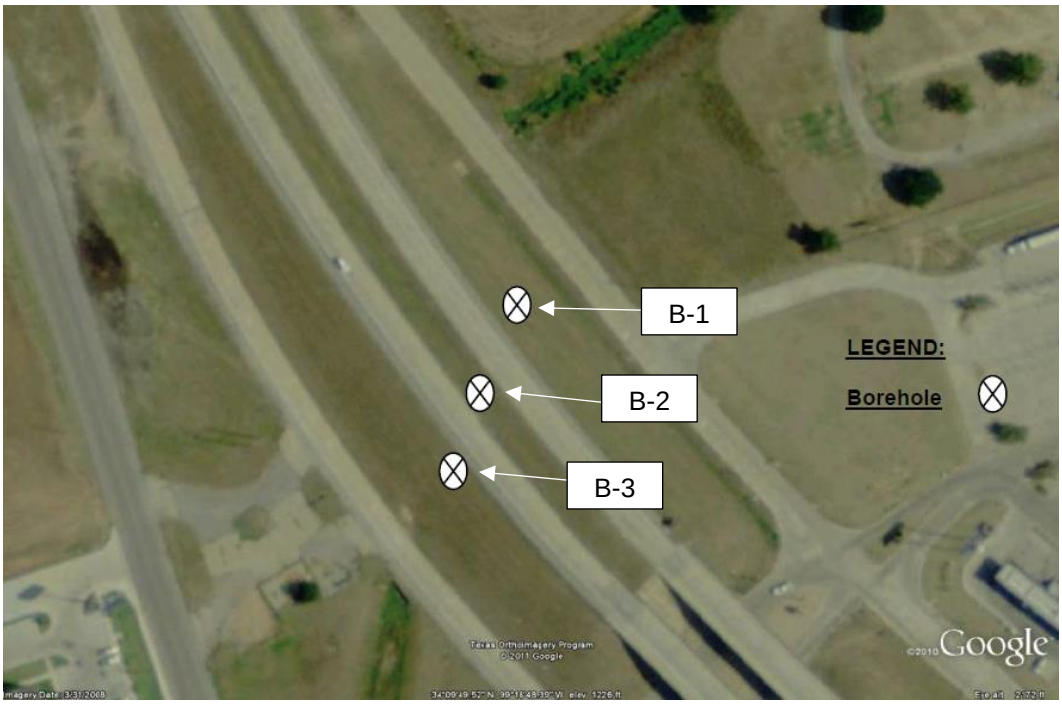

Figure 4-14 Borehole Locations at Vernon Project (Mamaqani, 2014)

Table 4-4 Sieve Analysis Results for Vernon Project (Najafi, 2013)

Sample ID	Soil Depth, m (ft)	Soil Gradation %				USCS Classification	
		Gravel	Sand	Silt	Clay	Group Name	Group Symbol
B1	0.15-1.2 (0.5-4)	0	53	47	0	Silty Sand	SM
	1.5-1.98 (5-6.5)	0	43	56	2	Sandy Silt	ML
	5.6-6.1 (18.5-20)	0	94	5	0	Poorly Graded Sand	SP
B2	0.76-1.2 (2.5-4)	0	40	49	11	Sandy Lean Clay	CL
	1.5-2 (5.0-6.5)	0	72	26	2	Silty Sand	SM
	2.6-3 (8.5-10)	0	90	10	0	Poorly Graded Sand with Silt	SP-SM
	10.2-10.7 (33.5-35)	5	75	19	1	Silty Sand	SM
	13.2-13.7 (43.5-45)	9	73	17	1	Silty Sand	SM
	14.8-15.2 (48.5-50)	18	62	19	1	Silty Sand with Gravel	SM
B3	0.15-0.6 (0.5-2.0)	19	60	20	1	Silty Sand with Gravel	SM
	0.76-1.2 (2.5-4)	0	66	33	1	Silty Sand	SM
	5.6-6.1 (18.5-20)	0	70	28	2	Silty Sand	SM

Table 4-5 UCS Test Results for Vernon Project

Sample ID	Soil Depth, m (ft)	Unconfined Compressive Strength (qu), kPa (psi)	Undrained Cohesion (cu), kPa (psi)
B1	2.4-3 (8.0-10)	121.7 (17.6)	61 (8.8)
	3.9-4.6 (13-15)	135.5 (19.6)	68 (9.8)
B2	1.5-2.1 (5-7)	89.5 (13)	45 (6.5)
	2.4-3 (8-10)	87.5 (12.7)	44 (6.4)
	4.1-4.6 (13.5-15)	100 (14.5)	50 (7.3)
	5.6-6.1 (18.5-20)	114 (16.5)	57 (8.3)
	7.2-7.6 (23.5-25)	260 (37.7)	130 (18.9)
	8.5-9.1 (28-30)	86 (12.5)	43 (6.3)

Table 4-6 Soil Properties of Vernon Project

ID	Depth m (ft)	Soil Type	Friction Angle (Degree)	Modulus of Elasticity, MPa (psi)	Unit Weight, kN/m^3 (lb/ft^3)	Cohesion, kPa (psi)
B1	0-1.2 (0-4)	SM	38	16.8 (2,436)	20 (128)	23 (3.3)
	1.2-4.8 (4-16)	ML	30	80 (11,600)	19 (122)	64 (9.3)
	4.8-12.2 (16-40)	SP	34	19.5 (2,827)	17.5 (112)	2 (0.3)
B2	0-1.2 (0-4)	CL	20	20 (2,900)	20 (128)	45 (6.5)
	1.2-12.2 (4-40)	SM	35	10.8 (1,566)	18 (116)	10 (14.5)
B3	0-12.2 (0-40)	SM	37	13.8 (2,001)	19 (122)	15 (2.2)

Instrumentations

A Total Station TC407 survey instrument was used to measure the existing pavement surface to record settlement and/or heave. Four shoulder points were selected as shown in Figure 4-15 (Points A, B, C and D). For underground settlements, horizontal inclinometer (HI) system was used to monitor settlement and/or heave around the existing and new boxes. The HI employs a force-balanced servo-accelerometer that measures inclination from horizontal (vertical) in the plane of the probe wheels. A change in inclination indicates that movement has occurred. The amount of movement was calculated by finding the difference between the current inclination reading and the initial reading and converting the result to a vertical distance (Najafi, 2013). This system consisted of inclinometer casings, a horizontal probe, control cable, and a readout unit. To measure the soil settlement near the box jacking operation, three 3.34 in. (84.8 mm) casings were installed on each side of the highway as shown in Figures 4-16 and 4-17. To place these casings, a Horizontal Directional Drilling (HDD) rig was used (Najafi, 2013).

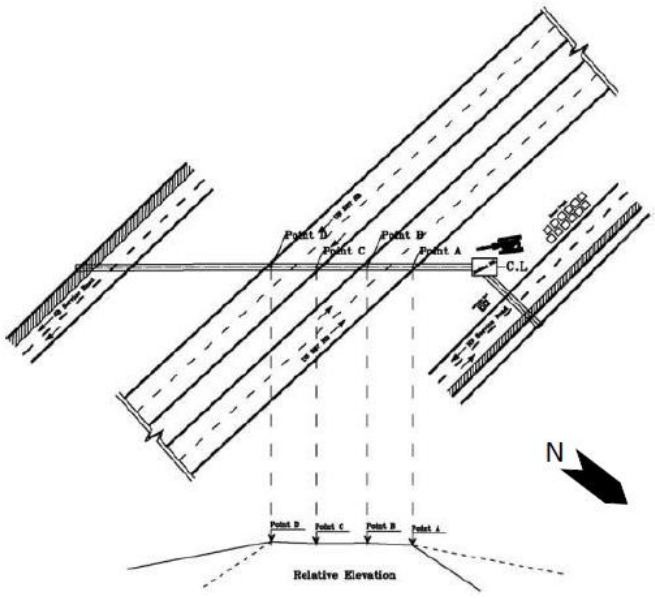

Figure 4-15 Total Station Points

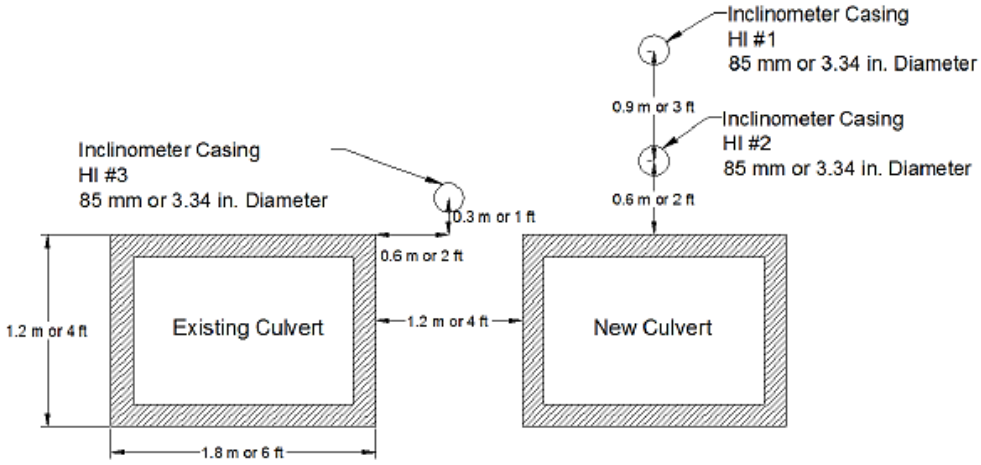

Figure 4-16 Inclinometer Installation Plan North Side (Tavakoli, 2012)

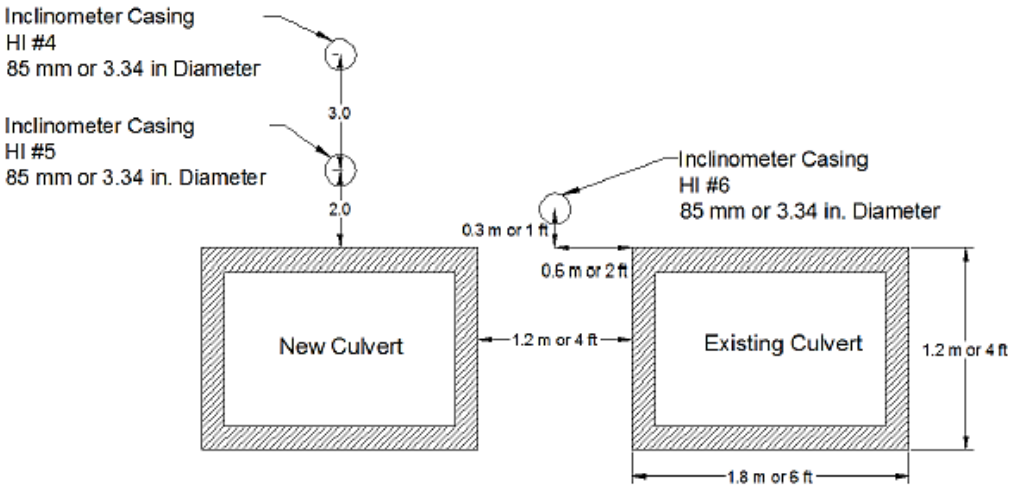

Figure 4-17 Inclinometer Installation Plan South Side (Tavakoli, 2012)

Field Results and FE Validation

Separate analyzes were performed for each case history (B-1, B-2 and B-3) to investigate the effect of different soil layers and depth on surface vertical settlement. The field data presented in Table 4-7 were used for vertical settlements and geotechnical soil properties were obtained from data provided in Table 4-6 for Mohr-Coulomb constitutive

model. An elastic concrete box with unit weight of 25 kN/m^3 (160 lb/ft^3), Poisson's ratio 0.2, Modulus of Elasticity 20 GPa (2.901e+6 psi) and liner thickness was selected 0.15 m (5.9 in.).

Model validation was conducted for all three locations (North, Middle and South sides) as shown in Figures 4-18 through 4-20 there are good agreements between field data and Finite Element Modeling results. As shown in Figure 4-21, there is no heave at the box invert even when all invert loads were lifted. This is mostly because less soil settlements occurs in the sand in the box invert to compensate vertical soil settlement. There were two surface ground settlements from Middle side (B-2) and the average surface was selected as the representative of the surface site settlement. In South Side (B-3) but there was almost large difference in the FEM result with the second point at the depth of 5 m (16.5 ft) from the ground surface. That was because the inclinometer reading was not functioning well or for some reasons the connection to data logger was disrupted (Mamaqani, 2014).

Table 4-7 Field Measurements Results (Najafi, 2013)

Location	Point	Vertical Settlements mm (in.)
North Side (B-1)	Surface	-10 (-0.4)
	HI #1	- 13.2 (-0.5)
	HI #2	-27.6 (-1.1)
Middle (B-2)	Surface (Point B)	-10 (-0.4)
	Surface (Point C)	-7 (-0.3)
South Side (B-3)	Surface	-8.5 (-0.3)
	HI #4	-8.9 (-0.4)
	HI #5	-20.1 (-0.8)

The overcut around box crown and both vertical sides was 50 mm (1.96 in) but as can be seen the maximum soil settlement in FEM is slightly higher than the field data. This is probably due to injecting bentonite slurry during the project execution. Bentonite slurry is injected into the annular space to reduce the friction force between the box and surrounding soils. However, the pressure of the slurry can prevent the soil from fully collapsing into the annular space and consequently reduce associated ground settlements.

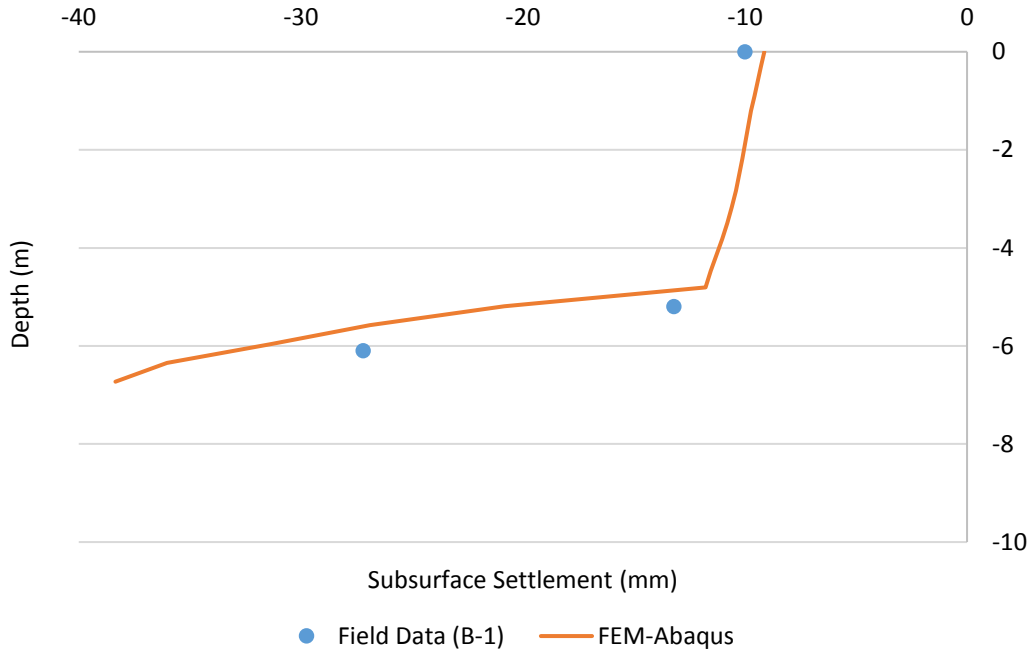

Figure 4-18 Model Validation Based on Field Data

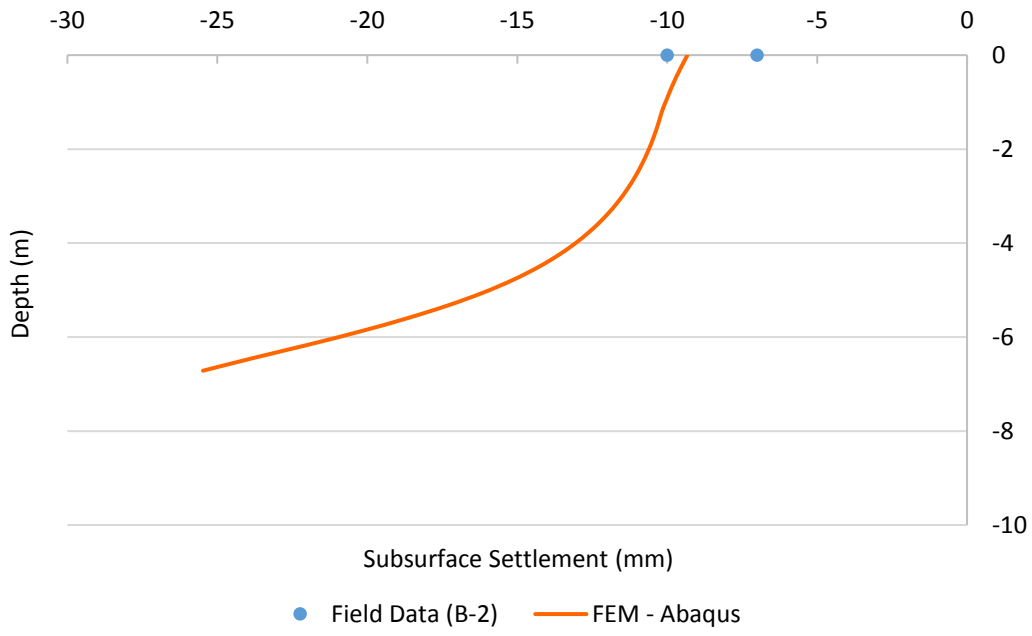

Figure 4-19 Model Validation Based on Field Data

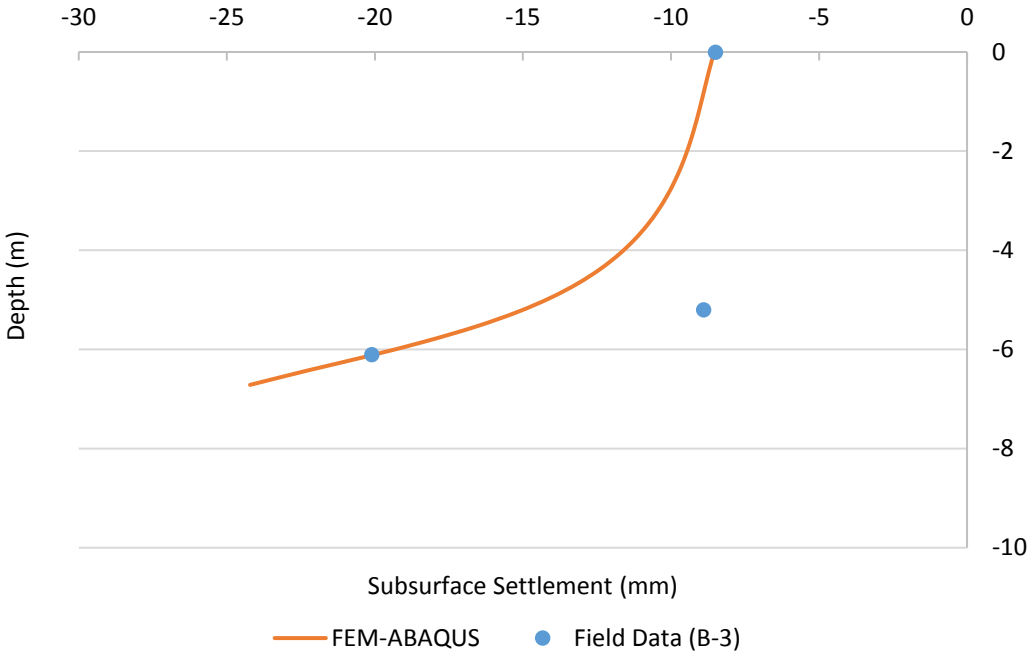

Figure 4-20 Model Validation Based on Field Data

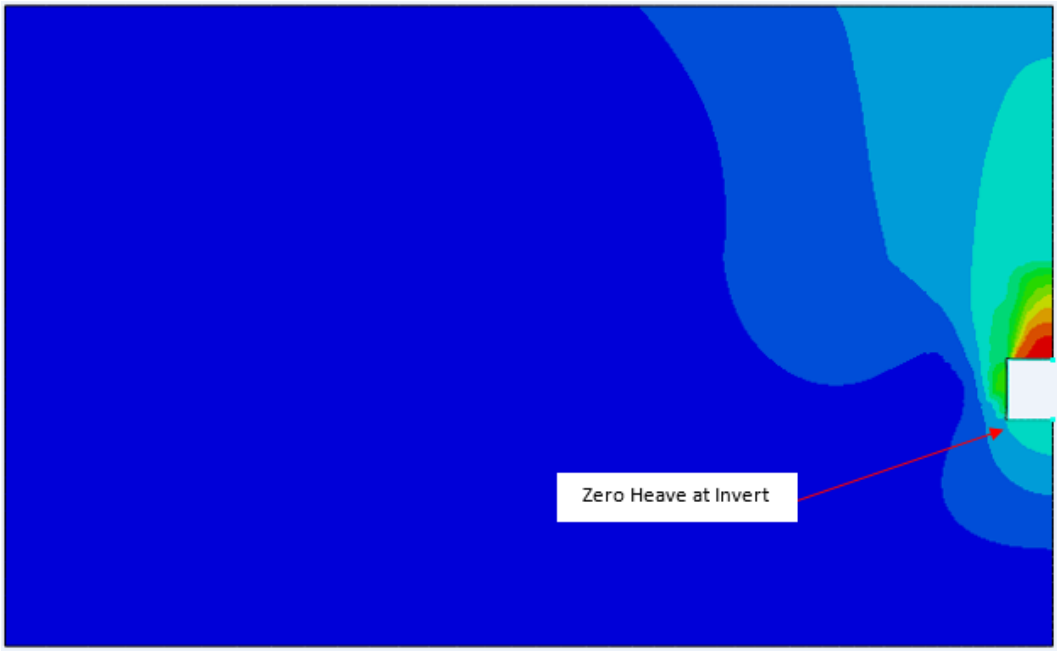

Figure 4-21 FE Analysis of Ground Settlement at North Side (B-1)

Navarro County Project (Shallow Installation)

The purpose for shallow box jacked implementation project at Navarro County, TX was to install a 2.7 m x 1.2 m (9 ft x 4 ft) box under an existing railroad. The cover depth (C) was 1.8 m (6 ft) and hand mining was used to excavate the shallow soil above the crown. The average overcut was 50 mm (1.98 in.). Figure 4-22 presents a schematic cross-sectional view of the box at Navarro County project.

Mamaqani, 2013 reported the soil properties as poorly graded sand with clay and gravel based on a relationship between SPT number and soil property as shown in Table 4-8 fifteen surface control points (five sets) were selected and monitored by the total station parallel to the railroad at 1.2 m (4 ft) intervals (Figure 4-23).

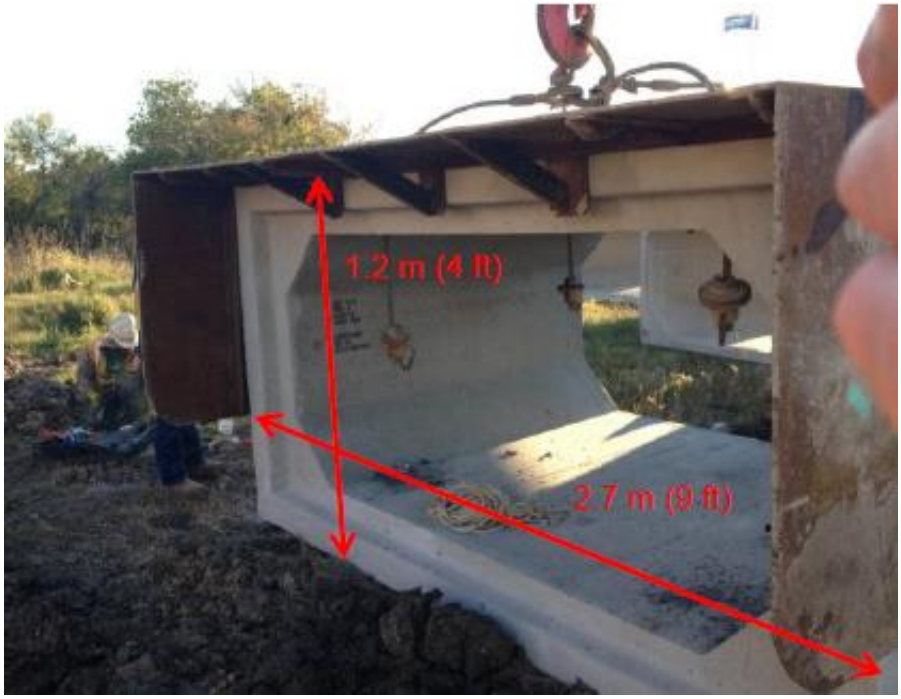

Figure 4-22 Cross Section View of the Box at Navarro County Project (Mamaqani, 2014)

Table 4-8 Soil Properties of Navarro Project

Depth m (ft)	USCS Symbol	N-Value	Friction Angle, (°)	Unit Weight kN/m^3 (lb/ft^3)	Modulus of Elasticity MPa (psi)	Cohesion kPa (psi)
0-1.2 (0-4)	SC-SM	26	34.5	17.6 (112)	13.12 (1,902)	7 (1)
1.2-2.4 (4-8)		10	32	16 (102)	8 (1,160)	7 (1)
2.4-4.3 (8-14)		45	37	19.5 (124)	19.2 (2,784)	10 (1.45)

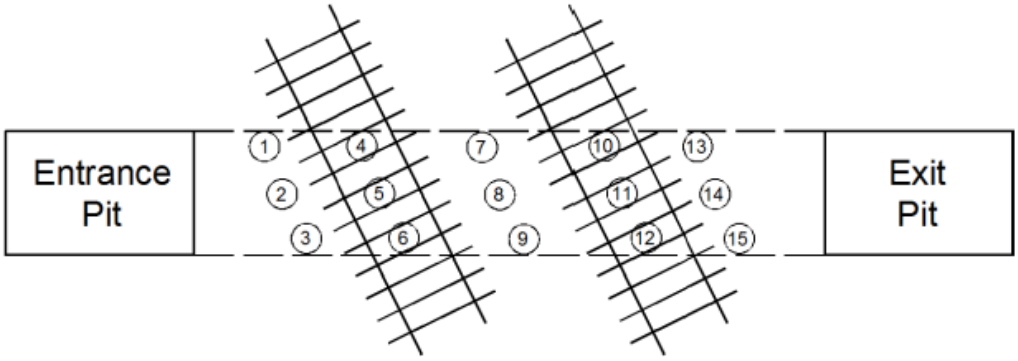

Figure 4-23 Location of Control Points

The results from surface ground settlements for each set is summarized in Table 4-9. The average value of surface vertical settlement at control points were considered as a representative value for finite element analysis as shown in Figure 4-24. Load at the invert was lifted in three consecutive steps and little or no heave occurred at the excavated zone (Figure 4-25).

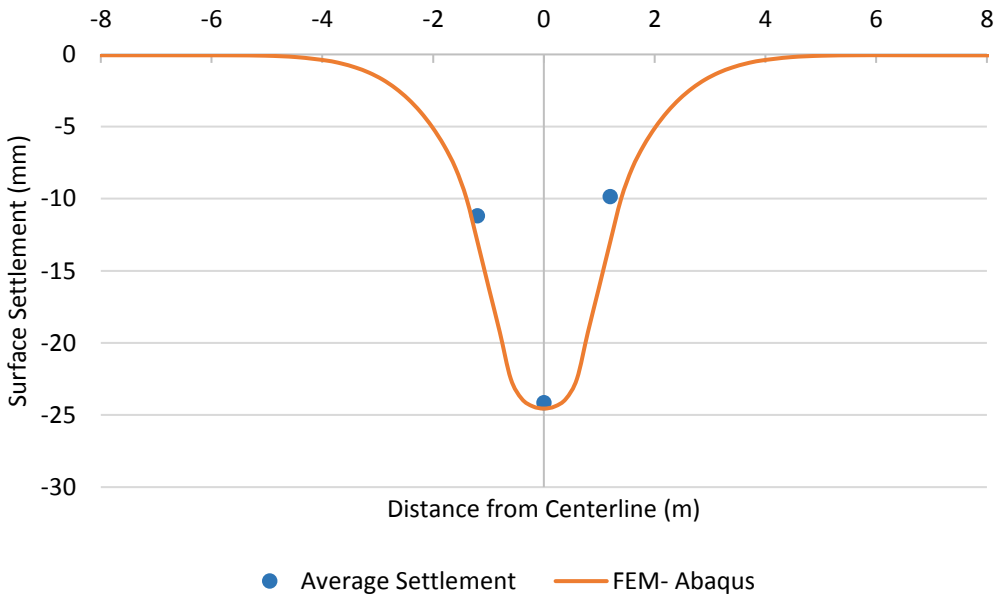

Figure 4-24 Model Validation Based on Field Data at Navarro County Project

Table 4-9 Surface Vertical settlement in Navarro County Project (Mamaqani, 2014)

Distance from Centerline m (ft)	Point #	Vertical Settlement mm (in.)	Average Vertical Settlement mm (in.)
-1.2 (-3.3)	1	-11.2 (-0.44)	-11.2 (-0.44)
	4	-9.3 (-0.36)	
	7	-12.1 (-0.48)	
	10	-11.3 (-0.44)	
	13	-12.1 (-0.48)	
0	2	-24.5 (-0.96)	-24.16 (-0.97)
	5	-23.4 (-0.92)	
	8	-30.2 (-1.19)	
	11	-20.3 (-0.8)	
	14	-22.4 (-0.88)	
1.2 (3.3)	3	-9.5 (-0.37)	-9.86 (-0.39)
	6	-10.2 (-0.4)	
	9	-9.4 (-0.37)	
	12	-10.8 (-0.43)	
	15	-9.4 (-0.37)	

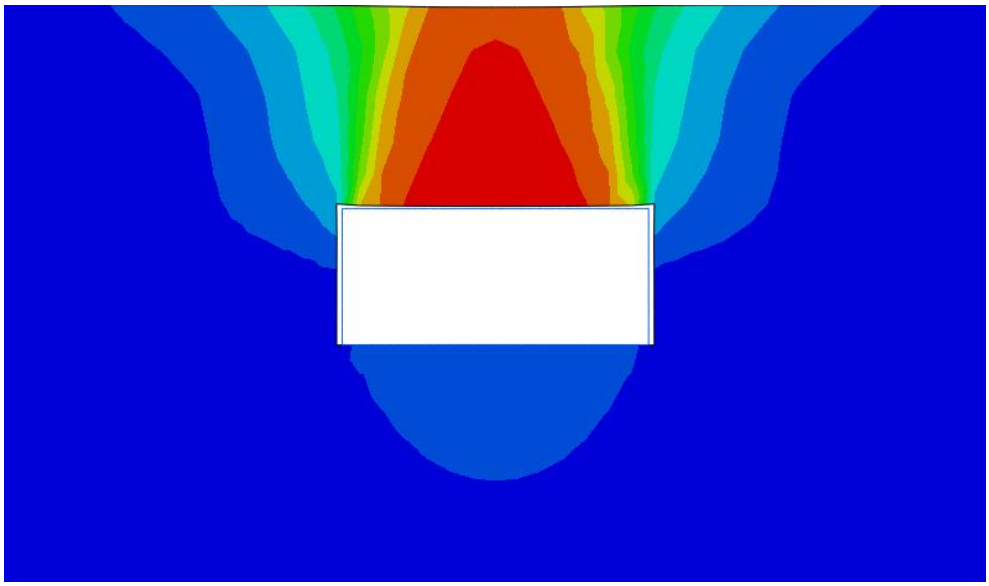

Figure 4-25 FE Analysis of Ground Settlement at Navarro County Project

PIPE JACKING PROJECT

Marshall, 1998, studied the effects of construction related factors such as lubrication, Pipeline alignment, operation stoppage and ground condition on jacking load by four experimental pipe jacking projects. He categorized the projects into four different projects for different site conditions. One of his research objectives was to monitor the ground response by measuring settlements around the tunnel and ground pressures above and perpendicular to the intended line. Ground conditions included a wide range of soils from highly plastic London clay to sand and gravel. Three inclinometer access tubes with settlement magnets and an array of road nails measured the ground settlement. Push-in pressure cells were installed close to the line of the tunnel to record changes in ground stresses close to the tunnel (Marshall, 1998). Three project specifications are provided in Table 4-10, model validation will be carried out and the results will be reported in the next section.

They assumed the ground loss at the tunnel face was negligible because the face was constantly supported by slurry pressure in microtunneling projects or the excavations are in stiff clay in hand mining excavations. For the relatively small diameters involved, the tunnel faces in stiff clay are highly stable and only very small settlements due to elastic unloading of the ground occurred (Milligan and Marshall, 1995).

Project Number 6

Project number 6 was conducted in Leytonstone, London in 1993. Pipe size was l.5 m (60 in.) internal diameter, 1.8 m (71 in.) outer diameter. Excavation was carried out by hand using pneumatic tools within a simple steerable shield in the highly plastic London clay. This comprised five boreholes to depths of 5 m to 12 m along the centerline of proposed tunnels. Representative disturbed and undisturbed samples were taken at regular intervals or at changes of stratum. Relatively unweathered highly plastic London

clay composed of stiff grey fissured silty clay with sandy laminations was encountered at depth. The material was classified as essentially firm to stiff, becoming stiff at depth (Marshall, 1998). Soil properties was obtained from Zymnis, (2009), and Wongsaroj, (2005), for finite element simulation as presented in Table 4-11. The model validation along with ground settlement prediction by Gaussian method are provided in Figure 4-27. As shown in Figure 4-27, both empirical and numerical curves show higher values than measured values for both 8 and 35 days measured settlements.

The outside pipe diameter was 1.8 m (5.9 ft) while excavated tunnel diameter was 1.83 m (6 ft). This gave an approximate volume loss equal to 3.36%, which was expected to show the similar settlement volume. The H/D ratio was 4.7 in clayey soil, which is categorized as deep excavation. The results from FEA shows the maximum ground settlement at the centerline was equal to 8.22 mm (0.32 in.). Using Equation 3-3 for clayey soil condition, the volume of ground loss at the surface would be equal to 3.43%, which shows very good agreements between the field analysis and FEA.

Table 4-10 Projects' Specifications (Marshall, 1998)

Project Number	6
Ground	London Clay
Excavation Method	Hand
Internal Pipe Diameter	1,500 mm (60 in.)
Depth to Axis	8.5 m (28 ft)
Drive Length	75 m (246 ft)
Monitoring Period	Short Term

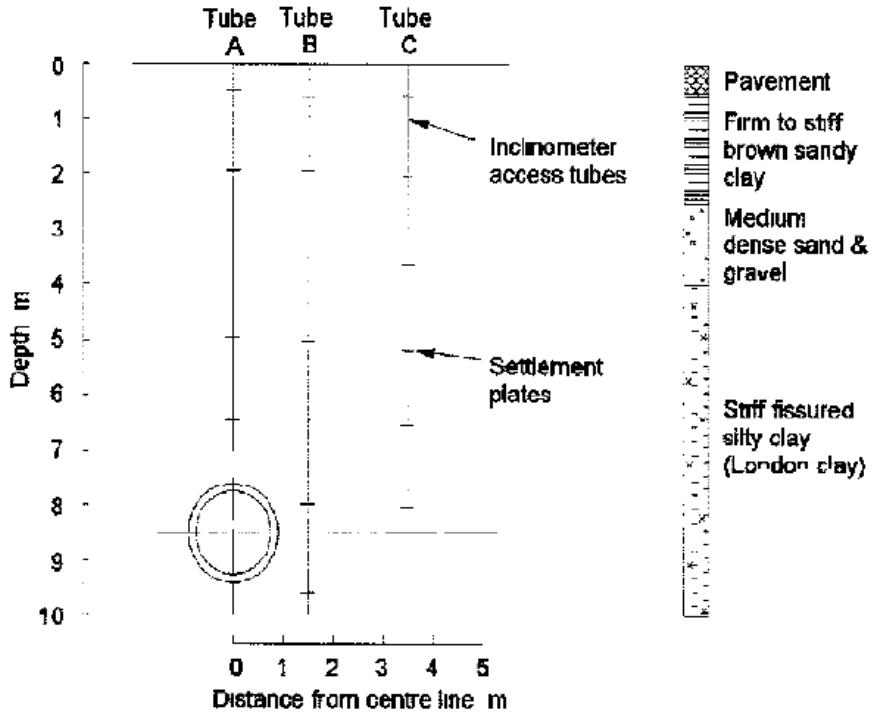

Figure 4-26 Instrument Arrays at Site 6 (Marshall, 1998)

Table 4-11 Soil Properties of Site 6 (Adapted from Zymnis, 2009 and Wongsaroj, 2005)

Depth m (ft)	Friction Angle, (Degree)	Unit Weight kN/m^3 (lb/ft^3)	Modulus of Elasticity MPa (psi)	Coefficient of Earth Pressure at Rest, K_0	Cohesion kPa (psi)
0-2.5 (0-8.2)	25	20 (128)	20 (2,900)	0.58	12 (1.74)
2.5-4 (8.2-13.1)	35	20 (128)	20 (2,900)	0.43	8.0 (1.16)
4-20 (13.1-65.6)	24	20 (128)	30 (4,350)	1.5	10 (1.45)

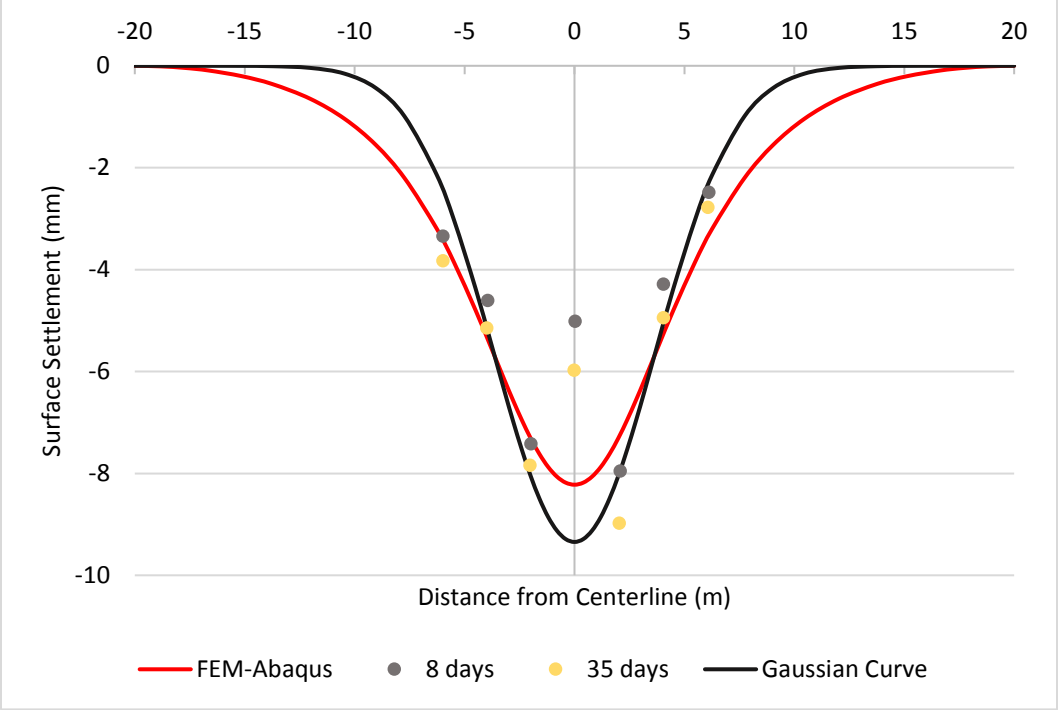

Figure 4-27 Model Validation Based on Field Data at Site 3

TUNNELING METHODS IN CLAYEY SOILS

Case 1: Centrifuge Tests in Stiff Clay

Loganathan et al., (2000), conducted a series of centrifuge tests with a model scale of 1/100 was used, with a nominal centrifuge acceleration of 100 g. The tunnel was assumed to deform in a plane strain condition. Centrifuge Tests aimed to present; (a) details of the centrifuge model setup; (b) measured ground deformations and comparisons with empirical and analytical methods of estimation; and (c) tunneling-induced performance of a single pile and a pile group (Loganathan et al., 2000). Three tests of 6 m (19.7 ft) diameter tunnel with different tunnel depths such as 15 m (49.2 ft) for test 1, 18 m (59.0 ft) for test 2 and 21 m (68.9 ft) for test 3 were studied. The ground settlement analysis was carried out under undrained condition and the volume loss value of 1% was considered for

all tests. Figure 4-28 shows Model validation for surface vertical settlement and Figure 4-29 represents the subsurface ground settlements above the pipe's crown. All geotechnical soil properties were summarized in Table 4-12. The results for surface settlements, subsurface settlements and horizontal movements for Tests 2 and 3 and also additional test at depth 25 m below surface ground are presented in Appendix A. Box with the same cross-sectional area (A=28.3 m^2) and width (W=D=6 m) was modeled. Appendix B presents results for comparison of pipe and box at different depth of installations.

Results for finite element modeling as presented in figure 4-28, shows reasonably good agreement with the Gaussian normal distribution curve and measured data. However, there is an under-predicted value for maximum surface settlement at the tunnel crown and wider values at the far field. The calculated value of volume loss from FEA is 0.9%, which is almost the same as expected. On average, almost 50% of full loads at the pipe invert (25% of tunnel periphery at the bottom) was kept in order to reduce unrealistic heave at the tunnel invert.

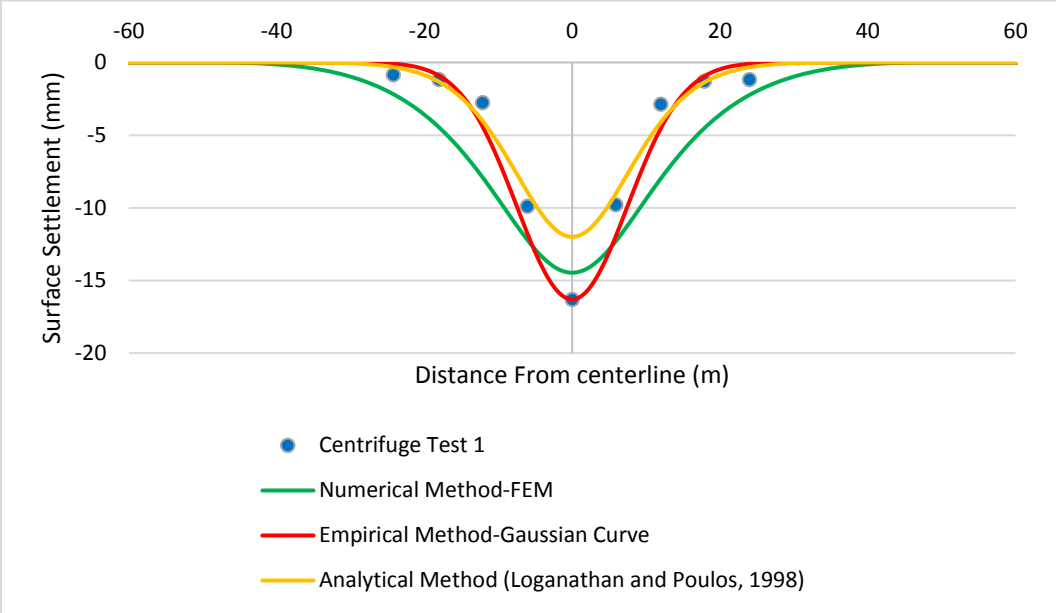

Figure 4-28 Model Validation for Centrifuge Test 1

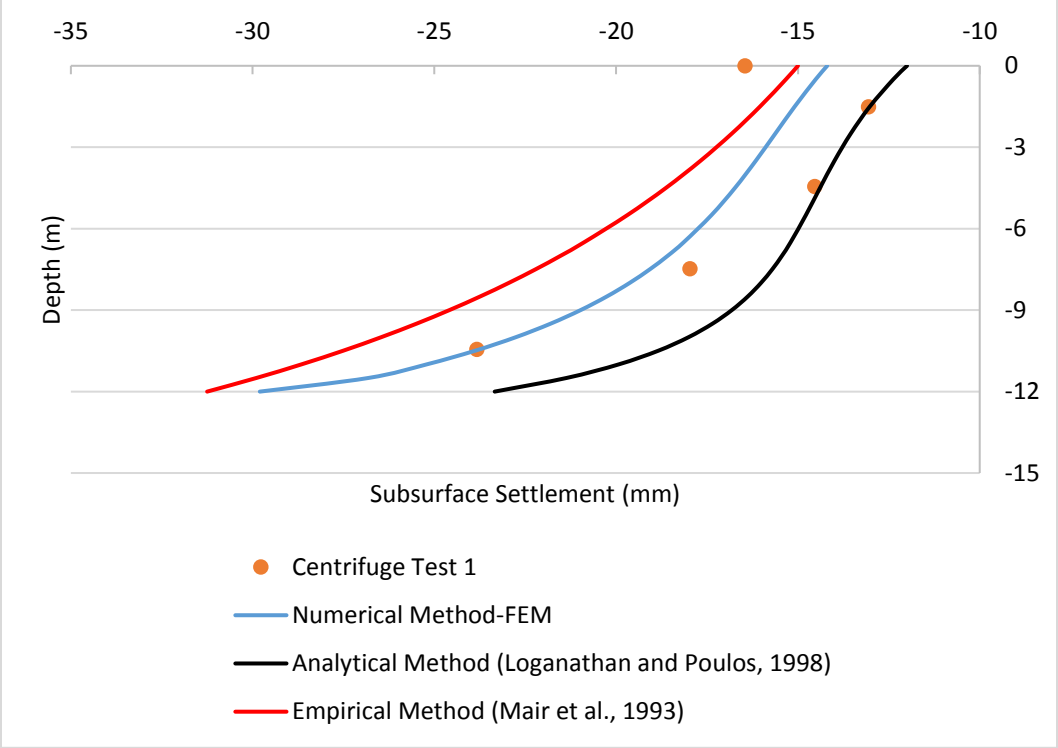

Figure 4-29 Subsurface Settlement above the Crown (Centrifuge Test 1)

Case 2: Centrifuge Test in Soft Clay

Ong (2007) reported the result for a centrifuge test with 60 mm (2.36 ft) diameter of model tunnel (i.e., 6 m (19.7 ft) diameter in prototype scale) under 100 g acceleration. Test was carried out in the Geotechnical Centrifuge Laboratory, National University of Singapore using soft clay condition from a slurry of Malaysian kaolin clay. The tunnel depth to diameter, H/D ratio of 2.5 was considered for the centrifuge test. A green field soil settlement due to tunneling with a volume loss value of 3.3% was examined. Figure 4-30 shows model validation for surface vertical settlement.

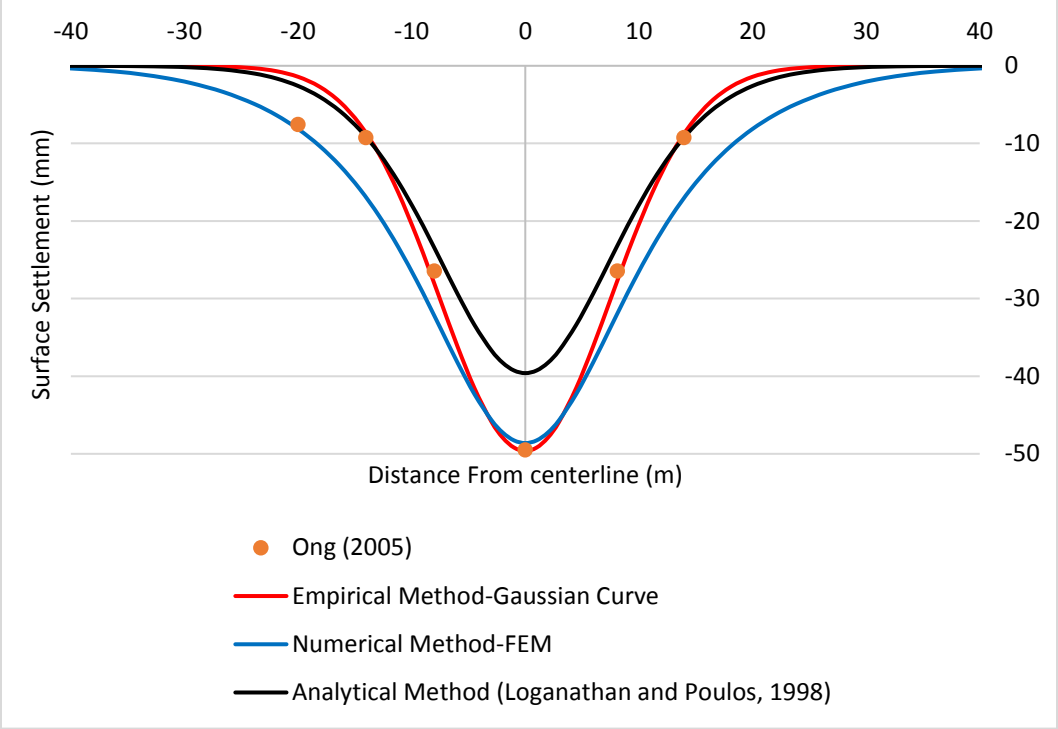

Figure 4-30 Model Validation for Surface Settlement

Case 3: Green Park Tunnel

A tunnel of approximately 4.14 m (13.6 ft) diameter was excavated through stiff fissured heavily over-consolidated London clay to create the Green Park 60 Tunnel at UK [Attewell and Farmer (1974), cited by Loganathan and Poulos (1998)]. The tunnel was excavated manually at 29.4 m (96.5 ft) below ground level. Undrained analysis with volume loss of 1.6% was used for the FE analysis as per recorded field data from the project. Figure 4-31 shows Model validation for surface vertical settlement. Unlike other methods, analytical methods give underestimated surface settlement value for the same volume loss value of 1.6%. Numerical approach shows a well-fitted data at the centerline and wider results at the far field with an estimated volume loss of 2% (25% over estimation). Table 4-12 presents geotechnical soil properties, tunnel geometry and construction method for this project.

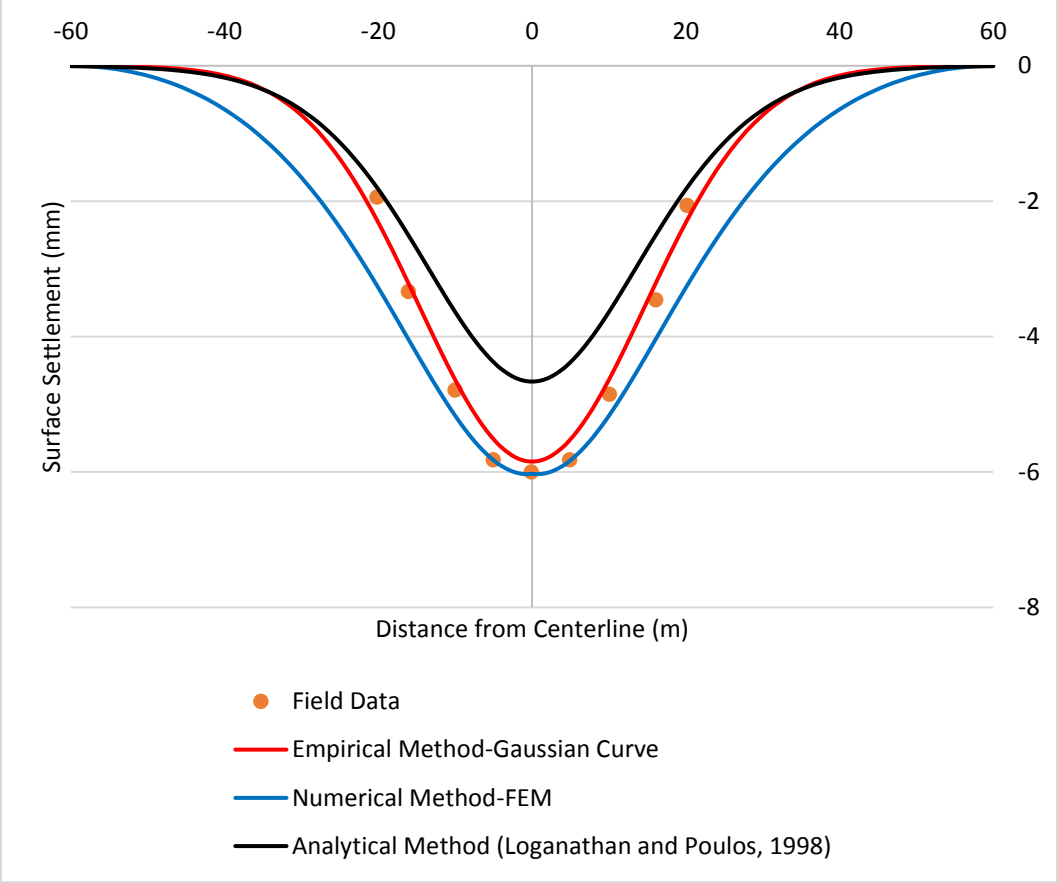

Figure 4-31 Model Validation for Surface Settlement

Case 4: Heathrow Express Trial Tunnel

The Heathrow express trial tunnel, an open face tunnel of 8.5 (28.0 ft) m diameter as presented in detail in Table 4-12, was excavated for a link between central London and Heathrow Airport. A tunnel was located at 29 m (95.2 ft) depth below ground level. The soil consists of stiff London clay with C_u of 50 to 250 kPa. Details of tunnel and soil information and field measurements were stated in Deane and Bassett (1995), and Loganathan and Poulos (1998). The undrained volume loss of 1.4% obtained from empirical data was adopted for the FE analysis. The boundary, which is 5-D in the lateral direction and 2-D from the tunnel axis to the bottom boundary, satisfies the lateral and bottom boundary

effects. Figure 4-32 shows Model validation for surface vertical settlement. The volume loss value obtained from FEA is 1.49%, which is almost perfectly fitted to the measured data. Both numerical and analytical methods illustrate under estimated values while the empirical method shows more realistic value as compared to measured data.

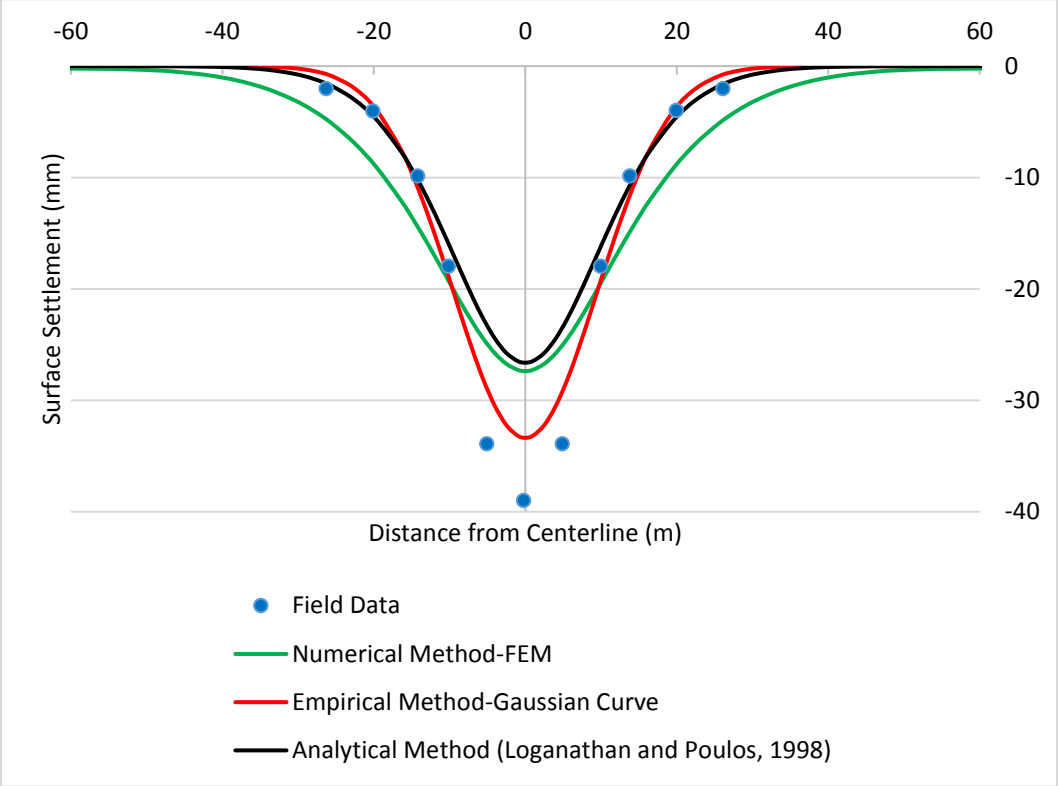

Figure 4-32 Model Validation for Surface Settlement

CHAPTER SUMMARY

This chapter presented research methodology including model generation, sensitivity analysis and 2-D tunneling simulations. Various real-life case histories for box jacking, pipe jacking and tunneling methods were introduced. Finite element simulation procedure was adopted for each model and the results were used in comparison with real life case studies for validation and accuracy.

Table 4-12 Soil Properties, Tunnel Geometry and Construction Methods for Tunneling Projects (Adapted from Su, 2015)

Cases	Geometry			Volume Loss V_L (%)	Soil Type	Geotechnical Soil Properties				Excavation Method	References
	Tunnel Diameter (D), m (ft)	Depth to Axis (H), m (ft)	H/D			Unit Weight kN/m^3 (lb/ft^3)	Modulus of Elasticity MPa (psi)	Friction Angle (Degree)	Cohesion kPa (psi)		
Centrifuge Test 1	6 (19.7)	15 (49)	2.5	1	Stiff Kaolin Clay	16.5 (106)	30 (4,351)	0	75 (10.9)	-	Loganathan et al., (2000)
Centrifuge Test 2		18 (59)	3								
Centrifuge Test 3		21 (69)	3.5								
Centrifuge Test	6 (19.7)	15 (49)	2.5	3.3	Kaolin Clay	16.39 (105.3)	5.2 (754)	23	20 (2.9)	-	Ong et al., (2000)
Green Park Tunnel	4.14 (13.6)	29.4 (96)	7.1	1.6	Stiff Fissured Clay	19 (122)	40 (5,800)	0	175 (25.4)	Hand	Loganathan and Poulos (1998)
Heathrow Express Trial Tunnel	8.5 (27.8)	19 (62)	2.2	1.4	Stiff London Clay	19 (122)	35 (5,076)	0	160 (23.2)	Open Face Shield Tunneling	Loganathan and Poulos (1998)

Chapter 5 RESULTS AND DISCUSSION

This chapter presents the results for underground construction of different pipes and boxes in specific soil conditions based on the case histories discussed in Chapter 4. In Chapter 5, the following parameters are studied:

1. Vertical surface and subsurface settlements induced by box from medium to large size installation,
2. Vertical surface and subsurface settlement induced by pipe installation,
3. Effect of box height (rise) on surface and subsurface settlement,
4. Effect of box width (span) on surface and subsurface settlement,
5. Effect of soil condition (sand and clay) on both pipe and box installations,
6. Effect of overcut excavation (volume loss) on surface settlement,
7. Horizontal soil movement induced by pipe and box installations at different installation depths,
8. Effect of layered soil on vertical and horizontal ground settlement.

LOAD DISTRIBUTION AROUND THE PIPE AND BOX

The nature of load distribution around the box and pipe is completely different as shown in Figures 5-1 and 5-2. This difference lead to different ground settlement around the structure and on the ground surface. Pipes are able to distribute loads more uniformly so with the same structural thickness, a circular cross section shows less deformation than rectangular one. Another difference between pipe and box is the difference between overcut excavations around pipe and box. In the other words, the maximum gap in pipe is at pipe crown but there is approximately uniform over excavation around the box.

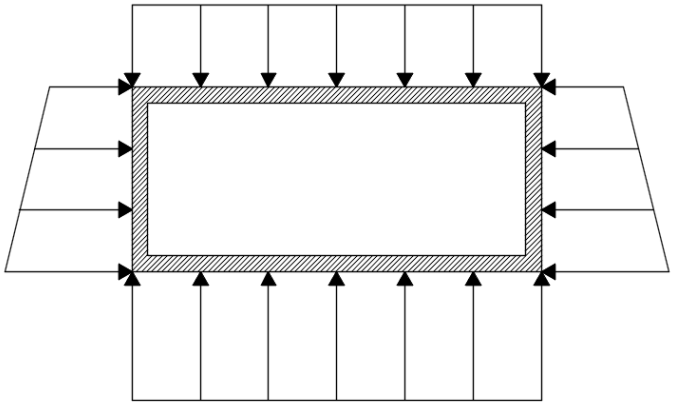

Figure 5-1 Soil Load Distribution around Buried Box

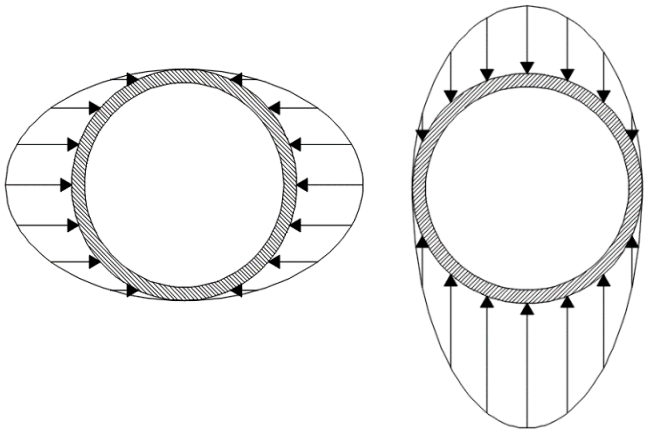

Figure 5-2 Horizontal and Vertical Soil Load Distribution around Buried Pipe

EFFECT OF BOX WIDTH ON SURFACE AND SUBSURFACE SETTLEMENT

Sandy Soils

Dilation of the ground above the tunnel may occur in sandy soils during the period of settlement but the expansion is likely to be quite small in loose cohesionless soils (O'Reilly et al., 1980). The stress relaxation is different over pipe and box crown due to different geometry and different soil movements around both structures.

Boxes with different geometries (i.e., different W/H_1 and same cross-sectional area) show different surface and subsurface settlements. A series of studies were carried out to investigate effect of box geometry in sandy soil conditions using the data obtained from the TxDOT Project at Vernon. Five different box widths range from 1.1 m (3.6 ft) to 2.4 m (7.9 ft) were generated for this study. The box rise (height) were calculated in a way that the box cross-sectional area was kept the same as the original box with net area equal to 2.16 m^2 (23.25 ft^2). The depth to axis for all boxes were equal to 7.3 m (23.9 ft). Table 5-1 shows box dimensions.

Figure 5-3 illustrates relationship between vertical settlement above box centerline and box span (W) and Figure 5-4 shows ground surface settlements for different box sizes. Box span was nearly doubled in size from 1.1 m (3.6 ft) to 2.4 m (7.9 ft). The ground surface settlement was also doubled while the settlement just over the crown showed a four-time increase (10 mm (0.4 in.) for H/W=5.2 to almost 40 mm (1.58 in.) for H/W=3.0). This clearly shows the direct relationship between box span and vertical settlement. However, this conclusion might not be always true where box with H/W=5.2 found to have less subsurface settlement than box with H/W=6.6. The reason is probably because the latter has less perimeter than the former. Therefore, it allows for less soil settlement around the box so causes less overall ground settlement than expected.

Table 5-1 Box Dimensions

Depth to Axis (H), m (ft)	Box Span (W), m (ft)	Box Rise (H_1), m (ft)	Perimeter m (ft)	H/W	Equivalent Diameter (D), m (ft)	H/D
7.3 (24)	1.1 (3.6)	2.0 (6.6)	6.2 (20.4)	6.6	1.66 (5.4)	4.4
	1.4 (4.6)	1.55 (5.1)	5.9 (19.4)	5.2		
	1.6 (5.2)	1.35 (4.3)	5.9 (19.4)	4.6		
	1.8 (5.9)	1.2 (3.9)	6.0 (19.6)	4.0		
	2.4 (7.9)	0.9 (3.0)	6.6 (21.8)	3.0		

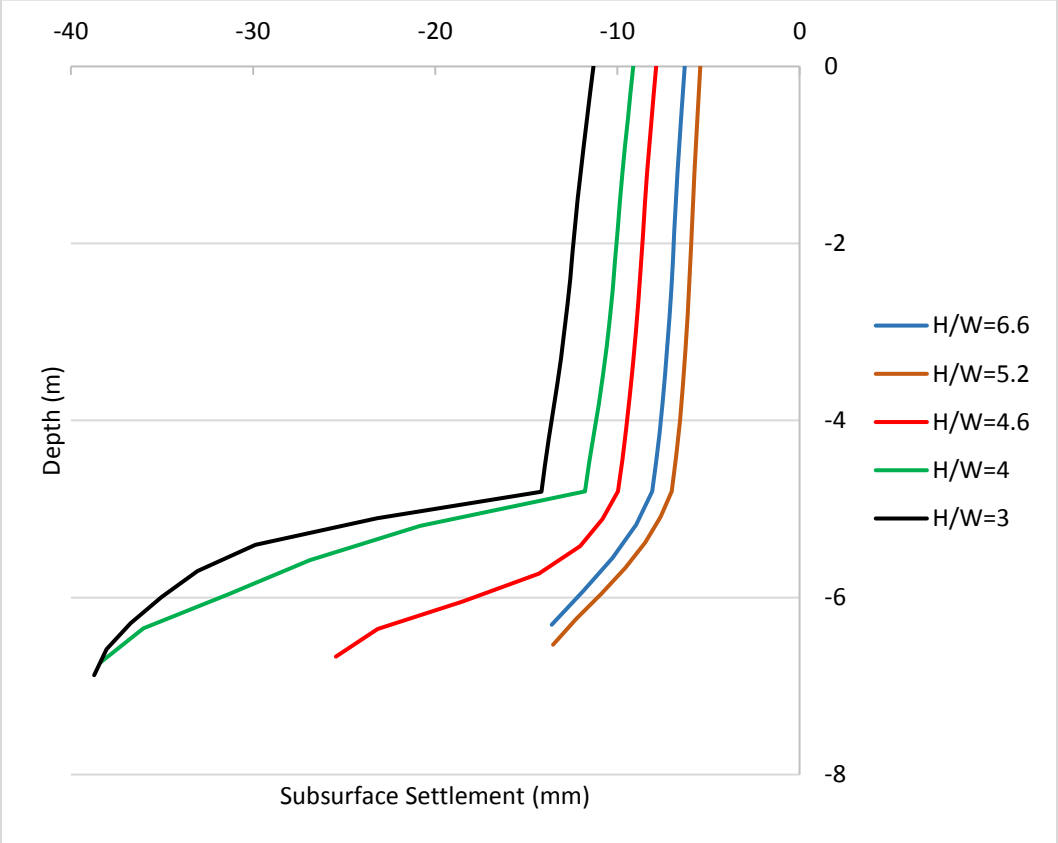

Figure 5-3 Relationship between Subsurface Ground Settlements and Box Sizes

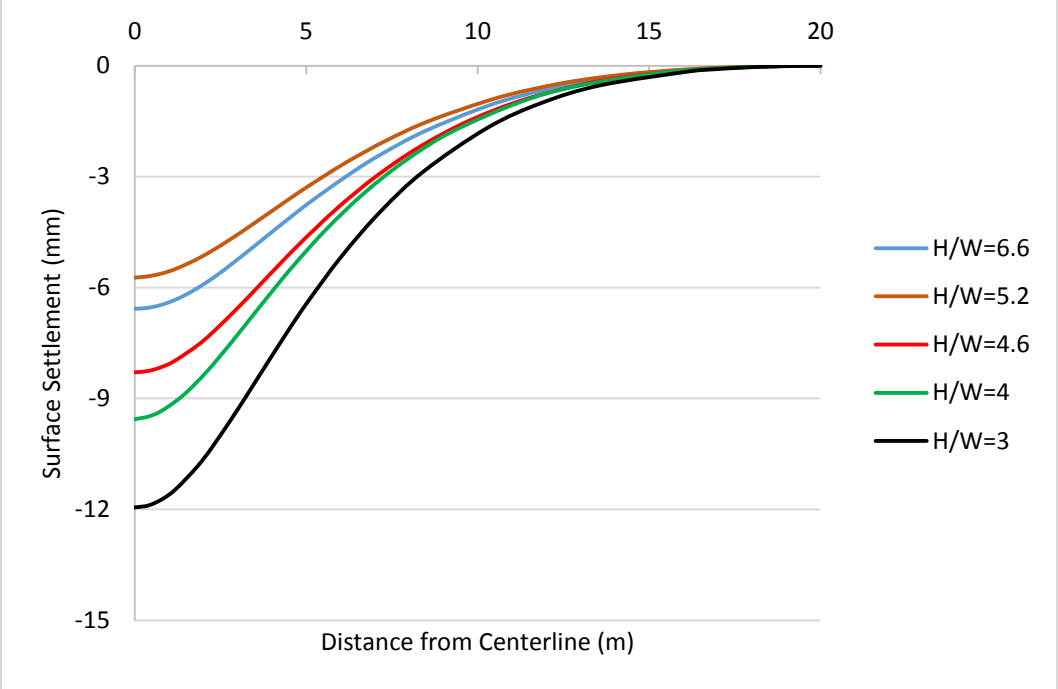

Figure 5-4 Relationship between Surface Ground Settlements and Box Sizes

Another finite element analysis was carried out to investigate the effect of pipe and box shape on surface ground settlement. Similar to previous model, the same cross-sectional area and same depth to axis was selected and FE models were generated for both pipe and box sections so, a depth to diameter (H/D) ratio of 4.4 was considered for all analyzes. The excavated area for the box jacking project was 2.16 m^2 (23.25 ft^2), which is equal to a volume loss of 9.26%. The same volume loss was applied to the pipe with a total gap area of 75 mm (2.95 in.) above the pipe crown. The result is presented in Figure 5-5. Pipe with the same cross-sectional area shows 60% less vertical settlement than box due to different load distribution pattern as shown in Figure 5-1. Table 5-2 presents the results obtained from finite element analysis.

Table 5-2 Settlement Trough Parameters

Type	i, m (ft)	S_V max, mm, (in.)
Box	4.28 (14.0)	9.56 (0.38)
Pipe	4.23 (13.9)	5.88 (0.23)

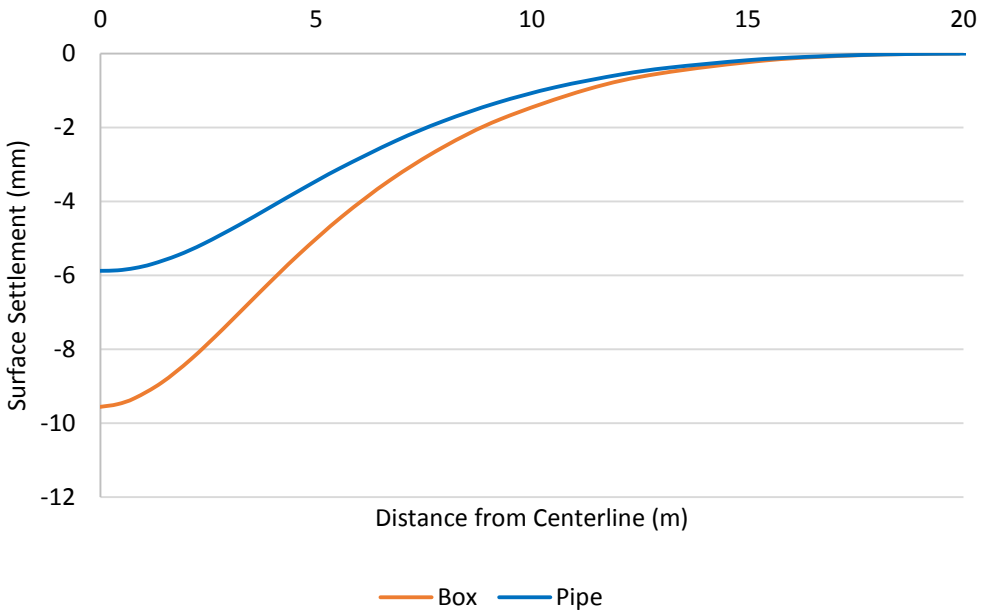

Figure 5-5 Effect of Structural Geometry on Ground Surface Settlement

EFFECT OF OVERCUT EXCAVATION IN SAND

Sandy Soil

Figure 5-6 illustrates relationship between size of overcut excavation and maximum surface settlement in box installation for the installation depth of 6.7m, (H/W=4) with 50 mm (1.97 in.) overcut. As shown in Figure 5-6, maximum surface settlement increases with increase in size of overcut excavation. However, it shows a reduction trend with overcut increase as it was supposed to show an increase in volume loss or vertical settlement. One reason for this it that the analysis was conducted based on immediate box installation. Therefore, soil had no time for final relaxation and collapsing into the overcut

area. The Gaussian method as shown in Figure 5-6 shows an overestimate values compared to field data (18 mm (0.71 in.) compared to 11.5 mm (0.45 in.)). Figures 5-7 and 5-8 show the schematic results from numerical analysis for the effect of overcut on pipe and box respectively.

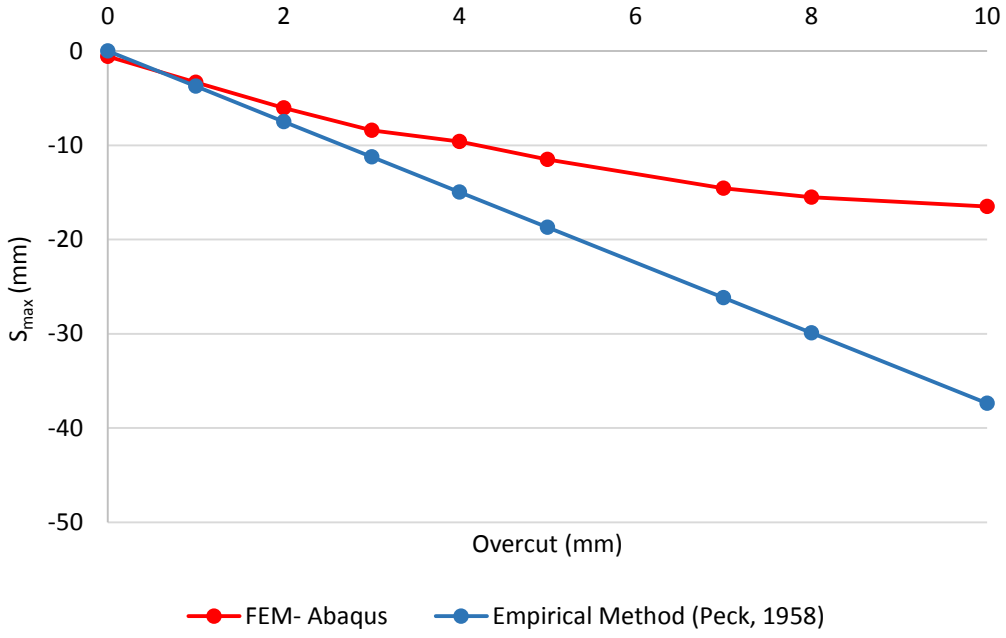

Figure 5-6 Relationship between Overcut Excavation and Maximum Surface Settlement

Pipe and box with the same width (diameter) also follow different settlement patterns. Another study was carried out to investigate the effect of same structure width by keeping box width (W) equal to pipe diameter (D). The box width from past analysis (W=D=1.8 m) was used for this study as well. It resulted in 18% higher cross-sectional area of pipe compared to the box section. The study aimed to study the effect of overcut for different structural shapes at different depth of installations in sandy soil condition (silty sand) as shown in Figure 5-9. It was observed that the box even with smaller cross-sectional area still showed higher maximum surface settlement. For the structure installed in shallower depths, there was higher surface settlement with an increasing trend with

increasing in overcut excavation. The reason can be explained by Terzaghi's vertical stress theory (Chapter 2). In the other words, in the shallower depths, soil's stress relaxation is not mobilized well so it tends to collapse into the gap area. According to Figure 5-10, vertical stress is mobilized well and does not transfer the whole settlement to the surface ground but almost all settlements are transferred to the ground surface in the shallow installations as illustrated in Figure 5-11.

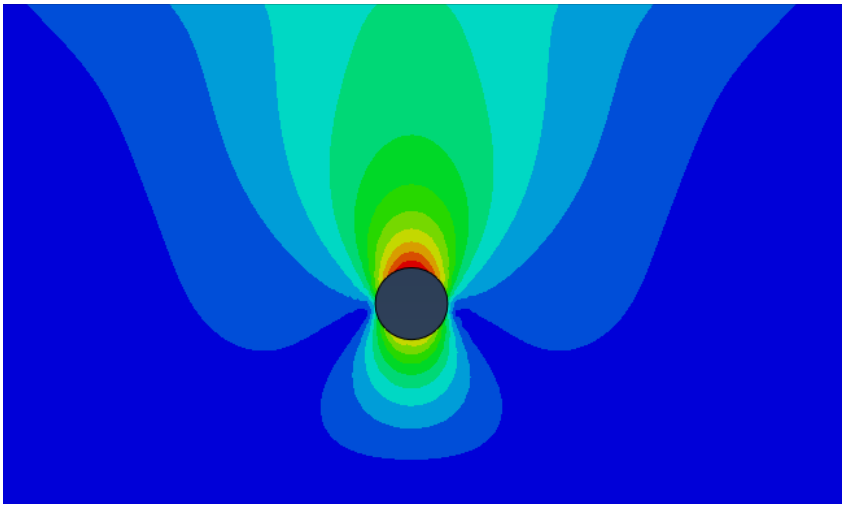

Figure 5-7 Effect of Overcut on Vertical Soil Settlement on Pipe

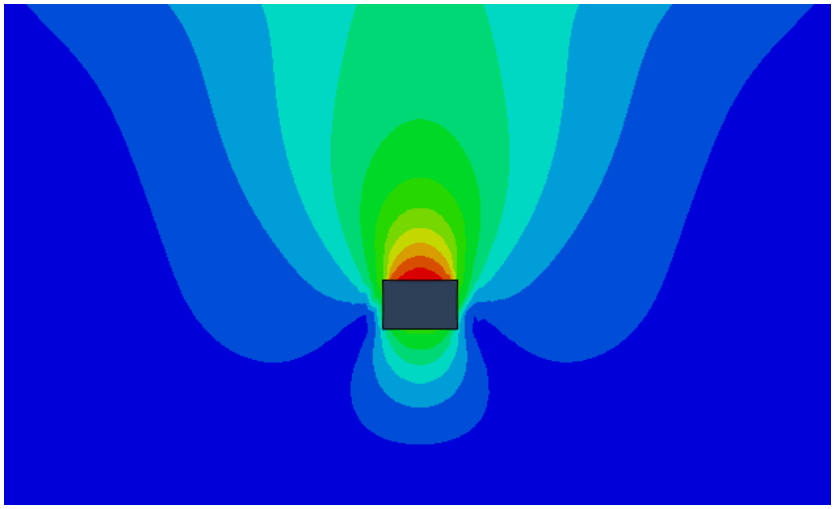

Figure 5-8 Effect of Overcut on Vertical Soil Settlement on Box

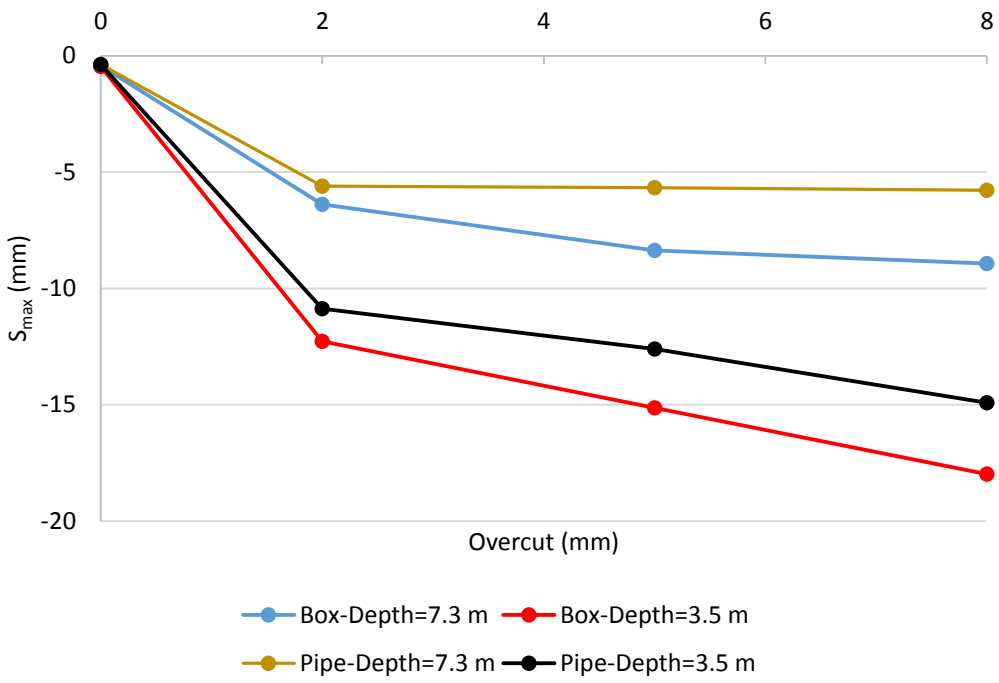

Figure 5-9 Relationship between Installation Depth and Maximum Surface Settlement for Different Overcut Excavations

Excavation in sand is very dependent to gap size and shape of excavation. Subsurface ground settlement varies significantly for box installation at depth 7.3 m (11.5 ft) when the overcut changes from 20 mm (0.79 in.) to 80 mm (3.15 in.). However, it becomes less dependent when pipe is installed. The pattern is similar in shallow pipe and box installations. Although pipe shows less settlement than box, they both are very dependent to size of overcut installation.

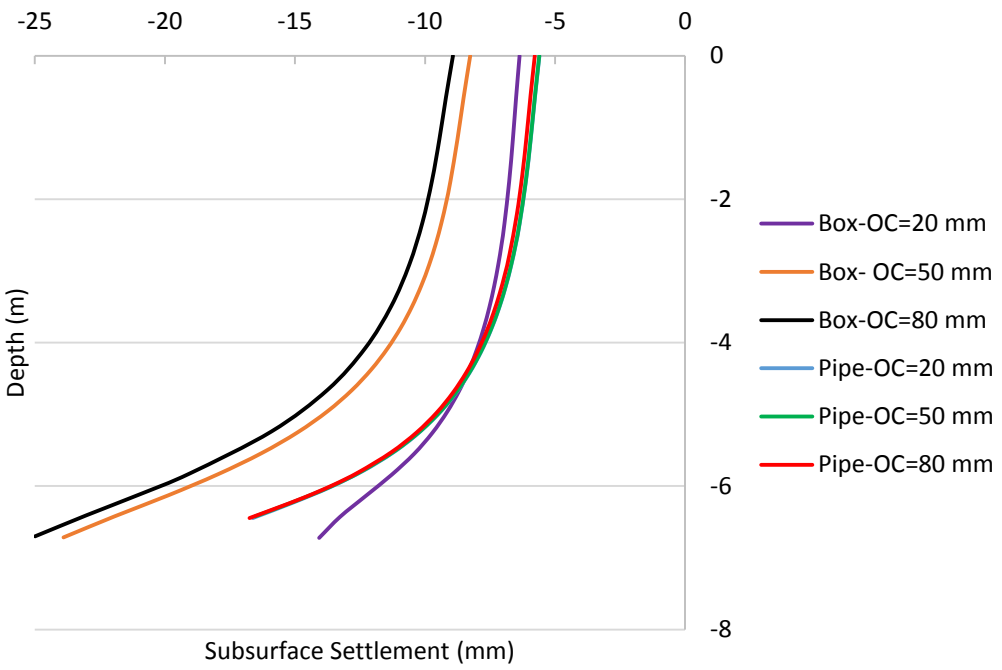

Figure 5-10 Comparison of Subsurface Settlement for Box and Pipe with Different Overcut Excavation (Depth to Axis= 3.5 m (24.0 ft))

Layered Soil

The model in layered sandy soils also showed very similar pattern to results shown in Figure 5-6. Finite element analysis was based on the results obtained from Navarro County Project (Figure 4-24) for box installations with cover depth of 1.8 m (5.9 ft) with W/H_1 ratio of 2.25 and volume loss equal to 8.0% (calculated from volume loss equal to overcut area). Study was performed further for volume losses of 5% and 2.5%. Results are presented in Figure 5-12. The results show that the construction depth has a major impact on maximum surface settlement for all volume loss values.

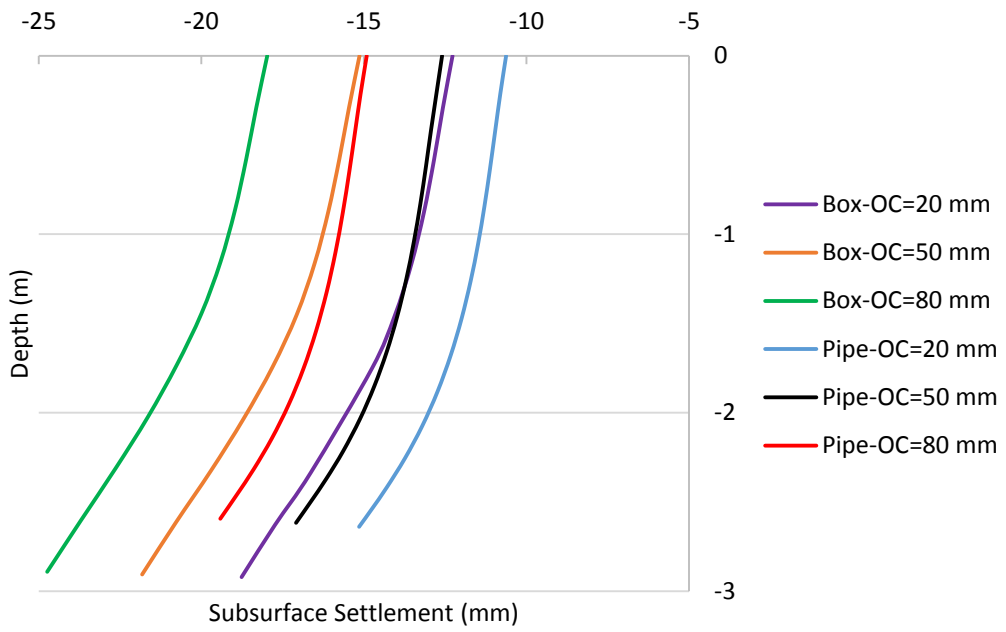

Figure 5-11 Comparison of Subsurface Settlement for Box and Pipe with Different Overcut Excavation (Depth to Axis= 3.5 m (11.5 ft))

Discussion on Ground Settlement in Sand

Figure 5-13 shows the effect of box width (W) on surface ground settlement. They all were considered in shallow depth of installations. Axis depth to width ratio (H/W) was 0.9, 2.0 and 3.7 for installation depths of 2.4 m, 5.5 m and 10.0 m respectively. When the installation depth is approximately doubled from 2.4 m to 5.5 m, an approximate 50% of the original vertical settlement is transferred to the surface ground, which is significant. The transferred volume loss keeps a substantial value of 40% when the installation depth is increased by four times. However, the vertical settlement in terms of equivalent pipe diameter to depth ratio (H/D) shows shallow to deep installation (1.45, 3.33 and 6.0), which is unable to interpret this huge volume loss.

Table 5-3 Settlement Trough Parameters for Shallow depth Box Installations

Depth m (ft)	i m (ft)	OC= 50.0 mm (1.97 in.)		OC= 30.0 mm (1.18 in.)		OC= 16.0 mm (0.63 in.)	
		S_{max} mm (in.)	Calculated i m (ft)	S_{max} mm (in.)	Calculated i m (ft)	S_{max} mm (in.)	Calculated i m (ft)
-2.4 (7.9)	1.08 (3.5)	-24.55 (0.97)	1.08 (3.5)	-20.75 (0.82)	1.10 (3.6)	-11.35 (0.45)	1.10 (3.6)
-5.5 (18.0)	2.48 (8.1)	-12.53 (0.49)	2.74 (9.0)	-11.00 (0.43)	2.76 (9.0)	-6.31 (0.25)	2.76 (9.1)
-10 (32.8)	4.5 (14.8)	-9.24 (0.36)	5.11 (16.8)	-8.29 (0.33)	5.23 (17.2)	-4.48 (0.18)	5.23 (17.2)

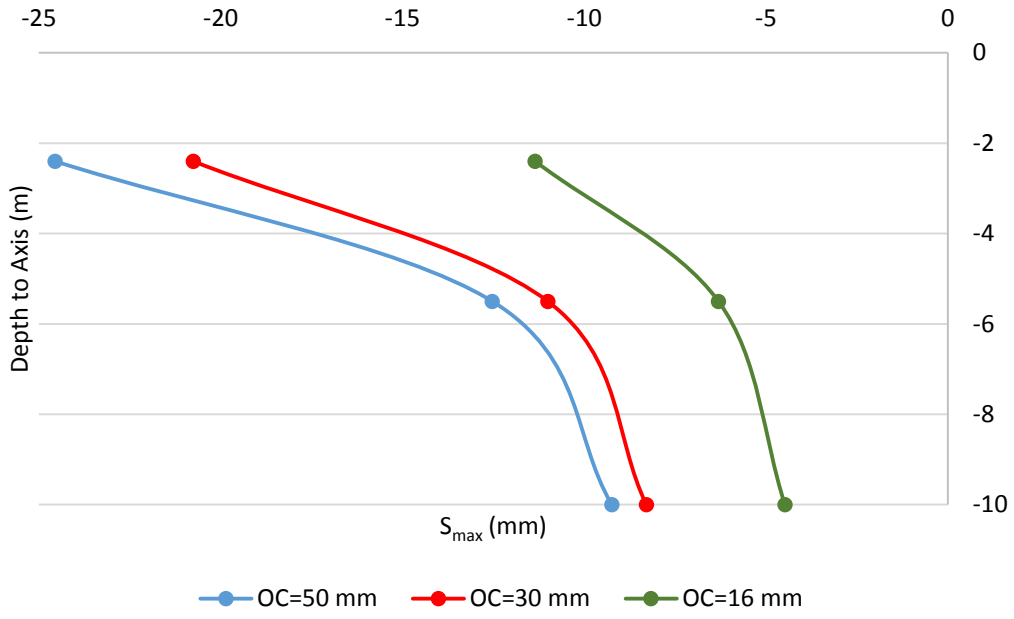

Figure 5-12 Relationship between Surface Settlement and Depth

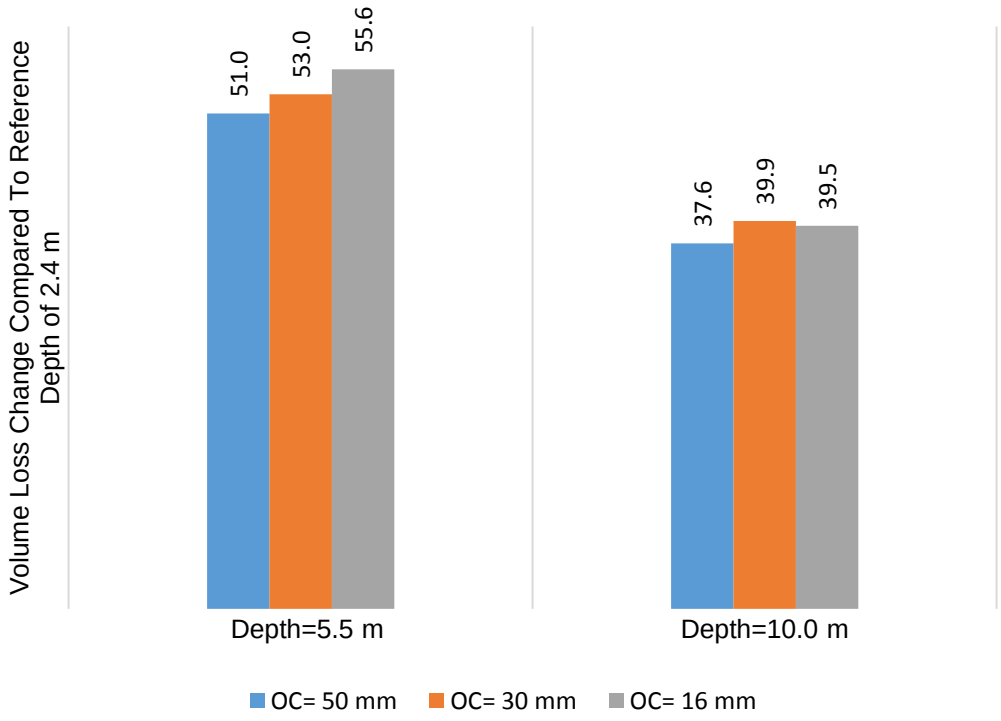

Figure 5-13 Comparison between Surface Settlement and Overcut Excavation

EFFECT OF CONSTRUCTION IN CLAYEY SOIL

Pipe jacking project with hand mining excavation was selected from Marshall, (1998) in clayey soil, which was underlain by terrace gravel soil layer. Marshall, (1998) reported the results for 8 days and 35 days after the pipe jacking operation was completed. Results obtained from field measurement have a very good agreement with the Gaussian Normal Distribution Curve. For FE analysis, total stress analysis was conducted for undrained condition in clayey soil. According to Marshall (1998), there was an average 30 mm (1.81 in.) maximum gap (OC) between pipe and excavated ground at the crown, which was equal to total volume loss of 3.36%. Using equation 2-4, a maximum ground surface of 9.35 mm (0.37 in.) was calculated at the centerline as shown in Figure 4-27.

The study was carried out to simulate the effect of box jacked operation with same cross-sectional area and to study the effect of vertical ground settlement at different depth of installations for pipe and box. Similar to the past studies, box width was equal to pipe diameter and a total overcut of 18.33 mm (0.72 in.) was equally applied around the box. Trough width parameter of 0.35 was selected for sandy soils and 0.5 for clayey soils. Settlement trough width (i) was calculated from the equation developed by O'Reilly and New (1991) as previously presented in Table 3-2.

Table 5-4 compares i parameter from finite element analysis for pipe and box and empirical method from Peck, 1968. Unlike sandy soils, surface settlements for both pipe and box in almost all installation depths are the same in the clayey soil. However, the results obtained from FEA show greater settlement trough than the analytical study, which gives wider and shallower surface settlement curve compared to empirical curve (Figure 5-14). Results from FEA for pipe and box at various depths are presented in Figure 5-15.

Table 5-4 Comparison between Finite Element and Empirical Method

Depth to Axis m, (ft)	Settlement Trough Width, i, m (ft)			Volume Loss (%)		
	Pipe	Box	Gaussian Curve	Pipe	Box	Gaussian Curve
3.5 (11.5)	1.24 (4.1)	1.23 (4.0)	1.23 (4.0)	2.15	2.48	3.36
5.5 (18.0)	2.90 (9.5)	2.75 (9.0)	2.15 (7.1)	3.33	3.38	
8.5 (27.9)	4.32 (14.2)	4.68 (15.4)	3.65 (12.0)	3.49	3.61	
12.5 (41.0)	6.00 (19.7)	6.33 (20.8)	5.65 (18.5)	3.63	3.43	
18.0 (59.0)	8.65 (28.4)	8.74 (28.7)	8.40 (27.6)	4.24	4.20	

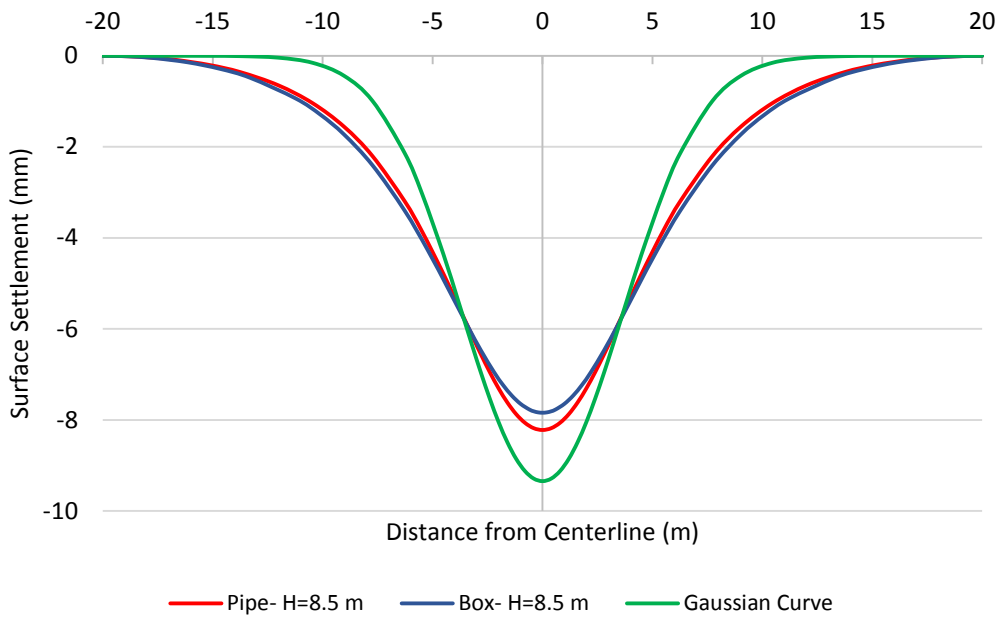

Figure 5-14 Comparison between Finite Element and Analytical Method

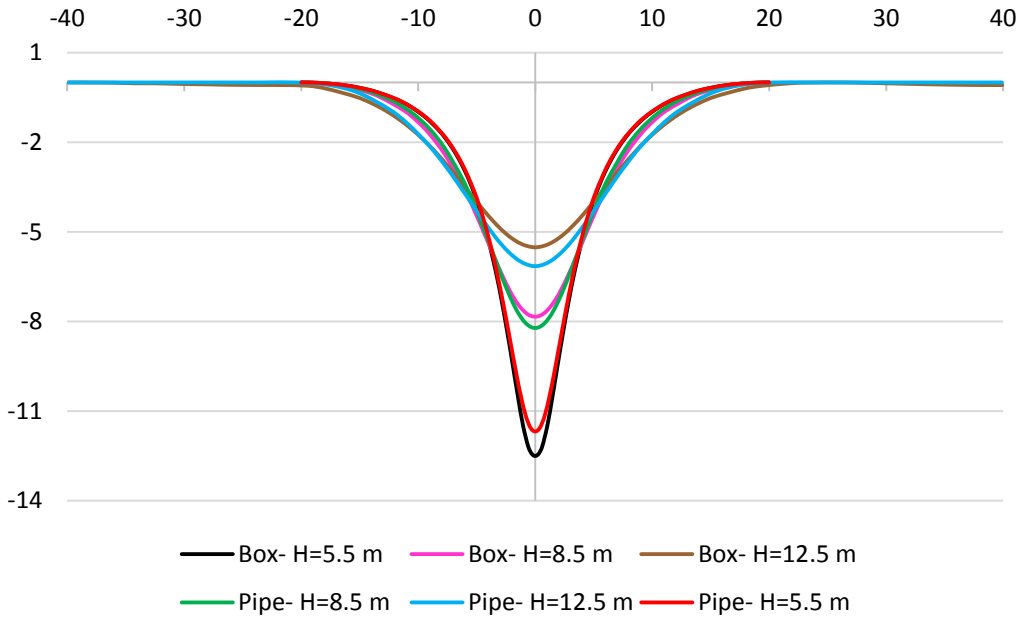

Figure 5-15 Comparison between Surface Settlement in Pipe and Box at Different Installation Depths

Results from maximum surface settlement and depth for pipe and box was plotted in Figure 5-16. It showed good fit between FEA and analytical method. However, maximum surface settlement in nearly shallow installation depths (H/D below 4) was underestimated by the finite element method. The field data and finite element analysis in layered clayey soil showed that the surface ground settlement in pipe jacking project fitted reasonably well to the analytical method. However, in hand mining excavation compared to closed face excavation, a larger overcut area was excavated and no face pressure was applied so lager volume loss was usually expected. It is also worth noting that the results from FEA are closer to the analytical method at the deeper installations and closer to empirical method at the shallower installations.

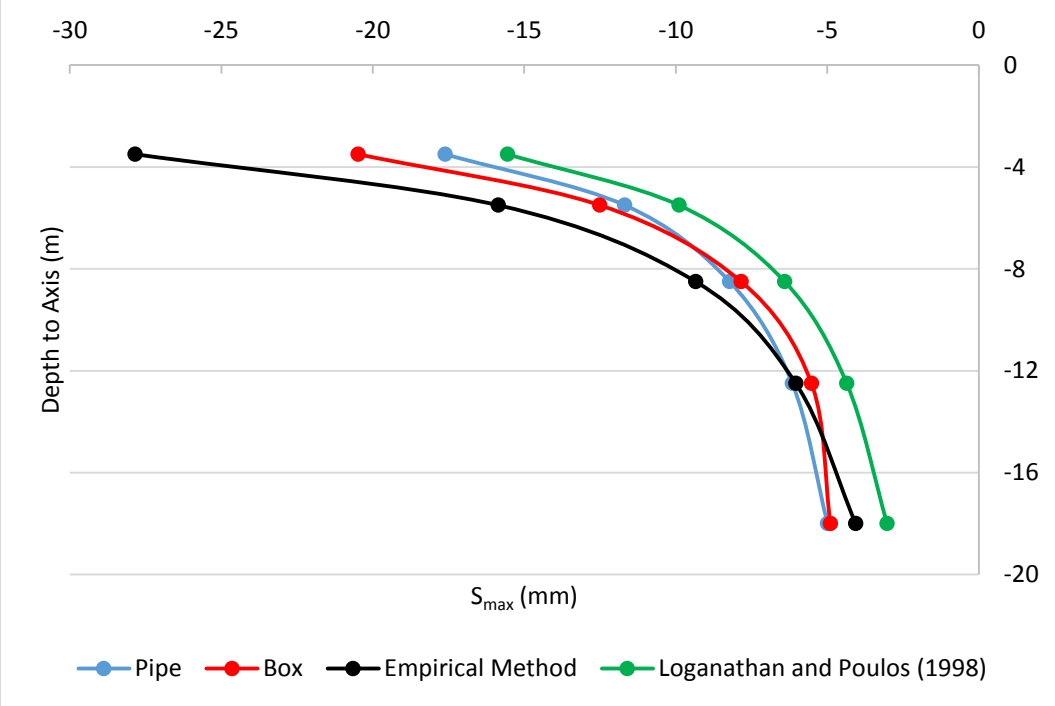

Figure 5-16 Relationship between Maximum Surface Settlement and Depth

EFFECT OF LARGE SIZE TUNNEL CONSTRUCTION IN SOFT CLAY

Laboratory Test (Ong, 2007)

Centrifuge laboratory test results for a 6 m (19.7 ft) tunnel diameter was selected for large size tunneling in soft clay. Ong, (2007) reported laboratory test results. Su (2015) plotted the relationship between volume loss and maximum surface settlement based on the results from FE analysis and found good match between the FEA and laboratory results. The results are presented in Figure 5-17. However, in higher volume losses (greater than 5%) FEM underestimated the maximum surface settlement results by approximately 17% compared to Gaussian method whereas only 3% by centrifuge test (Su, 2015).

The FE analysis was continued by adding two boxes with the same pipe cross-sectional area as shown in Table 5-5.

Table 5-5 Box Geometries in FE Analysis

Depth to Axis (H), m (ft)	Box Span (W), m (ft)	Box Rise (H_1), m (ft)	H/W	H/D
15 (49.2)	4.4 (14.4)	6.0 (19.7)	3.4	2.5
	6.0 (19.7)	4.4 (14.4)	2.5	

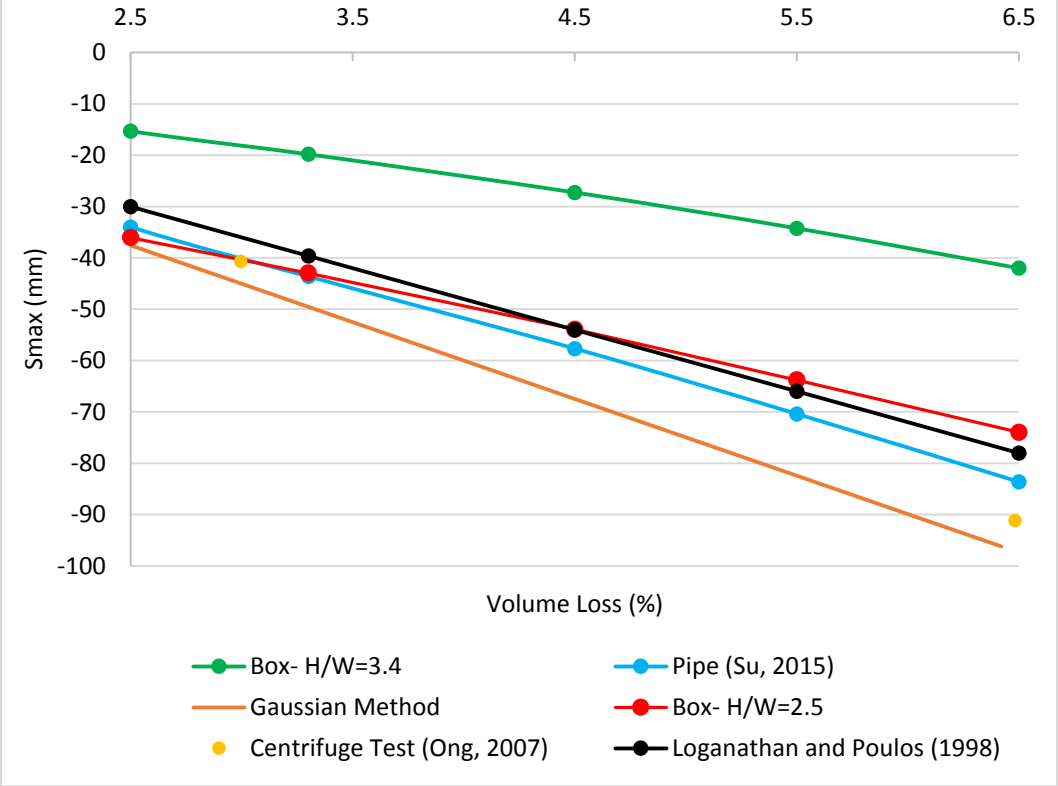

Figure 5-17 Relationship between Maximum Surface Settlement and Volume Loss

Results from box with H/W=3.4 showed similar maximum surface settlement to the pipe. Box with smaller width also showed less ground settlement than pipe. The analysis on the effect of box size also confirmed an underestimate surface settlement value as mentioned by Su (2015).

For the stiff clay with the same volume loss (1.6%) analyzes showed slightly higher settlement in box with width equal to pipe diameter. The study was conducted using data obtained from Green Park Tunnel from Loganathan and Poulos (1998). Larger ground surface settlement was observed in stiff clay than normal clay. This is because no soil relaxation was occurred while the tunnel was excavated resulting in an immediate volume change, which was fully transferred to the ground surface. Another important factor is the effect of depth of installation where the tunnel was constructed 29.4 m (96.5 ft) below

ground surface. As shown in Figure 5-18, the FE results for box showed higher ground settlements than other predictive methods in deep installation and less in the shallower depth of installations.

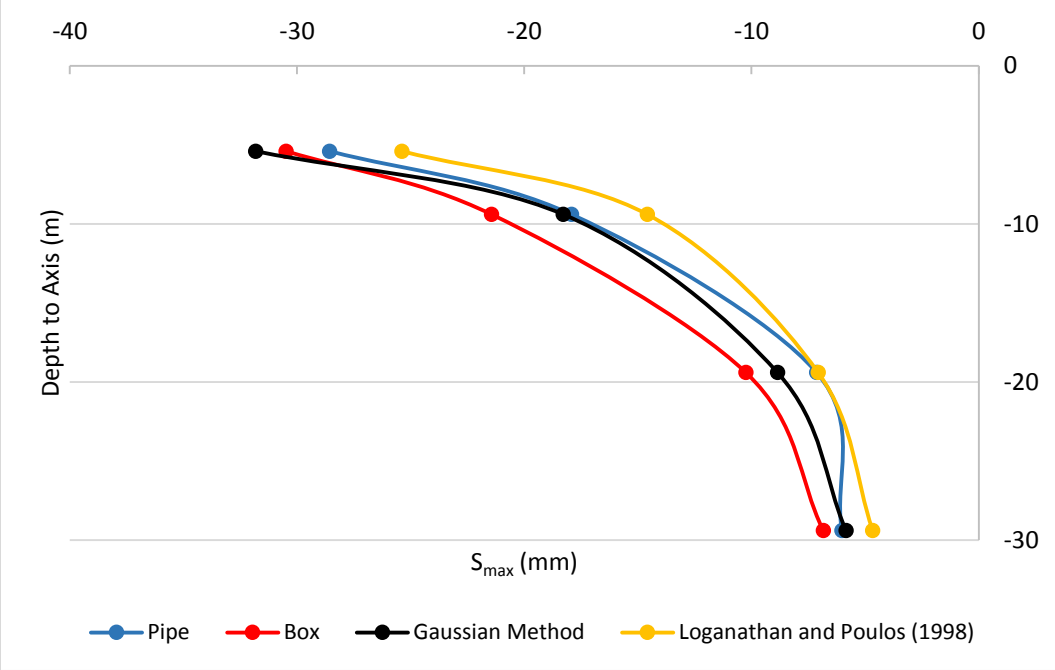

Figure 5-18 Relationship between Maximum Surface Settlement and Depth

Effect of Subsurface Settlement above Tunnel Crown

Effect of soil on subsurface ground settlement was studied in the past section. Results for box and pipe installation in stiff clay condition for deep installation (Green Park Tunnel) and shallow installation (Heathrow Express Trial Tunnel) as shown in Figures 5-19 and 5-20 respectively. The result from former case study showed higher settlement in box than pipe according to Figure 5-19 and almost the same vertical settlement over the crown for both pipe and box. Results from finite element analysis for pipe had a good match with data obtained from field measurement (Attewell and Farmer, 1974). For the latter case study, surface ground settlement was underestimated by finite element analysis for both

pipe and box, but it showed more accurate results as the measurements approached tunnel crown.

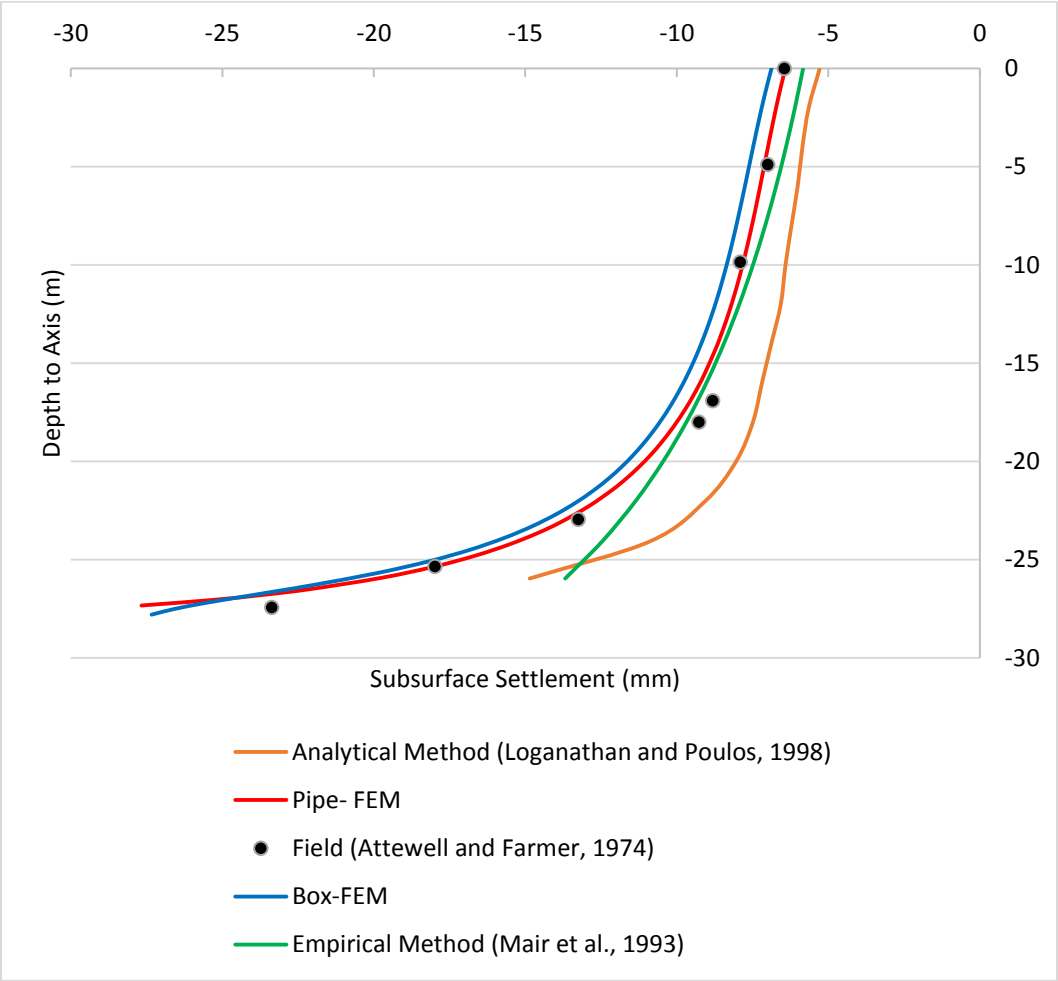

Figure 5-19 Subsurface Settlements above Centerline (Green Park Tunnel)

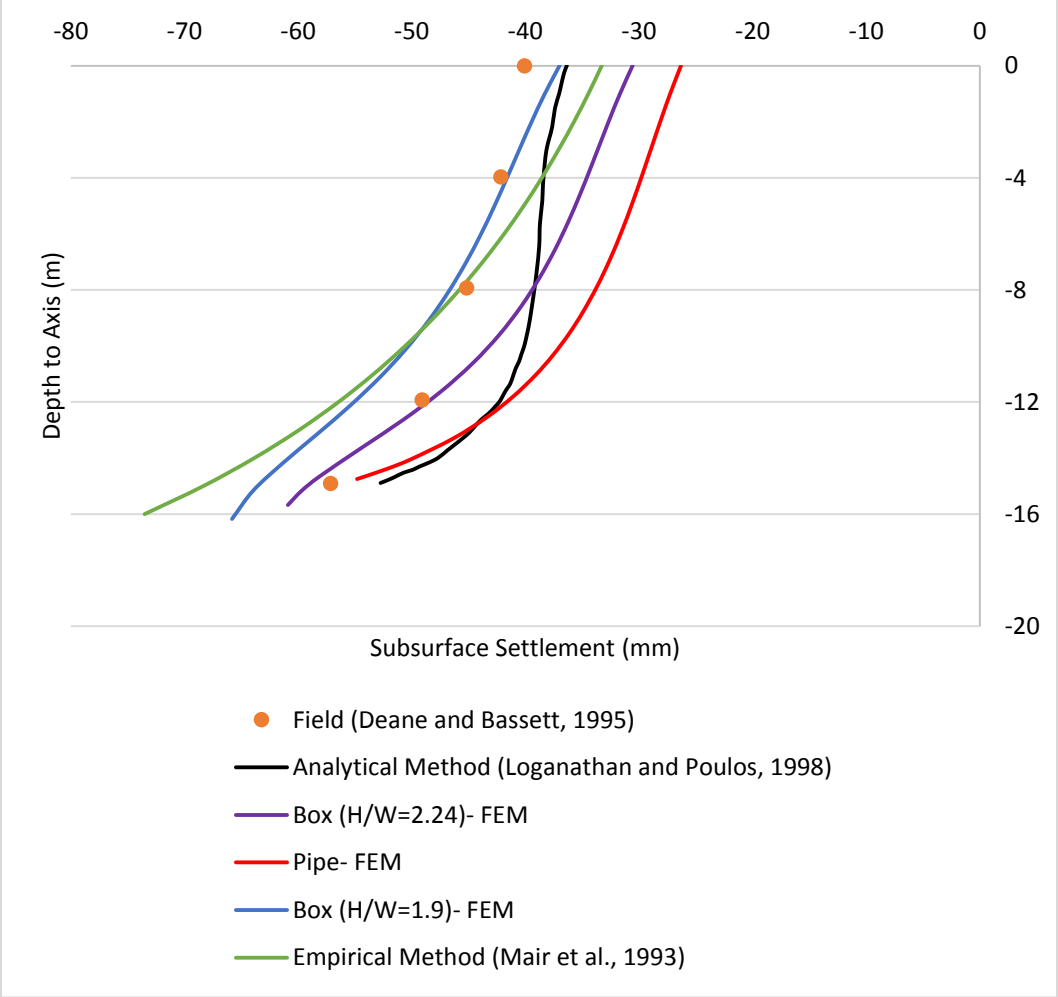

Figure 5-20 Subsurface Settlements above Centerline (Heathrow Express Trial Tunnel)

Effect of Subsurface Settlement Trough

Similar to surface settlement, box with W≥ D showed higher subsurface settlement trough than pipe. Study was conducted based data from Heathrow Express Trial Tunnel. Figure 5-21 compares finite element results for subsurface settlement trough at depth 3 m (9.8 ft), 5 m (16.4 ft) and 10 m (32.8 ft). Compared to Gaussian Distribution Curve, FE analysis underestimated the maximum surface settlement. To overcome with the same volume loss, a larger settlement trough parameter was obtained from the numerical

analysis (13.8 versus 9.5). Table 5-6 compares settlement trough width between pipe and box. The trough width parameter for pipe is approximately in good fit with the slope of curve proposed by Mair et al., (1993) as shown in Table 3-3.

Table 5-6 Calculated Settlement Trough Width for Pipe and box

Tunnel Shape	Settlement Trough Width, i, m (ft)				di/dz
	Depth=0 m	Depth=3 m	Depth=5 m	Depth=10 m	
Pipe	11.86	11.47	11.03	8.65	-0.321
Box (H/W=2.24)	11.20	10.80	10.34	8.65	-0.255
Box (H/W=1.9)	10.91	10.57	10.17	8.91	-0.2

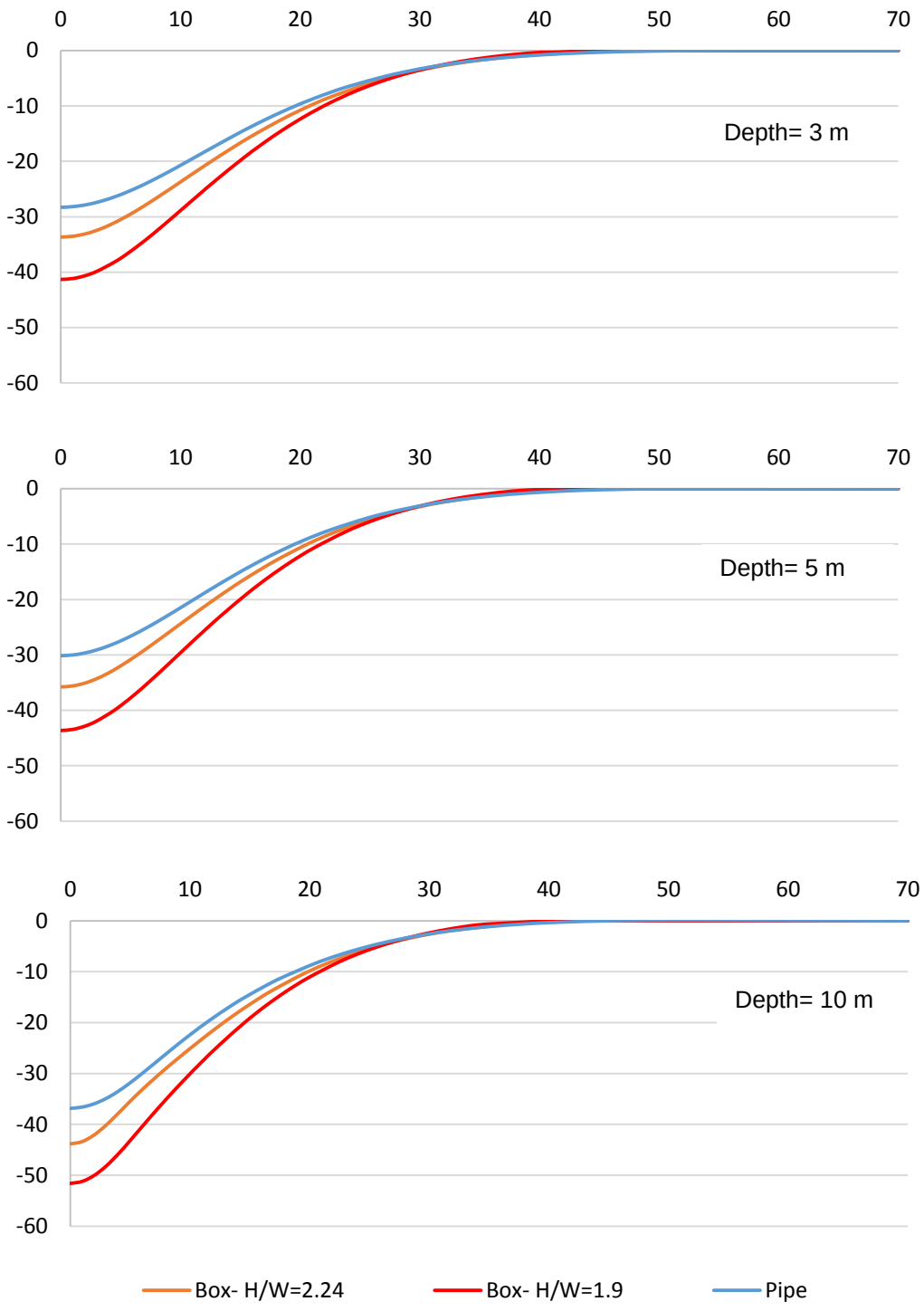

Figure 5-21 Subsurface Settlement at Depth 3 m, 5 m and 10 m

Effect of Horizontal Displacement

Horizontal (lateral) displacement of soil for pipe at distances of 9 m (29.5 ft) and 6 m (19.7 ft) from vertical centerline were presented in Figures 5-22 and 5-23 respectively. This study was carried out based data from Heathrow Express Trial Tunnel. The results from FEA were compared to analytical and field data measurements. The horizontal settlement analysis was continued 7 m (23 ft), after tunnel invert (depth= 30 m). Maximum lateral settlement occurred exactly at the tunnel springline. However, maximum horizontal displacement was overestimated at farther distances by the analytical method. There was a very good fit between field measurements and finite element analysis as shown in Figures 5-22 and 5-23.

Below the tunnel invert, settlements calculated from analytical and numerical methods were observed to diminish at a rapid rate with depth. At depth below 30 m (100 ft), FEA showed a horizontal heave, which was dissipated at the bottom of soil boundary at depth 40 m (130 ft), due to the boundary constrains. However, the heave existence cannot be confirmed because no field data was available below 30 m, so It may need deeper soil boundary (probably 50 m (160 ft)) until it can make sure that the boundary condition is not affecting the horizontal soil displacement. Appendix A provides more FE results for horizontal displacement based on Centrifuge Tests by Loganathan (2000).

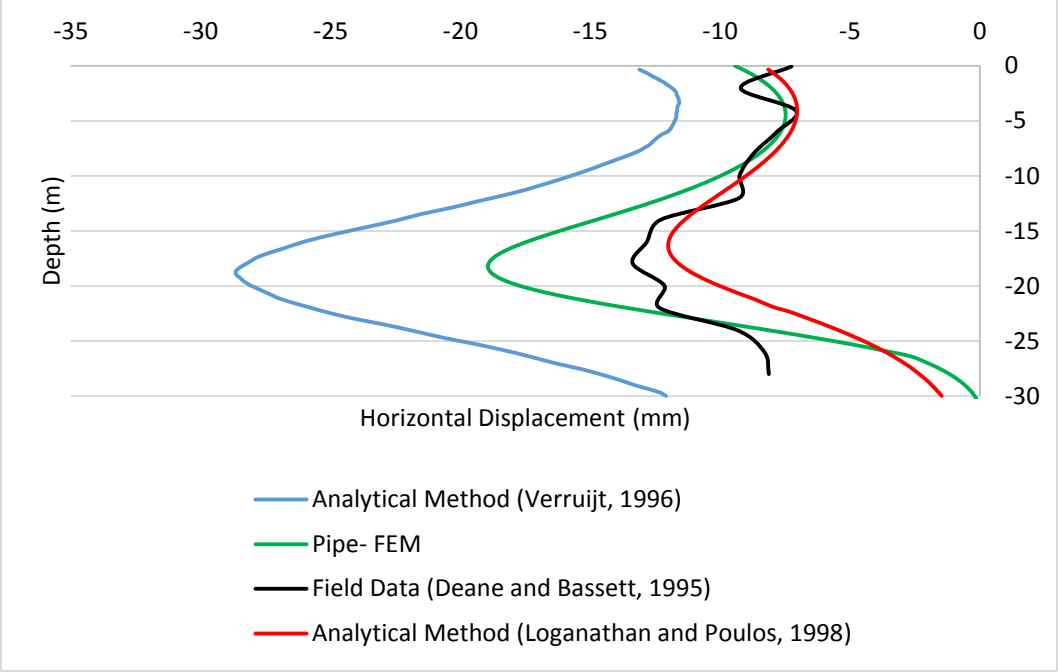

Figure 5-22 Horizontal Soil Displacement vs. Depth at x= 9 m (29.5 ft) from Tunnel Centerline

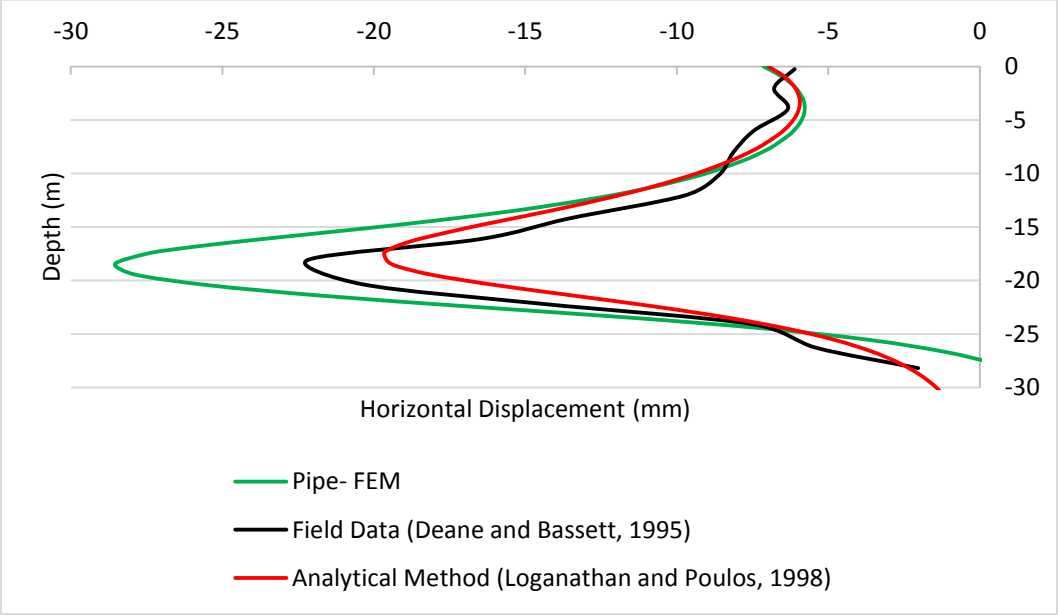

Figure 5-23 Horizontal Soil Displacement vs. Depth at x= 6 m (19.7 ft) from Tunnel Centerline

COMPARISON OF HORIZONTAL DISPLACEMENT IN PIPE AND BOX

The lateral settlement of soil at various distances of 6 m (19.7 ft), 9 m (29.5 ft), 15 m (49.2 ft) and 30 m (98.4 ft), from the tunnel vertical centerline for Heathrow Express Trial Tunnel were presented in Figures 5-24 through 5-27. As mentioned before, two box tunnels with different sizes were considered for this study. Box with span (width) of 10 m (32.8 ft) and span to depth ratio of 1.9 m (6.2 ft), showed higher horizontal displacements at lateral distance of 6 m (19.7 ft). However, an immediate settlement reduction occurred at lateral distance of 9 m (29.5 ft) from tunnel centerline. However, it still showed greater settlements at the surface for all case studies. Horizontal soil displacement for box and pipe with same diameter showed almost the same trend for all cases.

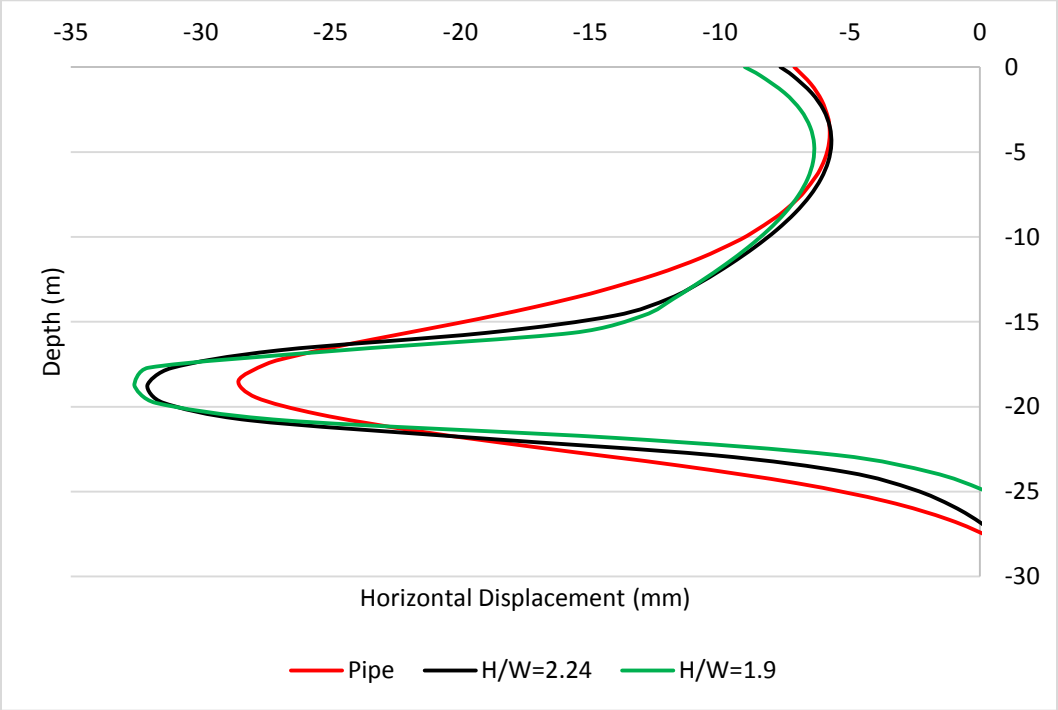

Figure 5-24 Horizontal Soil Displacement vs. Depth at x= 6 m (19.7 ft) from Tunnel Centerline

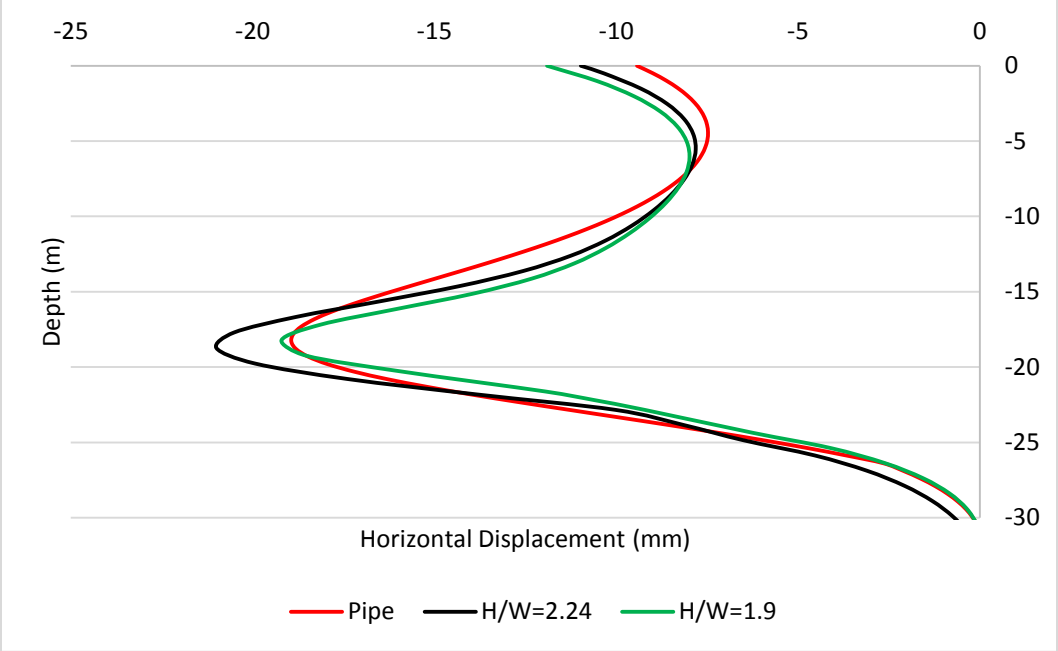

Figure 5-25 Horizontal Soil Displacement vs. Depth at x= 9 m (29.5 ft) from Tunnel Centerline

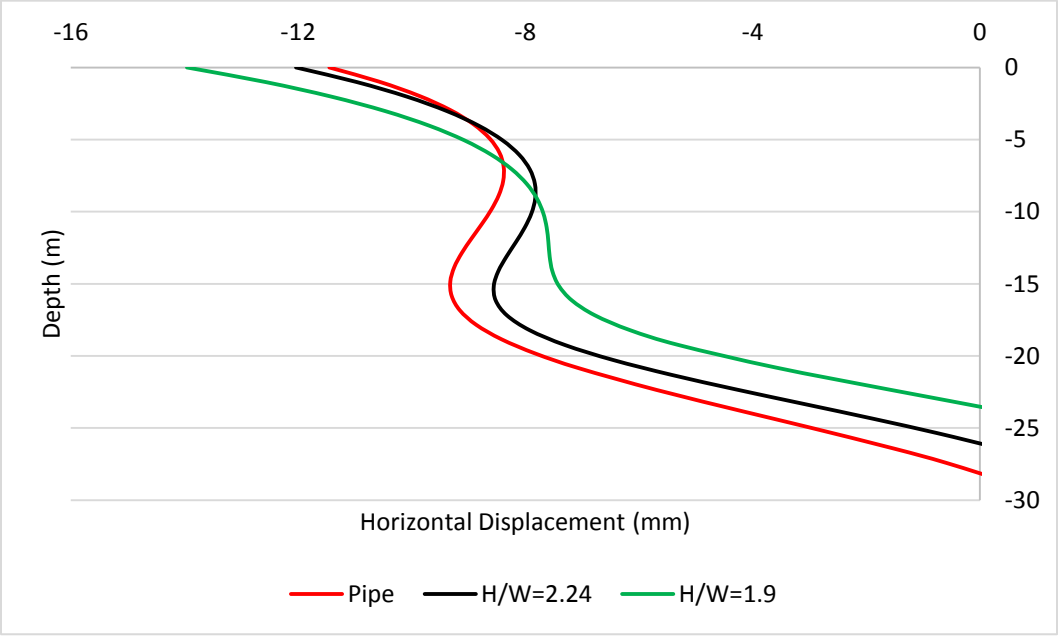

Figure 5-26 Horizontal Soil Displacement vs. Depth at x= 15 m (49.2 ft) from Tunnel Centerline

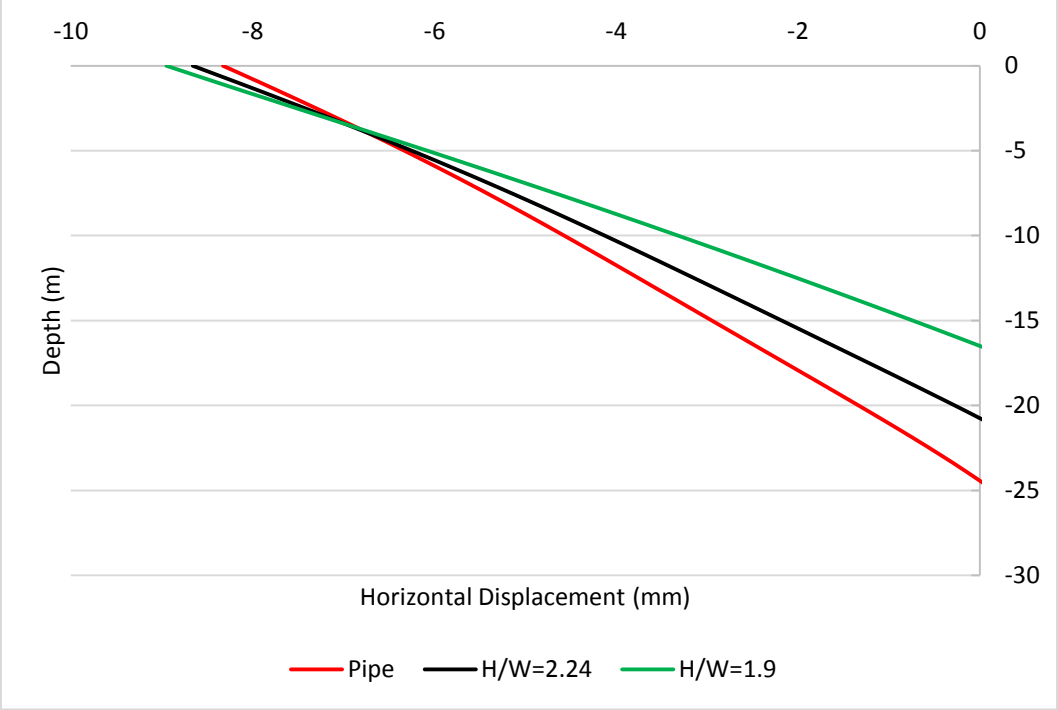

Figure 5- Horizontal Soil Displacement vs. Depth at x= 30 m (98.4 ft) from Tunnel Centerline

DISCUSSION ON EMPIRICAL GROUND SURFACE PREDICTION MODELS

As discussed in Chapter 3, various models are developed to increase the accuracy of existing empirical models. According to FE analysis in this study, Gaussian Distribution Curve, shows narrower and deeper curve than numerical analysis. Figures 5-28 through 5-32 compares between the performed numerical analysis in various soil conditions, tunnel shape and depth of installation as categorized from shallow installation to deep installation. Vorster (2005) suggested Modified Gaussian Curve to better fit the surface settlement for centrifuge test results as the Gaussian Curve was not satisfactory to accurately describe the soil settlement (Vorster, 2005).

Vorster suggested three values of 0.5, 1 and 1.5 for n. n=0.5 gives narrower curve while for n=1, the curve becomes Gaussian Curve. The parametric value of α=0.212

(n=0.5) was selected for Modified Gaussian Curve and the results were compared to the results from current study. Figure 5-28 shows the results from Green Part Tunnel as a case study for deep tunnel construction in clayey soil. The field data fitted with Gaussian method while the FE curve agreed with the Modified Gaussian Curve. Yield Density model showed very narrow results while Jacobsz model showed wider curve at the far fields.

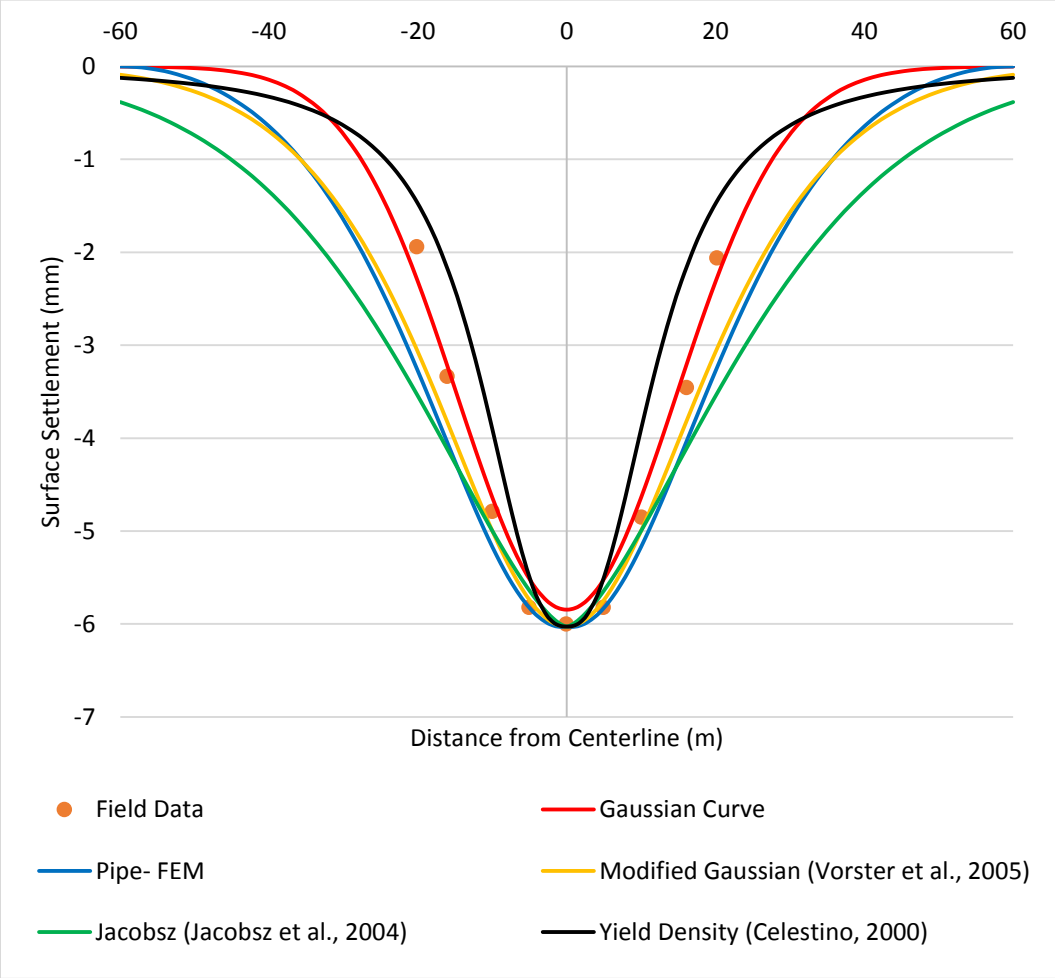

Figure 5-27 Comparison of Empirical Ground Surface Models- Deep Pipe Installation (Green Park Tunnel)

Vertical ground settlement for very deep box installation in stiff clay also showed good fit between Modified Gaussian Curve and numerical analysis while Jacobsz method still showed a wider curve in far fields as shown in Figure 5-29.

The trend in vertical surface settlement in shallow box installation in sandy soils was different from deep installation where the curve for numerical analysis agreed more with Gaussian Distribution Curve (see Figure 5-30 for data from Navarro box installation). Modified Gaussian Curve predicted the surface settlement very good from the centerline to near inflection point. For the box in deep installation in sandy soil as shown in Figure 5-31 (Vernon Project for layered soil, B1), there was an agreement between Gaussian Curve and FEA from the centerline to the inflection point and then showed good fit between Modified Gaussian Curve and FEA from inflection point to the far field. This was exactly similar to deep pipe installation (Marshall, 1998).

In conclusion, the Jacobsz method and yield Density Method do not predict the surface settlement well enough but both Gaussian and Modified Gaussian Curves are able to predict the vertical soil settlement for both pipe and box in different soil conditions.

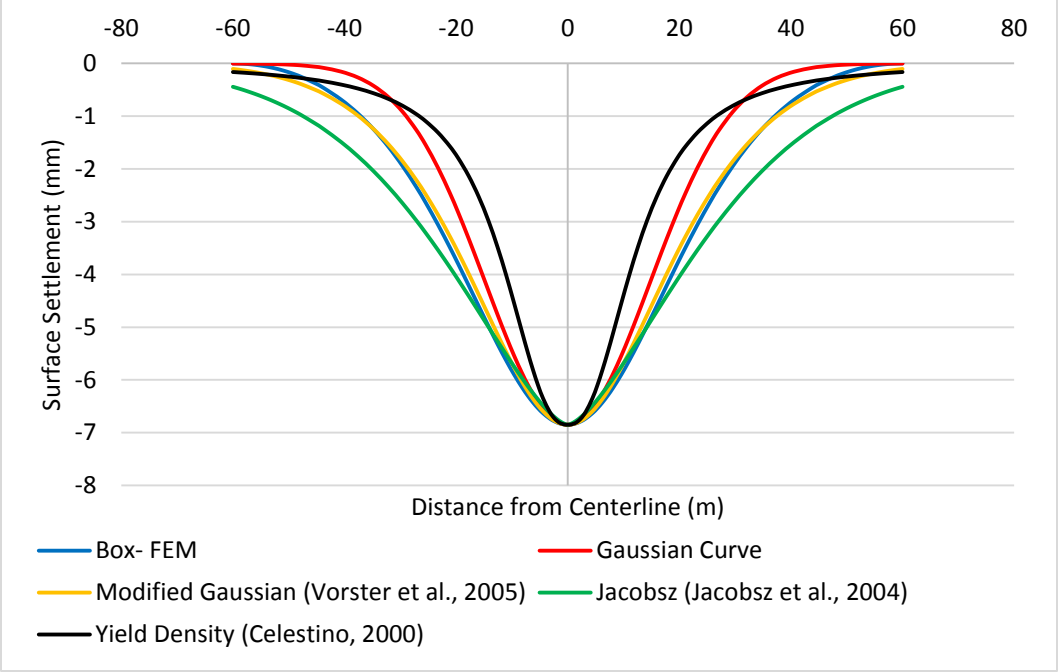

Figure 5-28 Comparison of Empirical Ground Surface Models- Deep Box Installation in Clay (Green Park Tunnel)

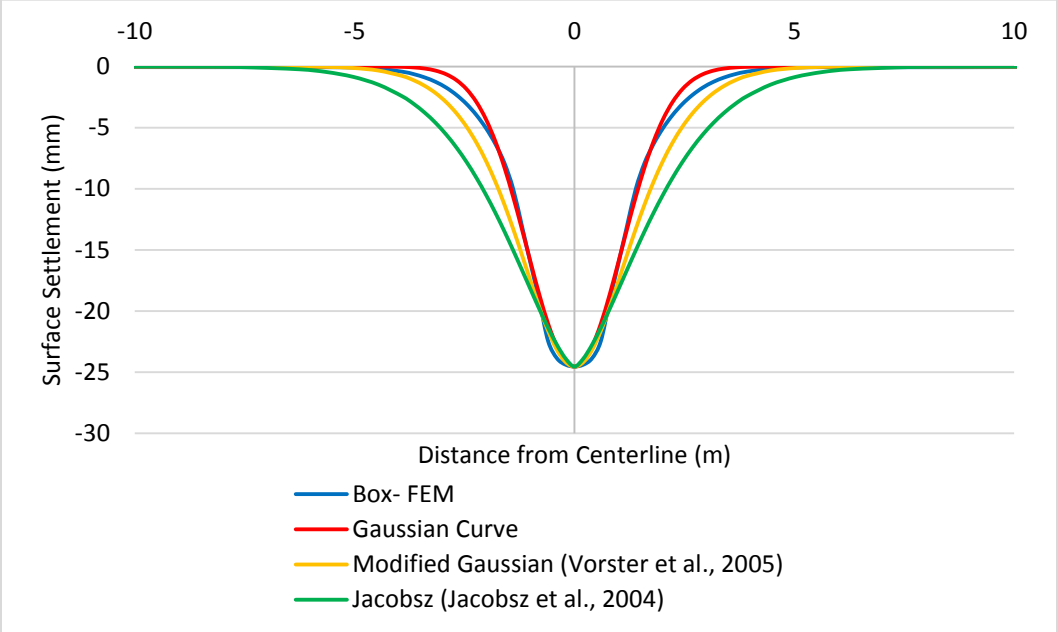

Figure 5-29 Comparison of Empirical Ground Surface Models- Shallow Box Installation in Sand (Navarro County Project)

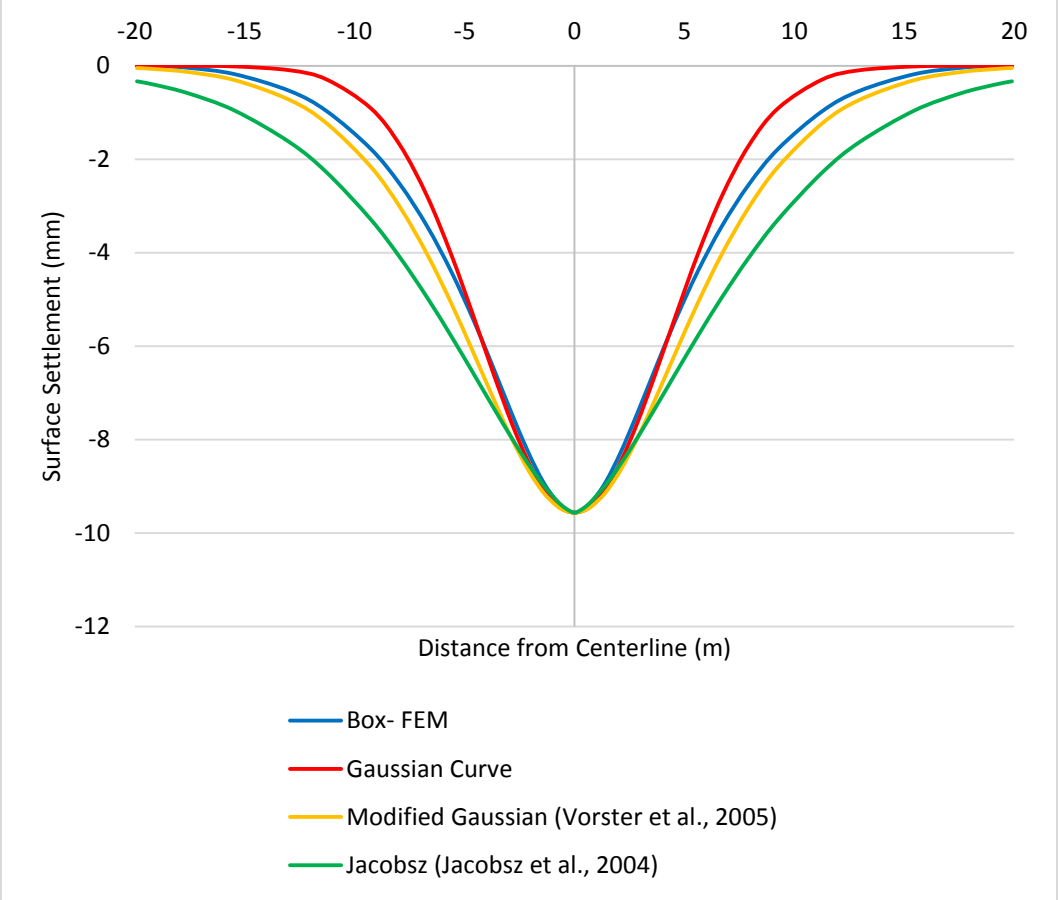

Figure 5-30 Comparison of Empirical Ground Surface Models- Deep Box Installation in Sand

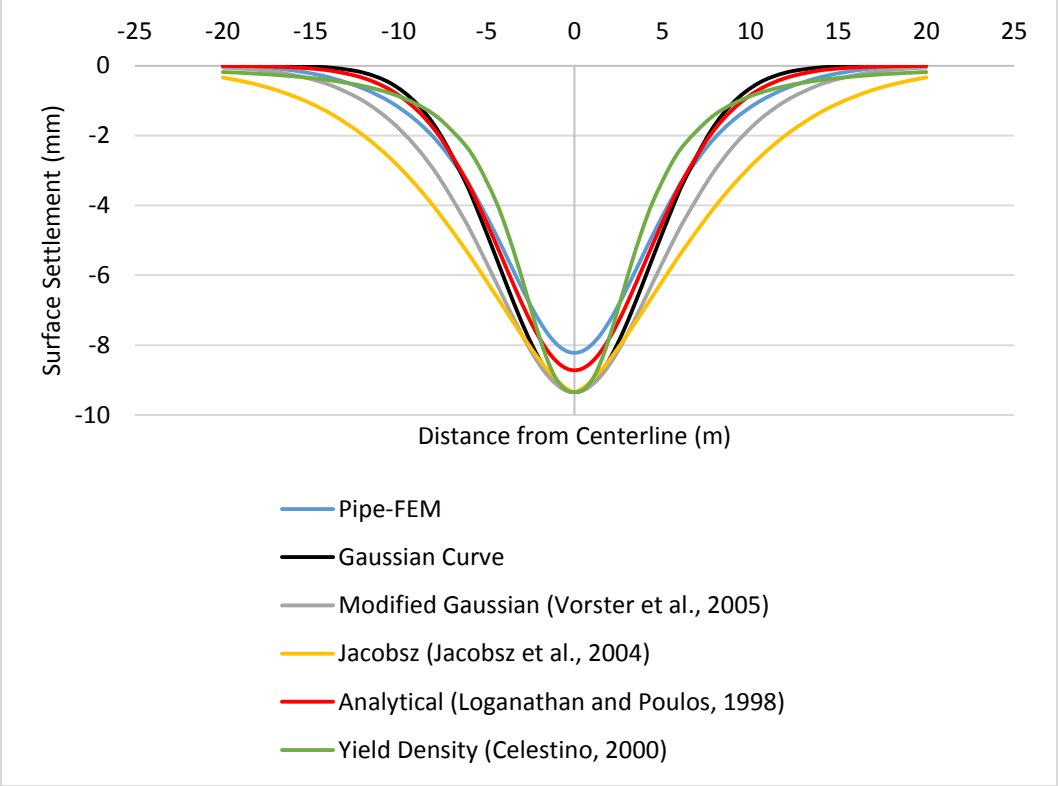

Figure 5-31 Comparison of Empirical Ground Surface Models- Deep Pipe Installation in Layered Clayey Soil (Marshall, 1998)

DISCUSSION ON EFFECT OF VERTICAL STRESS ABOVE PIPE AND BOX

Figures 5-33 and 5-34 present effect of vertical stress over pipe and box for models generated form data obtained from Heathrow Express Trial Tunnel at depth 5 m (16.4 ft) and 10 m (32.8 ft) from ground surface respectively. As can be seen at the centerline, the vertical stresses for pipe at both cases are less than that for box. This means for the same overcut, less stress distribution occurs over the pipes than box. In addition, effect of box span (width) can be seen in Figure 5-33. Vertical stress above box with smaller span is higher so less stress distribution occurs, and less ground settlement can be predicted. Figure 5-35 shows vertical stress contour above box from numerical analysis in Abaqus.

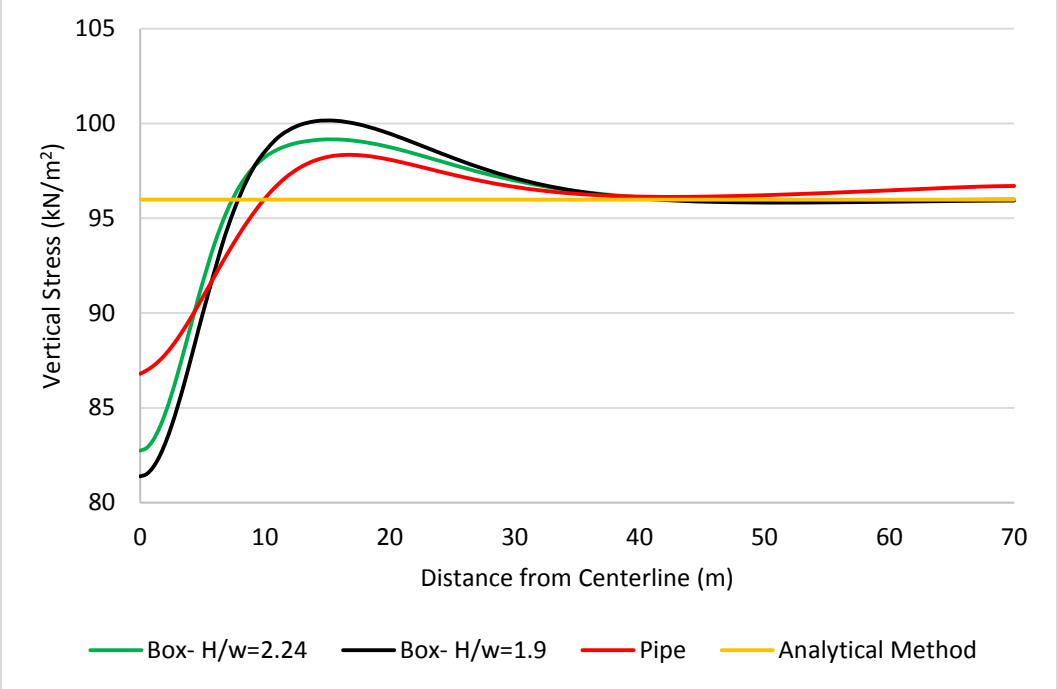

Figure 5-32 Vertical Stress above Pipe and box at Depth 5 m

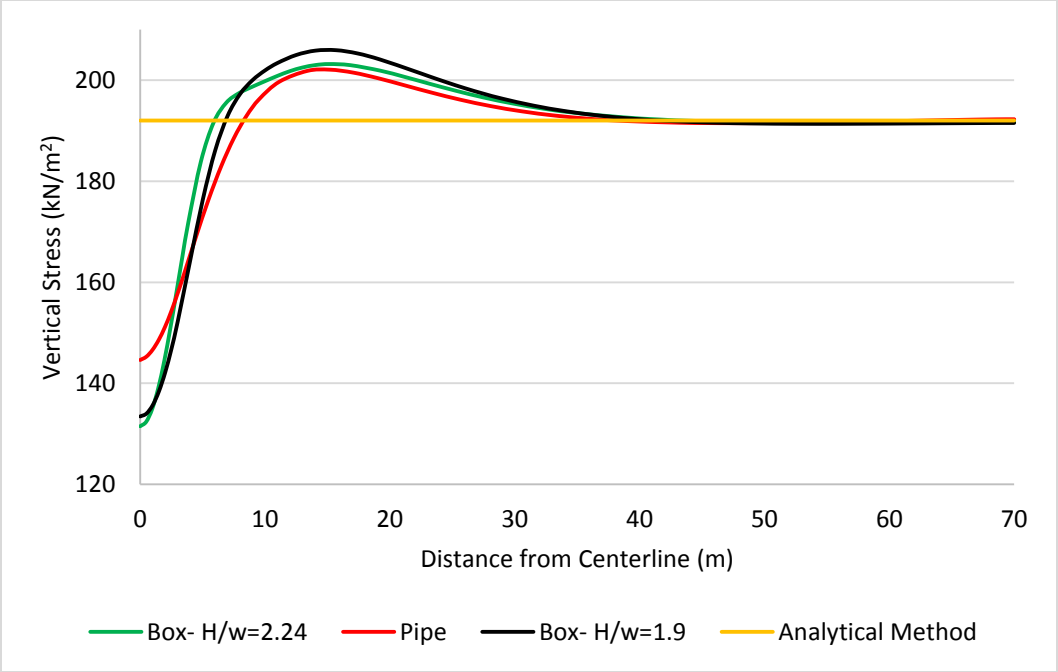

Figure 5-33 Vertical Stress above Pipe and box at Depth 10 m

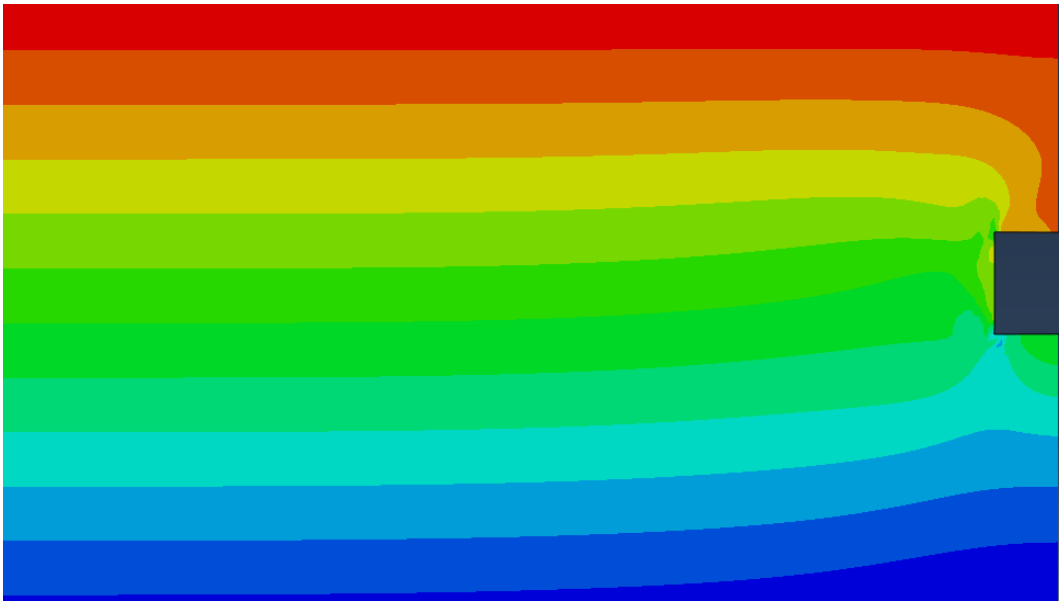

Figure 5-34 Vertical Stress Contour above Box

CHAPTER SUMMARY

This chapter presented results from finite element for pipe and box jacking in various soil conditions, depths and pipe/box sizes. Effect of overcut excavation in box jacking and volume loss in fine soils were also discussed. Results showed that box with same cross-sectional area and its width equal to pipe diameter, had greater surface, subsurface and horizontal soil displacement than pipes. It was also observed that empirical and analytical predictive methods could be applied for box with the same cross-sectional area as pipe. Other empirical methods such as Modified Gaussian Curve were fitted to the curves obtained from numerical analysis.

Chapter 6 CONCLUSIONS AND RECOMMENDATIONS FOR FUTURE RESEARCH

CONCLUSIONS

The advances in trenchless construction technology have brought many new tunnel installation methods in recent years. For example, box installations with high span sizes are carried out successfully in the world. A method of excavation is being developed where rectangular TBMs are reducing the size of the overcut and vertical surface settlements. Circular tunnels are still popular where the excavation methods are from hand excavation and microtunneling for the small to medium tunnel sizes and tunnel boring machines for large size tunnels. Various methods of underground pipe installation such as pipe jacking or segmental linings are selected based on the soil conditions, tunnel size, above surface conditions and project conditions.

In this dissertation, tunneling, pipe/box jacking, and ground conditions were simulated using finite element method and soil settlement was applied to the tunnel by applying step-by-step stress reduction method. Since the ground settlement is a rapid settlement, total stress condition was chosen for all soil types to consider the effect of undrained soil condition. The following summarizes the parameters considered in this study:

- Methods of tunnel construction with emphasis on hand mining and open shield tunneling,
- Soil condition from coarse materials to fine materials (sand and clay),
- Tunnel shape (circular or rectangular),
- Depth of installation,
- Volume loss or overcut size,
- Tunnel size,
- Surface and subsurface ground settlement, and

- Comparison of empirical, analytical and numerical methods for settlement prediction.

Simulated results from numerical analysis were compared to real-life case histories, empirical and analytical methods. Ground settlement pattern induced by pipe or box installations showed similarity between all methods. However, the magnitude of settlement was a function of overcut size (volume loss), soil conditions, tunnel shape, and tunnel depth from the ground surface. Various real-life case histories were selected from the literature to determine the effects of such parameters on vertical and horizontal ground displacements over the box and pipe. The most important findings of this research can be summarized as below:

- Boxes with the same cross-sectional areas and same overcut sizes with pipes show higher surface ground settlements than pipes in almost all soil conditions.
- Size of overcut excavation has a direct impact on vertical surface settlement. However, in sandy soils it presents a nonlinear relationship between size of overcut and surface settlement. In clayey soils, findings agree reasonably well with empirical method.
- Depth to axis to box width (span) ratio can be used as a surface settlement indicator. In other words, the less ratio, the higher surface and subsurface ground settlement and vice versa.
- There is no logical relationship between box height (rise) and surface ground settlement.
- Box with width equal to height ($W=H_1$) almost is an ideal box size because, in most cases, in has almost the minimum surface ground settlement as compared to other box shapes with the same cross section area.

- Total volume loss in clayey soil was transferred to the surface compared with 40% to 50% in sandy soil conditions.
- In general, Gaussian distribution curve was not able to estimate surface ground settlement accurately. This method overestimated maximum vertical surface settlement and underestimated settlement trough width.
- Other empirical methods such as Modified Gaussian distribution curves were able to accurately predict surface ground settlement.
- Vertical stress on top of box was minimum on the box centerline and increased until it reached its maximum on the edge of box. Then, it decreases away from the edge of box to reach expected value (e.g., γH).
- Higher soil stress disturbance above box than pipe was the most important factor causing higher surface settlement in boxes.

RECOMMENDATIONS FOR FUTURE RESEARCH

Based on the conclusions and findings of this study, the following recommendations for future study of ground settlement induced by trenchless technology constructions are provided:

- Consider the effects of live load on vertical surface and subsurface settlement
- Consider the effects of above ground structures on surface ground settlement induced by box and pipe installation.
- Study the effects of other trenchless technologies such as HDD, Pipe Bursting or Pipe Ramming on surface and subsurface ground settlement.
- Take into account effects of face loss on surface settlement with an emphasis on box with different installation depths.
- Develop the current study with 3-D modelling and compare the results with 2-D analyzes.

- Consider the effects of grouting on short-term and long-term surface settlements.

APPENDIX A – CENTRIFUGE TEST RESULTS

(Loganathan et al., 2000)

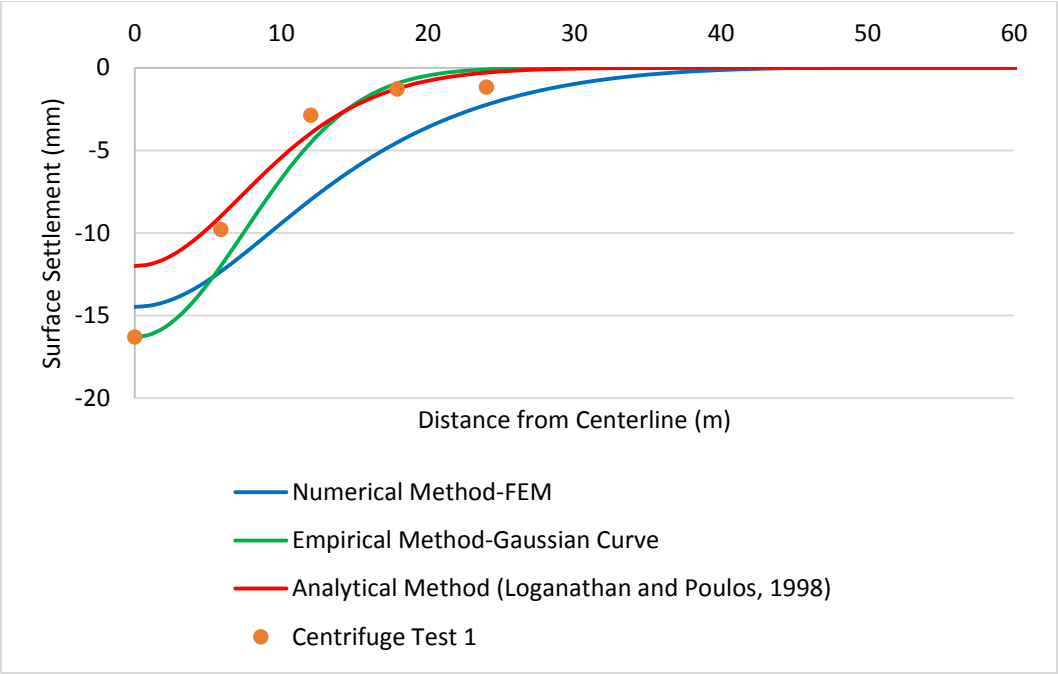

Figure A-1 Surface Settlement Results (Centrifuge Test 1)

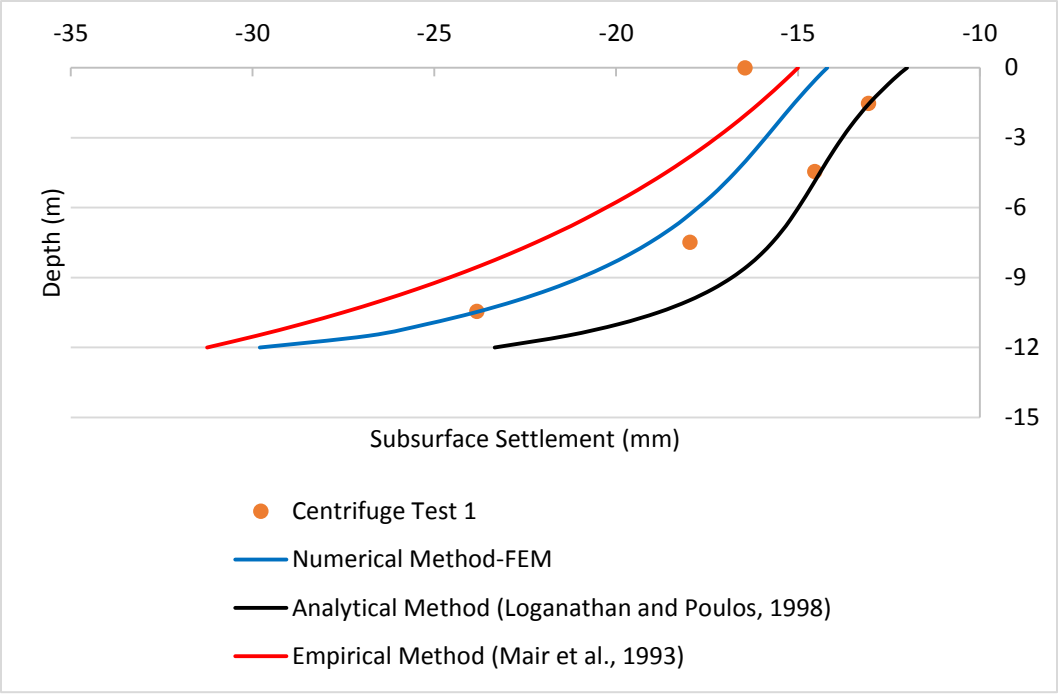

Figure A-2 Subsurface Settlement Results (Centrifuge Test 1)

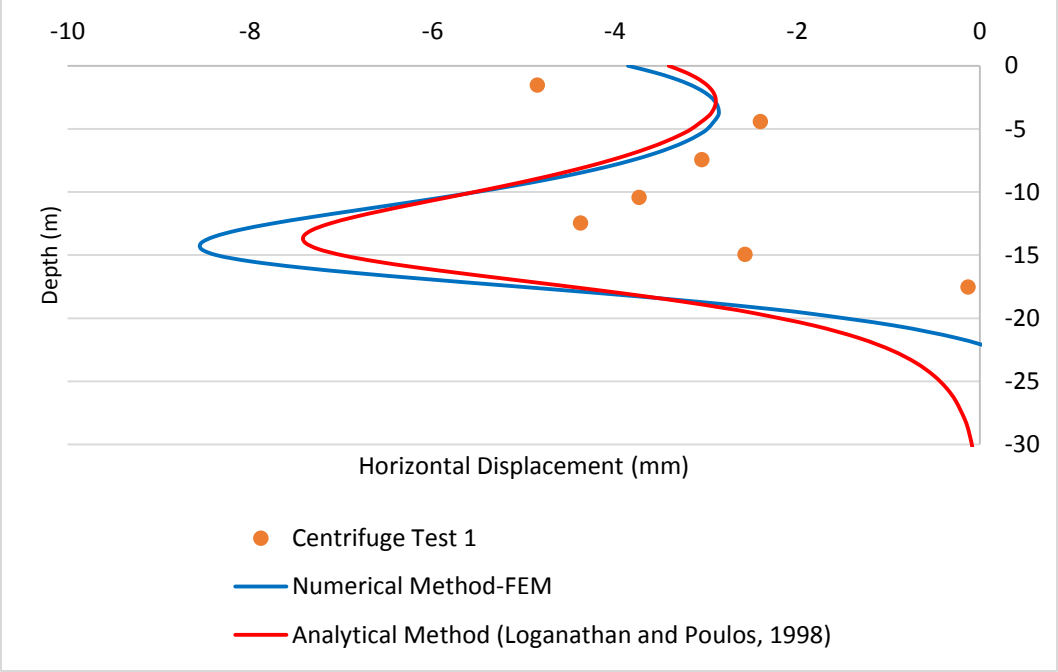

Figure A-3 Horizontal Displacement 5.5 m from Tunnel Centerline (Centrifuge Test 1)

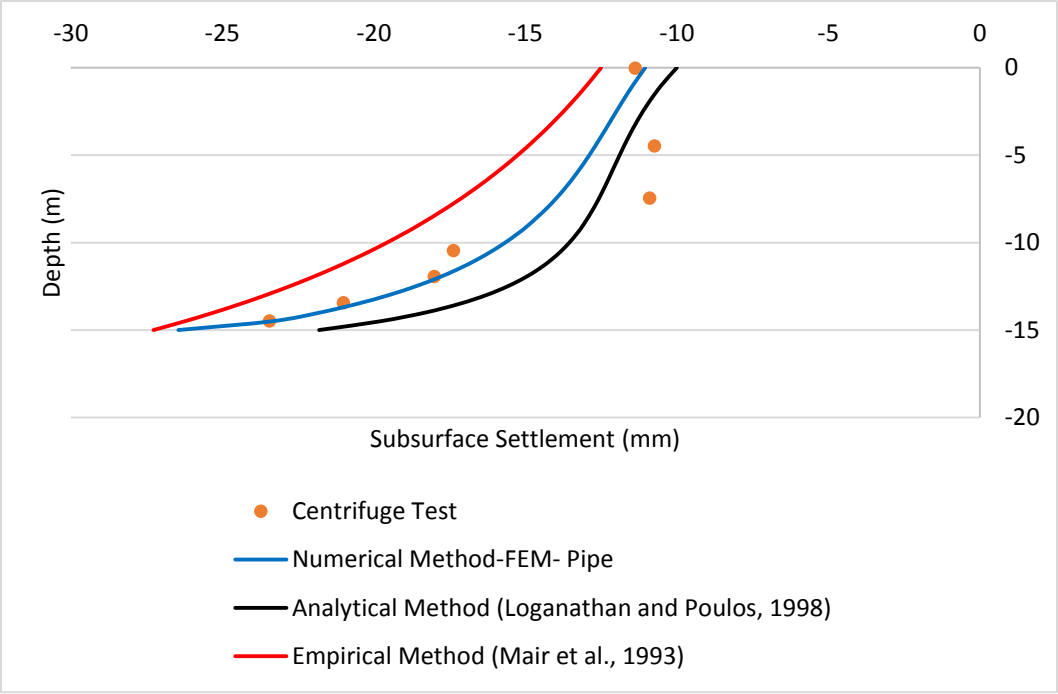

Figure A-4 Subsurface Settlement Results (Centrifuge Test 2)

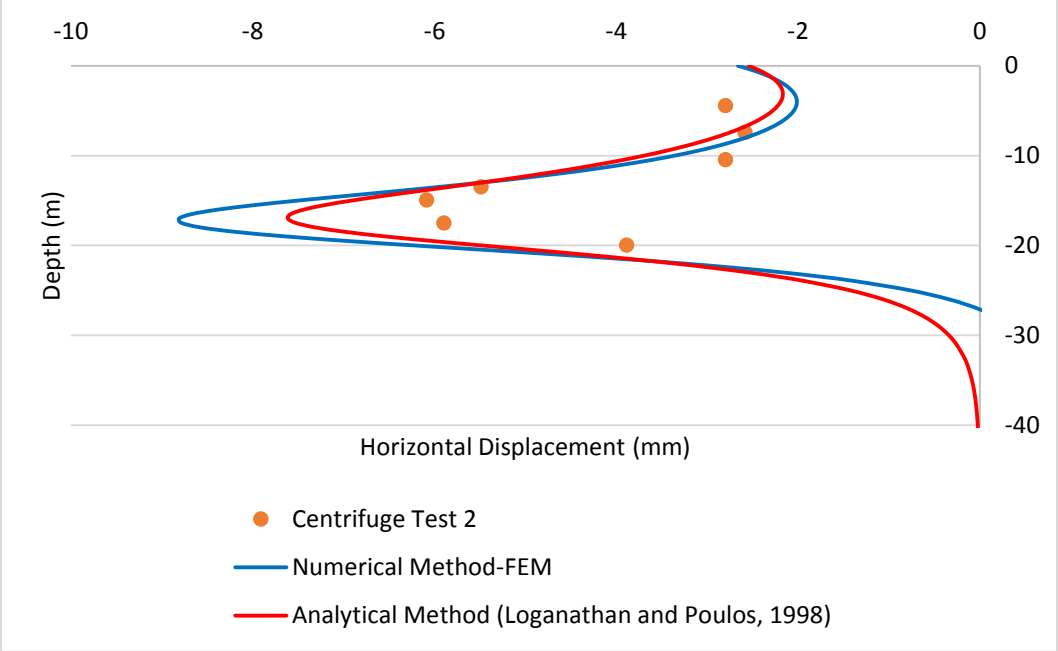

Figure A-5 Horizontal Displacement 5.5 m from Tunnel Centerline (Centrifuge Test 2)

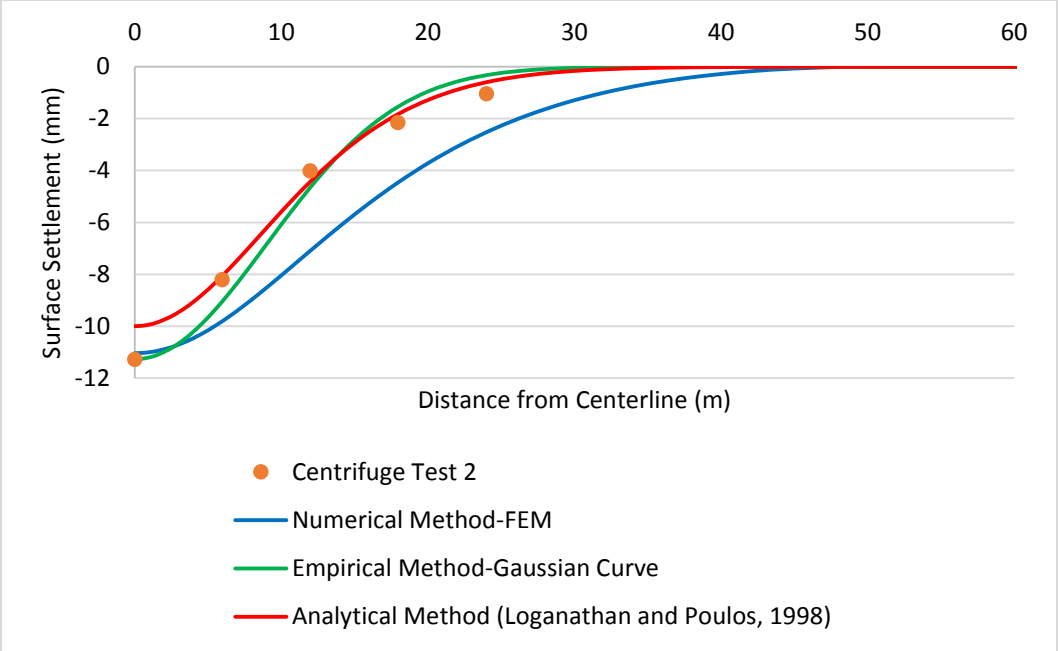

Figure A-6 Surface Settlement Results (Centrifuge Test 2)

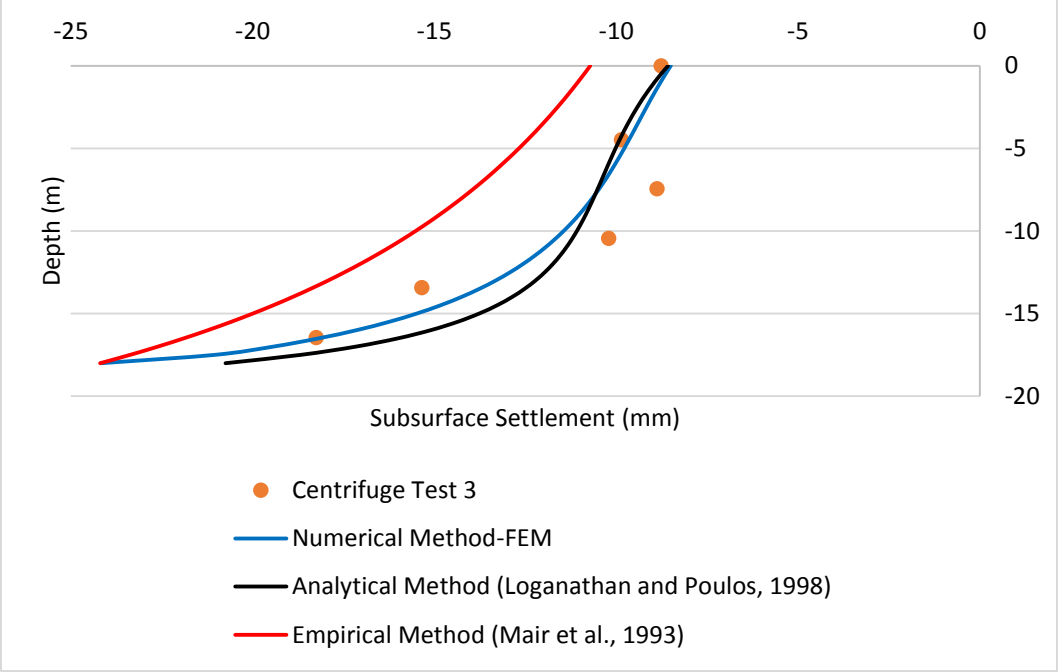

Figure A-7 Subsurface Settlement Results (Centrifuge Test 3)

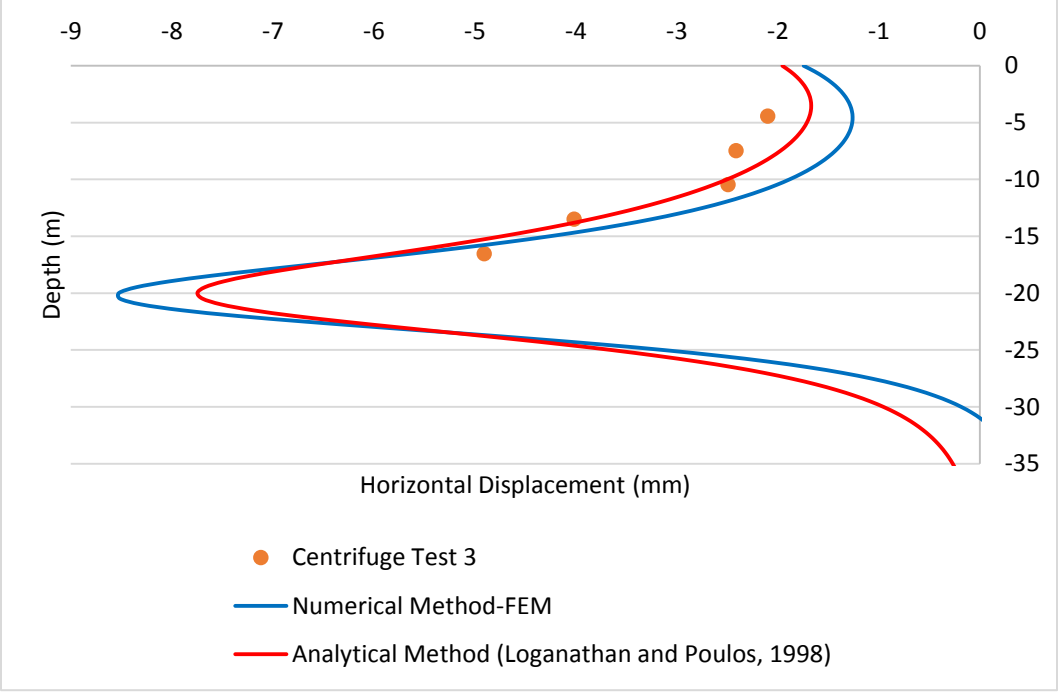

Figure A-8 Horizontal Displacement 5.5 m from Tunnel Centerline (Centrifuge Test 3)

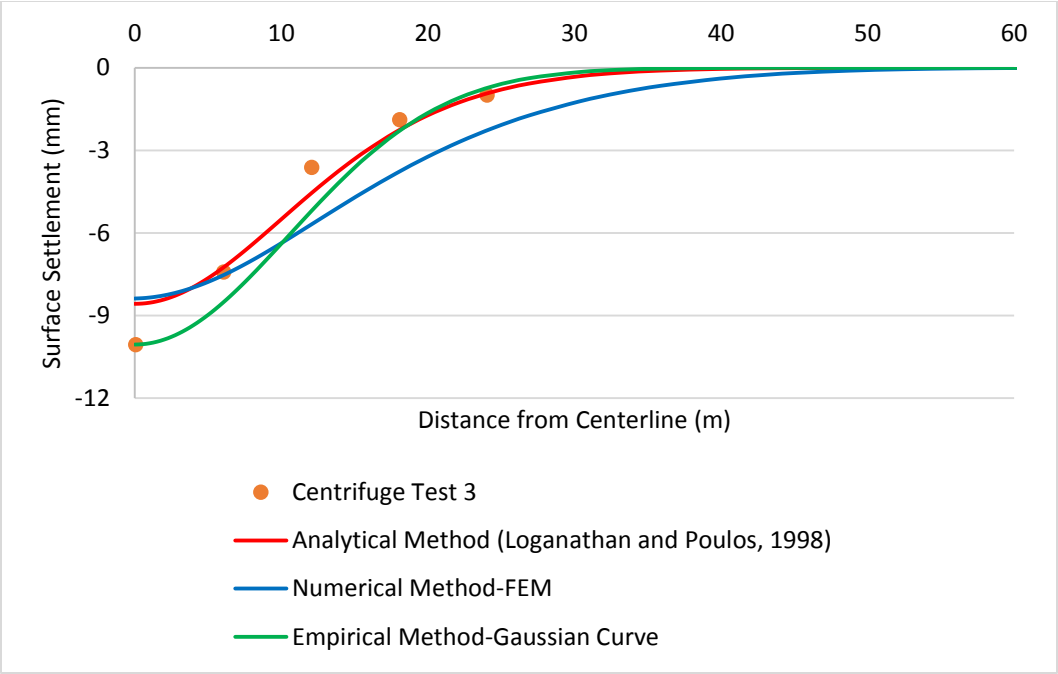

Figure A-9 Surface Settlement Results (Centrifuge Test 3)

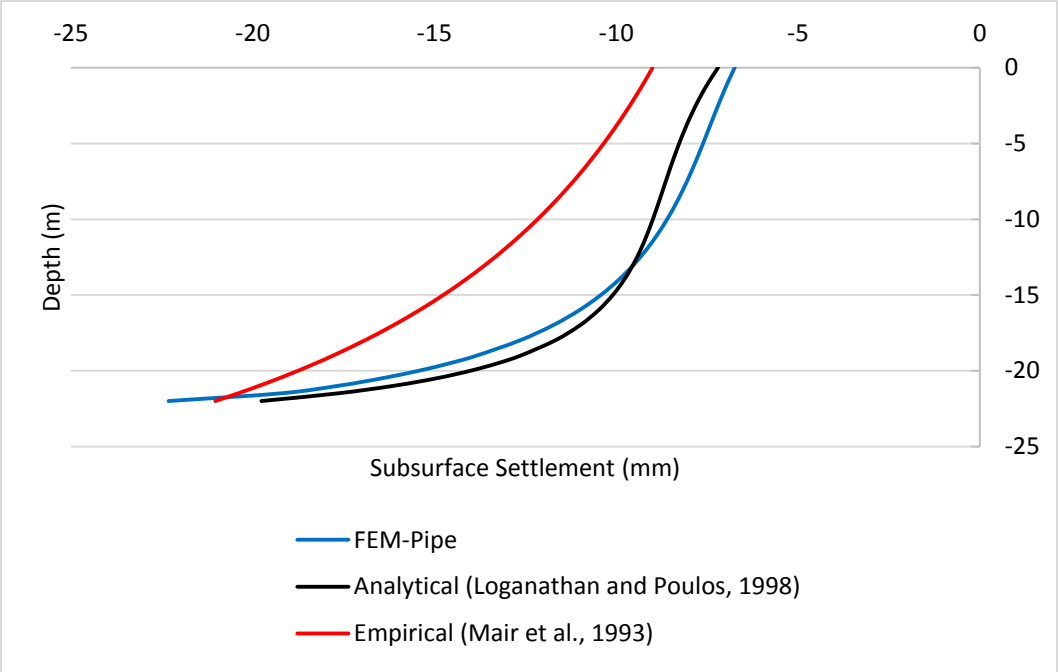

Figure A-10 Subsurface Settlement Results for Pipe (Depth to axis= 25 m)

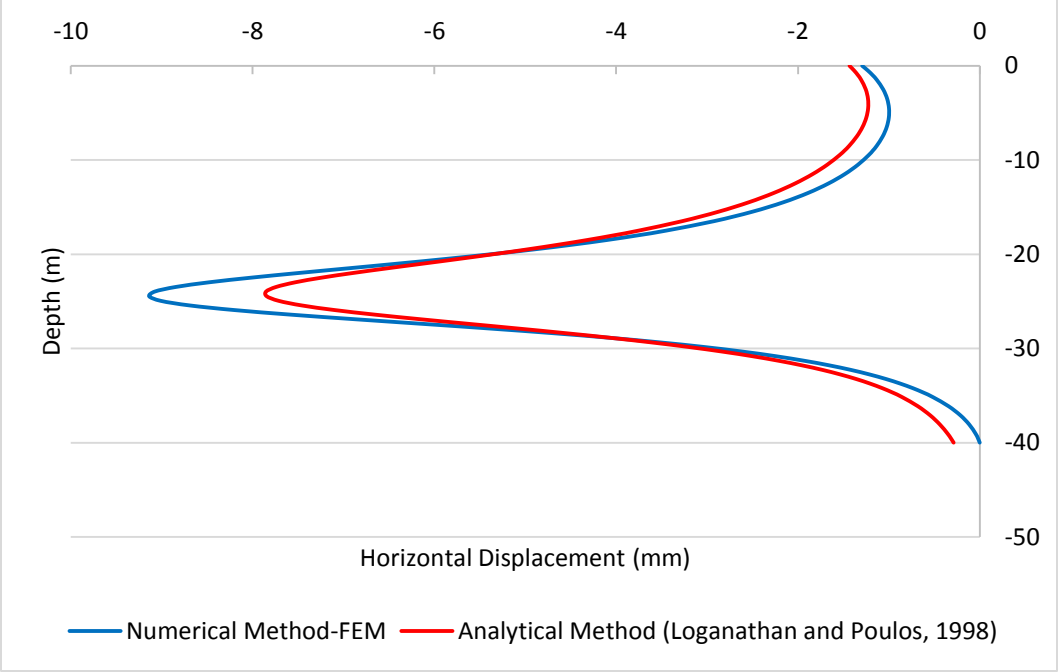

Figure A-11 Horizontal Displacement 5.5 m from Tunnel Centerline (Depth to axis= 25 m)

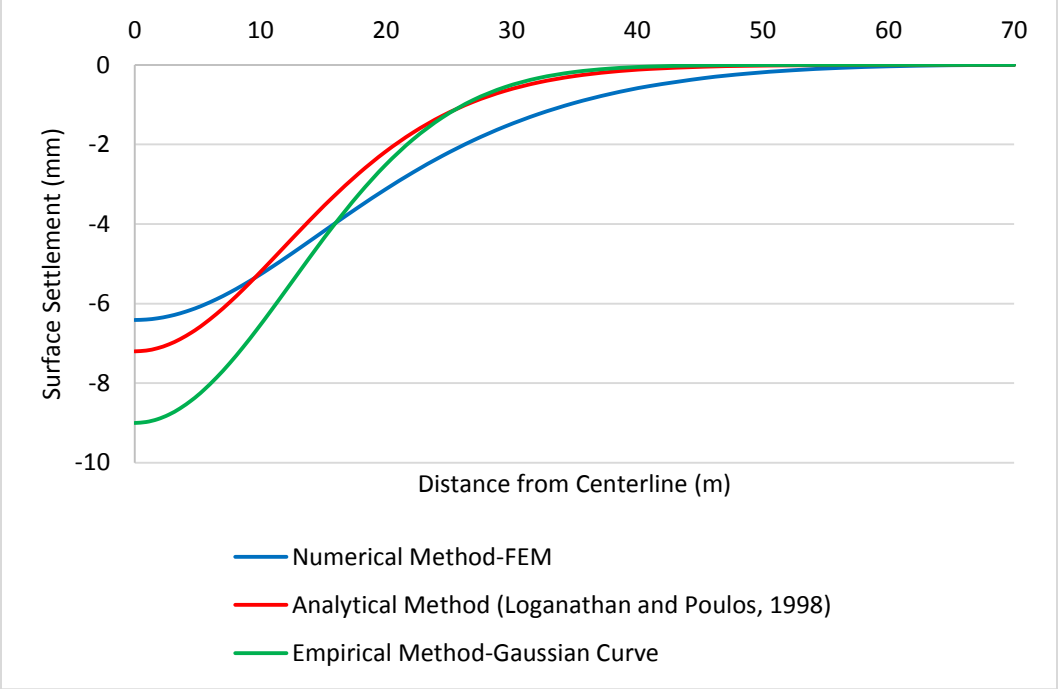

Figure A-12 Surface Settlement Results (Depth to axis= 25 m)

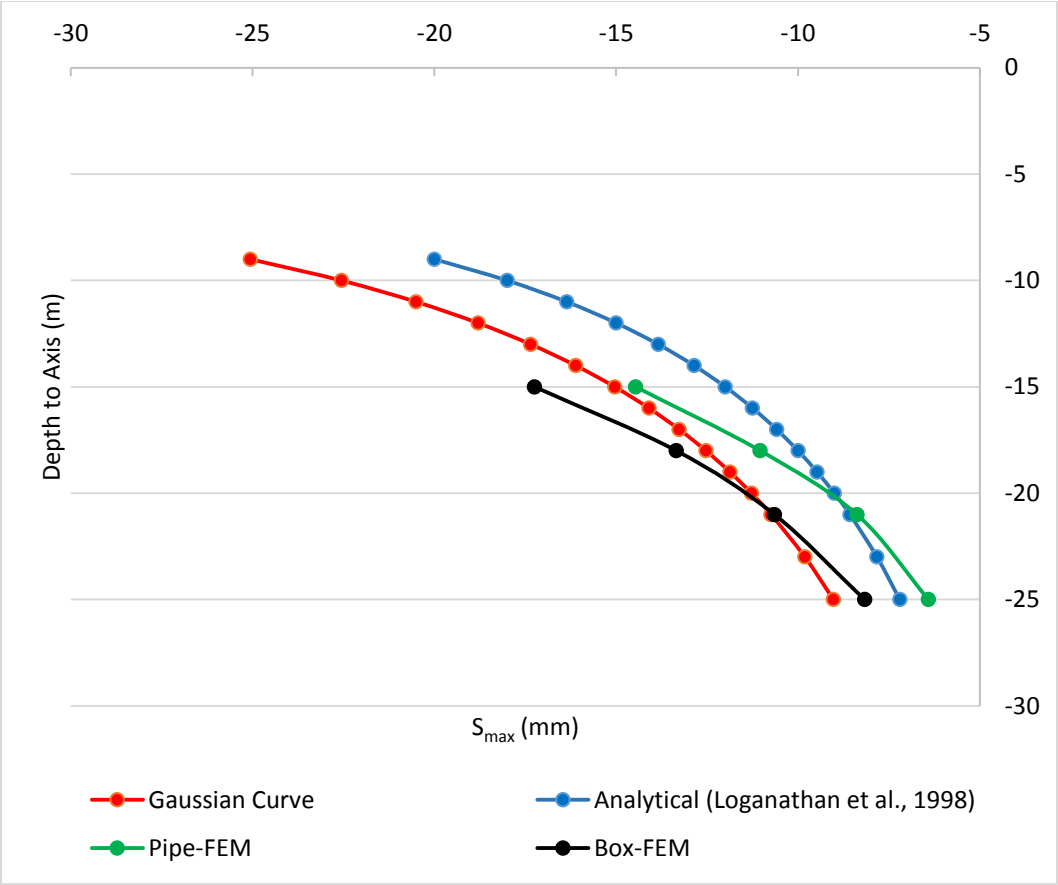

Figure A-13 Relationship between Maximum Surface Settlement and Depth

APPENDIX B – COMPARISON OF PIPE AND BOX (FINITE ELEMENT RESULTS)

(Based on data obtained from Loganathan et al., 2000)

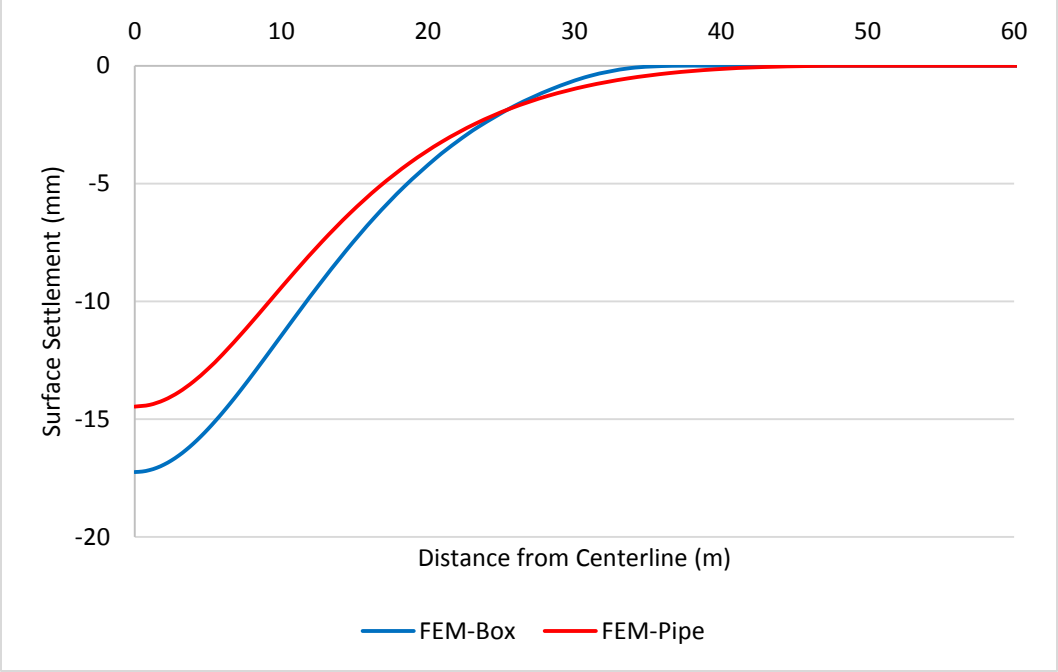

Figure B-1 Surface Settlement Results (Depth to Axis= 15 m)

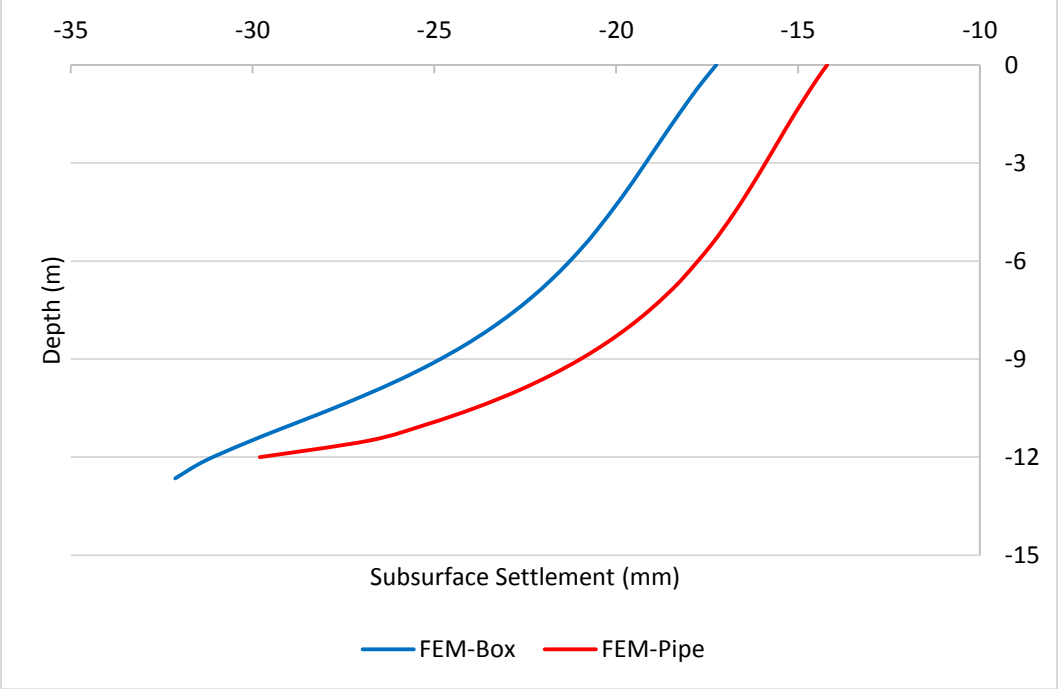

Figure B-2 Subsurface Settlement Results (Depth to axis= 15 m)

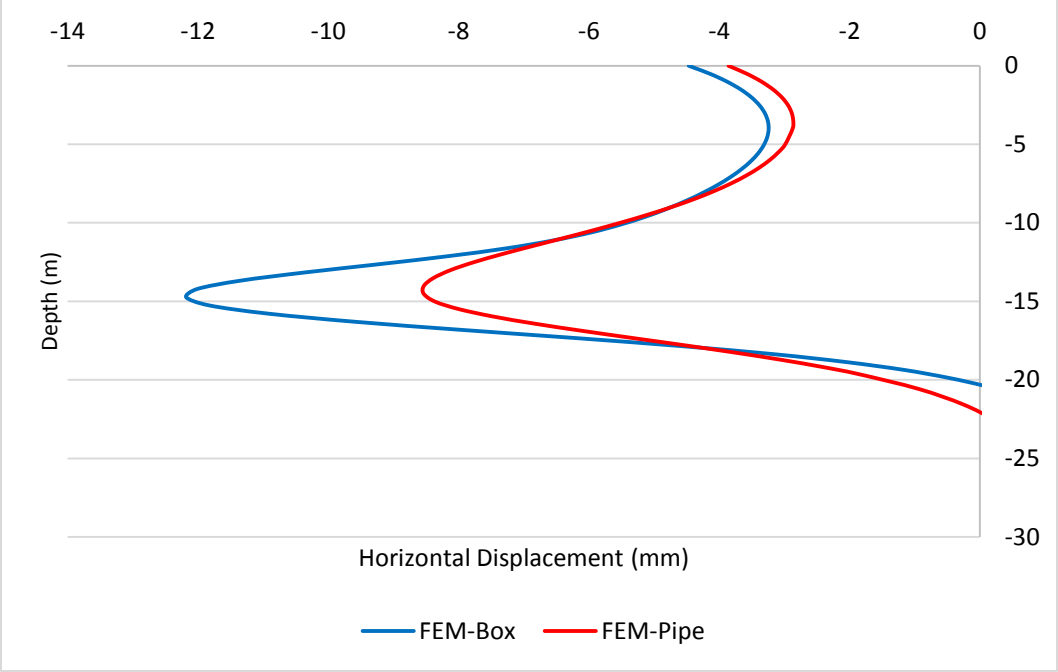

Figure B-3 Horizontal Displacement 5.5 m from Tunnel Centerline (Depth to axis= 15 m)

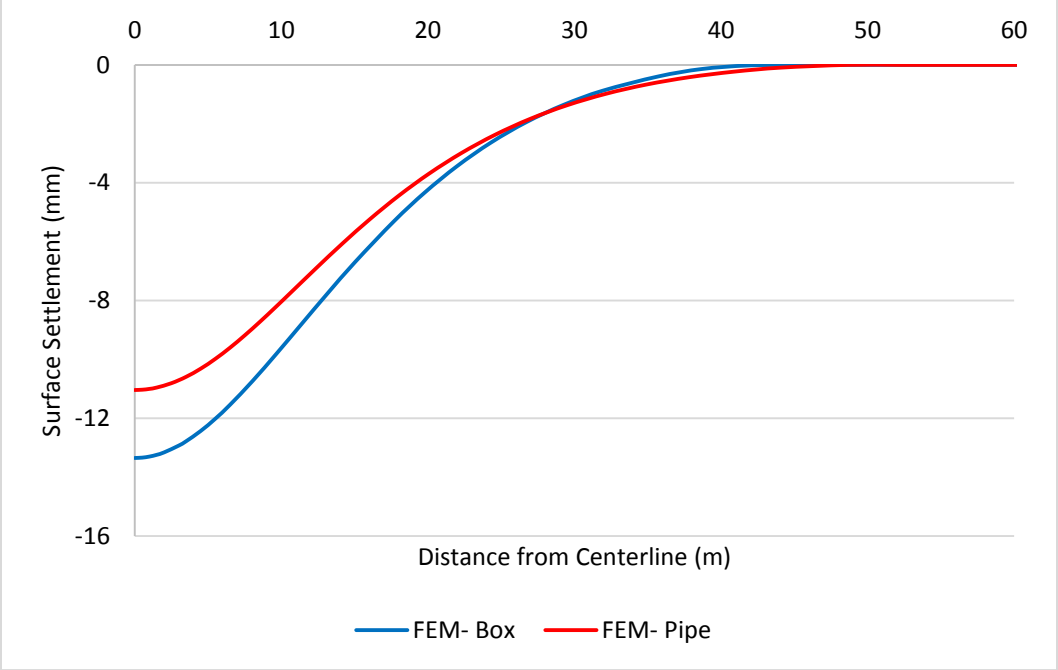

Figure B-4 Surface Settlement Results (Depth to Axis= 18 m)

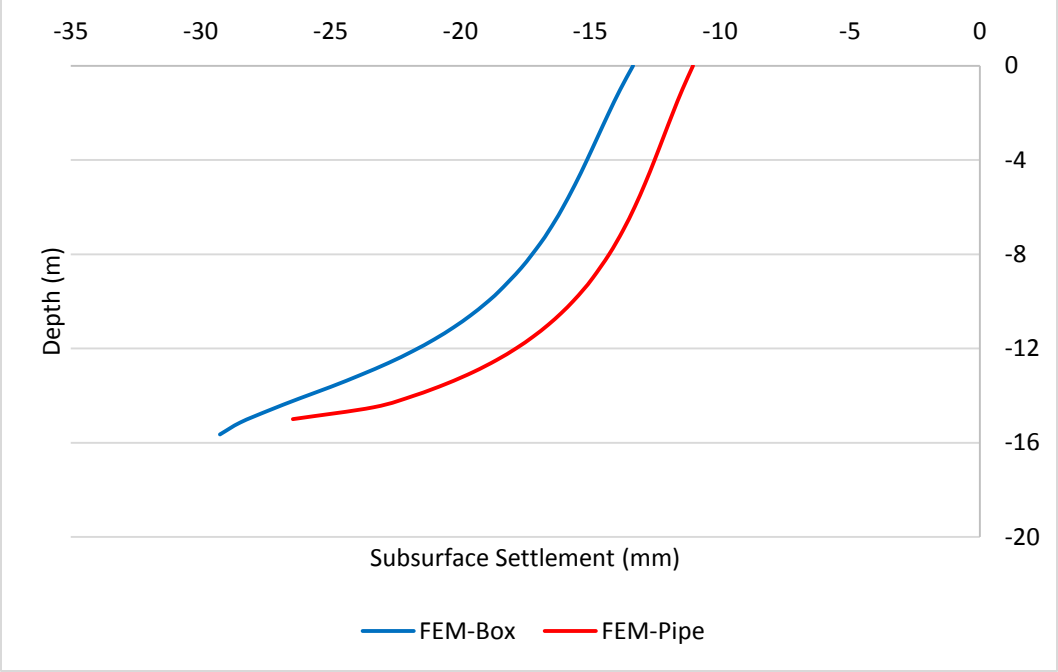

Figure B-5 Subsurface Settlement Results (Depth to axis= 18 m)

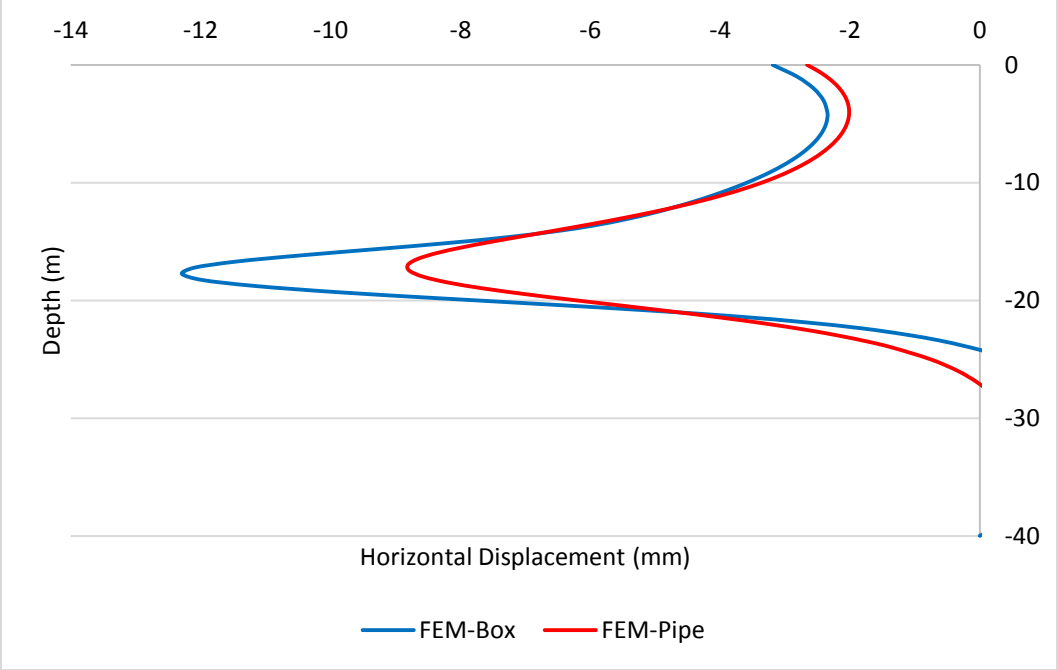

Figure B-6 Horizontal Displacement 5.5 m from Tunnel Centerline (Depth to axis= 18 m)

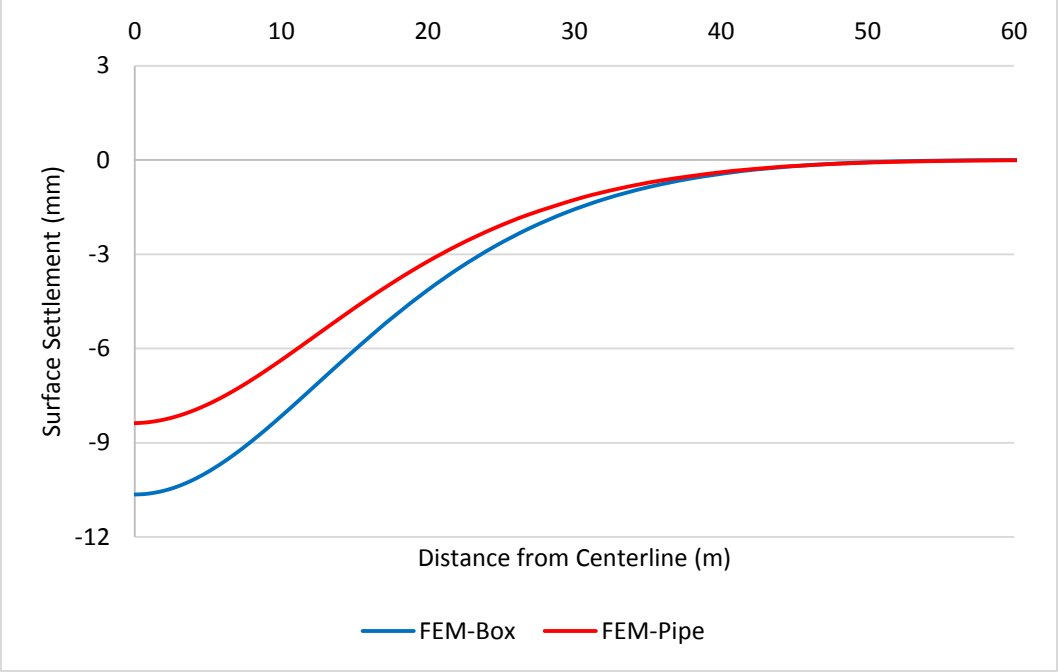

Figure B-7 Surface Settlement Results (Depth to Axis= 21 m)

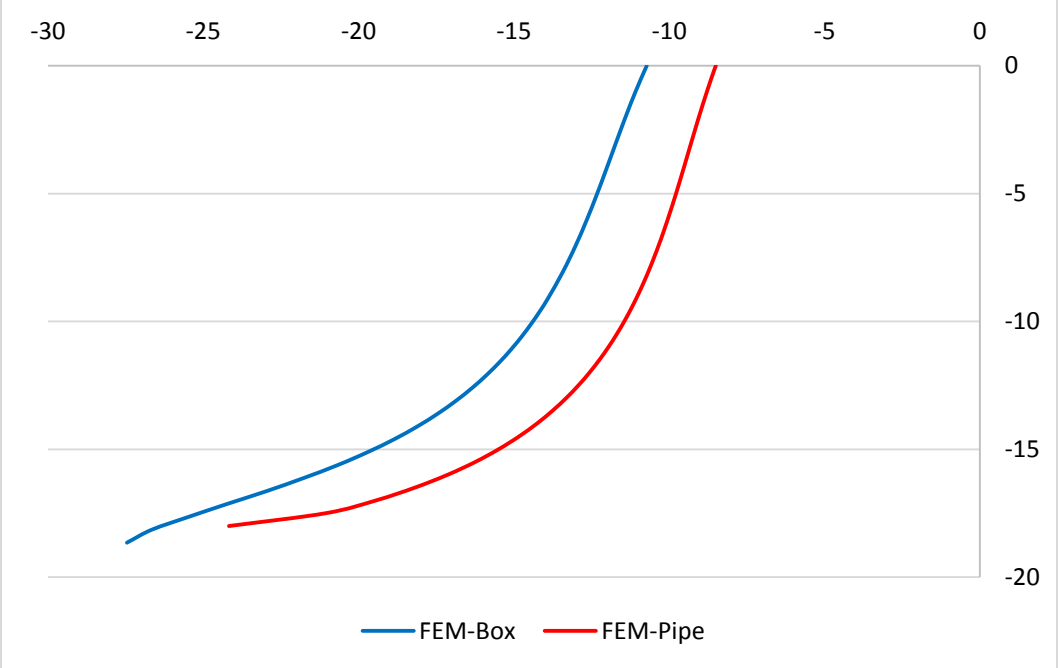

Figure B-8 Subsurface Settlement Results (Depth to axis= 21 m)

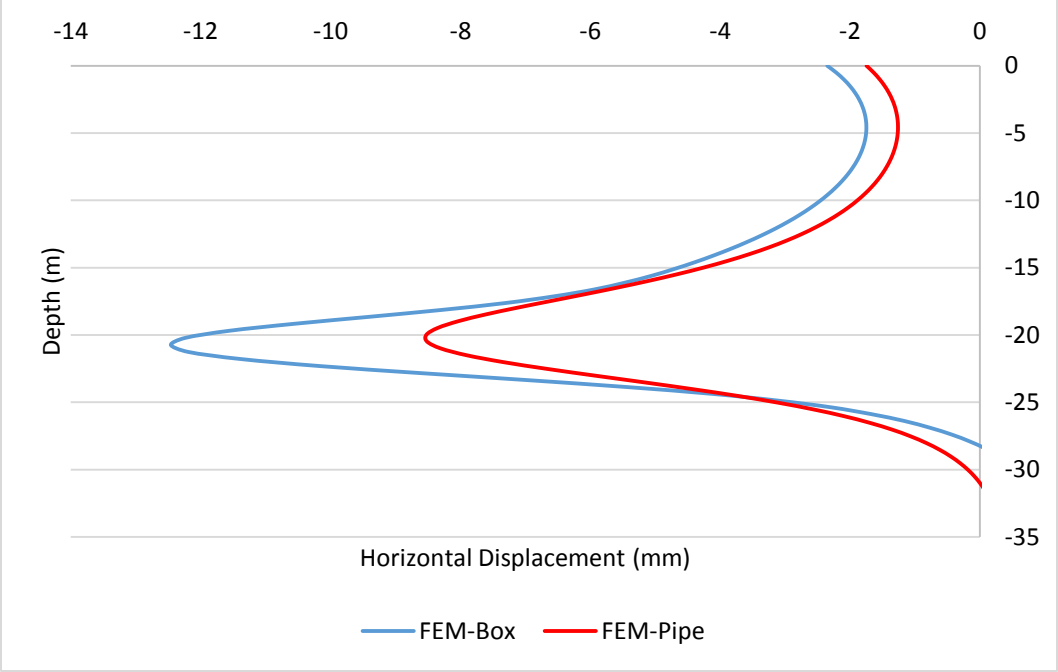

Figure B-9 Horizontal Displacement 5.5 m from Tunnel Centerline (Depth to axis= 21 m)

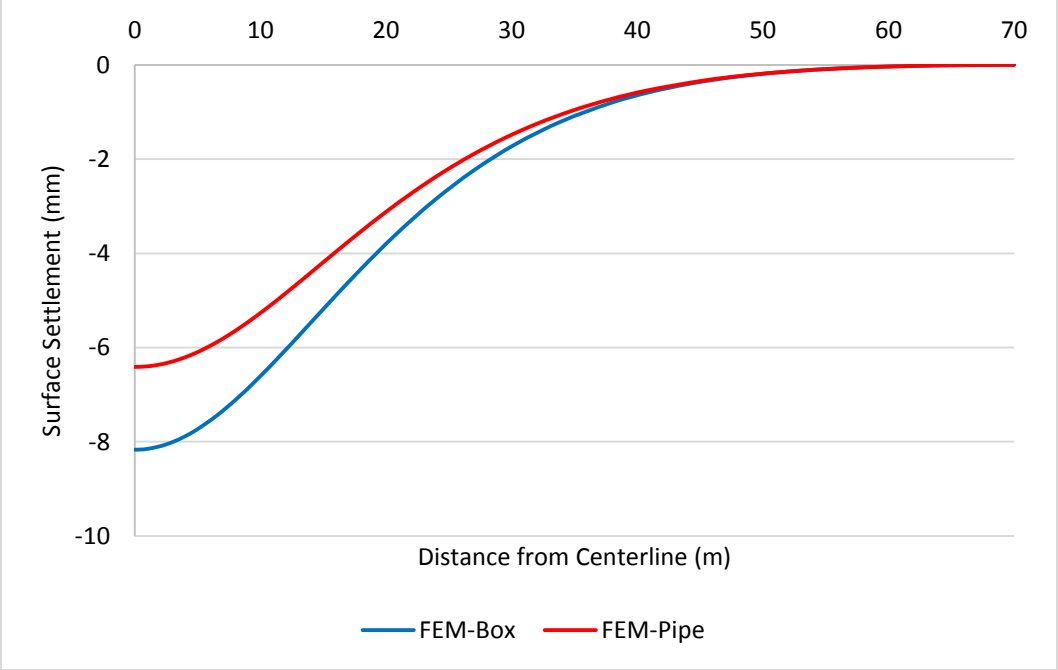

Figure B-10 Surface Settlement Results (Depth to Axis= 25 m)

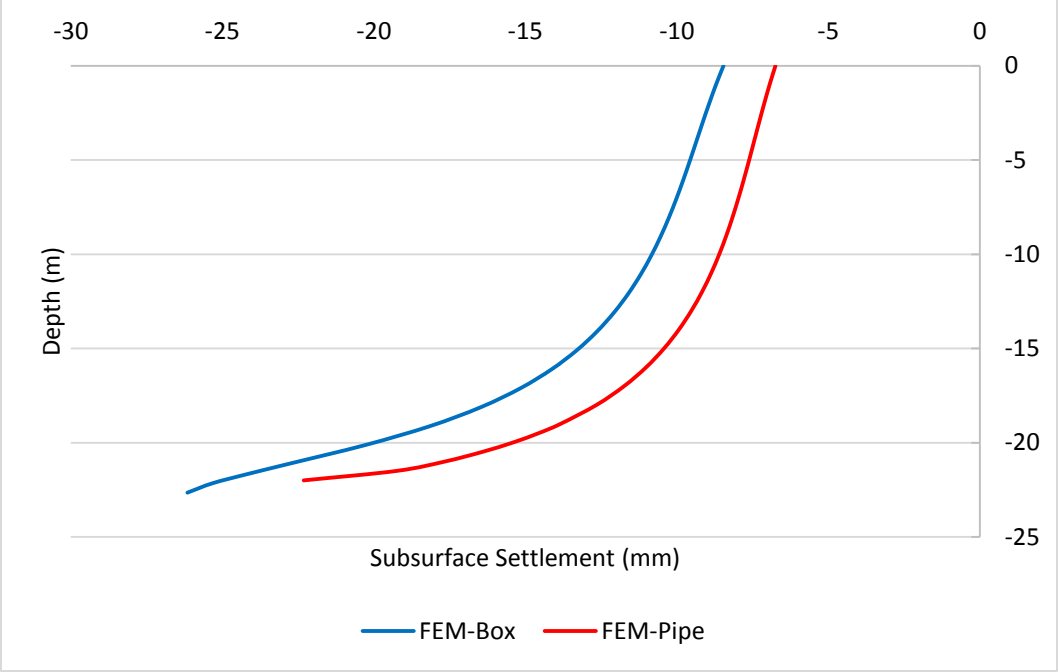

Figure B-11 Subsurface Settlement Results (Depth to axis= 25 m)

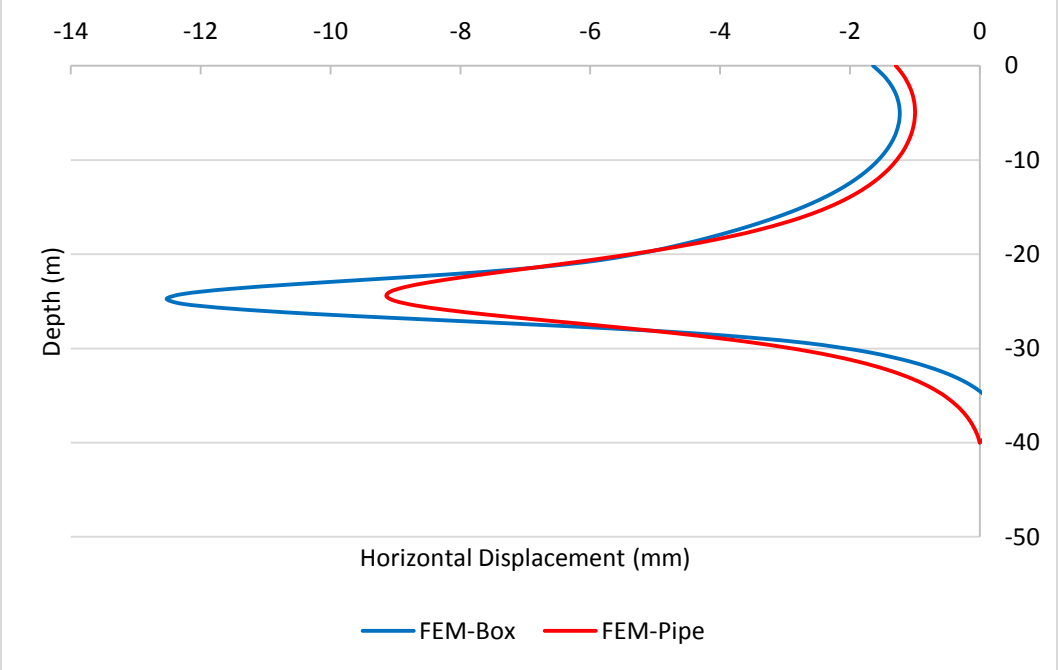

Figure B-12 Horizontal Displacement 5.5 m from Tunnel Centerline (Depth to axis= 25 m)

LIST OF ACRONYMS

2-D	Two Dimensional
3-D	Three Dimensional
AASHTO	American Association of State Highway and Transportation
ANN	Artificial Neural Network
ASTM	American Society for Testing and Materials
BJ	Box Jacking
EPBM	Earth Pressure Balance Machine
FEA	Finite Element Analysis
FEM	Finite Element Method
H	Depth to Axis
H/W	Depth to Box Width Ratio
H_1	Box Height (Rise)
HDD	Horizontal Directional Drilling
HDPE	High Density Polyethylene Pipe
HEB	Horizontal Earth Boring
i	Settlement Trough Width
LRFD	Load and Resistance Factor Design
MT	Microtunneling
MTBM	Microtunneling-Boring Machine
OC	Overcut
PJ	Pipe Jacking
PVC	Polyvinyl Chloride
RTBM	Rectangular Tunnel Boring Machine

TBM	Tunnel Boring Machine
TCM	Trenchless Construction Method
TRM	Trenchless Renewal Method
TT	Trenchless Technology
TxDOT	Texas Department of Transportation
UCS	Unconfined Compressive Strength
USCS	Unified Soil Classification System
V_L	Volume Loss
W	Box Width (Span)

LIST OF DEFINITIONS

Earth pressure balance (EPB) machine: Type of microtunneling or tunneling machine in which mechanical pressure is applied to the material at the face and controlled to provide the correct counterbalance to earth pressures to prevent heave or subsidence. The term is usually not applied to those machines where the pressure originates from the main pipe jacking rig in the drive shaft/pit or to systems in which the primary counterbalance of earth pressures is supplied by pressurized drilling fluid (Najafi, 2010).

Heaving: A process in which the ground in front of a tunneling or pipe jacking operation may be displaced forward and upward, causing an uplifting of the ground surface (Najafi, 2010).

Jacking: The actual pushing of pipe or casing in an excavated hole. This is usually done with hydraulic cylinders (jacks) but has been done with mechanical jacks and air jacks (Najafi, 2010).

Lubrication or Drilling fluid: A mixture of water and usually bentonite and/or polymer continuously pumped to the cutting head to facilitate cutting, reduce required torque, facilitate the removal of cuttings, stabilize the borehole, cool the head, and lubricate the installation of the product pipe. In suitable soil conditions water alone may be used (Najafi, 2010).

Microtunneling: A trenchless construction method for installing pipelines. Microtunneling uses all of the following features during construction: (1) Remote controlled, (2) Guided, (3) Pipe jacked, (4) Continuously supported (Najafi, 2010).

Pipe jacking: A system of directly installing pipes behind a shield machine by hydraulic jacking from a drive shaft, such that the pipes form a continuous string in the ground (Najafi, 2010).

Trenchless Technology: Also, NO-DIG, techniques for underground pipeline and utility construction and replacement, rehabilitation, renovation (collectively called renewal), repair, inspection, and leak detection, etc., with minimum or no excavation from the ground surface (Najafi, 2010).

Tunnel boring machine (TBM): (1) a full-face circular mechanized shield machine, usually of worker-entry diameter, steerable, and with a rotary cutting head. For pipe jacking installation, it leads a string of pipes. It may be controlled from within the shield or remotely such as in microtunneling. (2) A mechanical excavator used in a tunnel to excavate the front face of the tunnel (Najafi, 2010).

Tunnel: An underground conduit, often deep and expensive to construct, which provides conveyance and/or storage volumes for wastewater, often involving minimal surface disruption (Najafi, 2010).

REFERENCES

Acharya, R., Han, J., Brennan, J., Parsons, R. and Khatri, D., (2014). Structural Response of a Low-Fill Box Culvert under Static and Traffic Loading, Journal of Performance of Constructed Facilities. Volume 30, Issue 1.

Addenbrooke, T. I., Potts, D. M., and Puzrin, A. M., (1997). The Influence of Pre-Failure Soil Stiffness on the Numerical Analysis of Tunnel Construction. Geotechnique 47, No. 3, pp. 693-712.

Atkinson J H and Potts D M (1979). Subsidence above Shallow Tunnels in Soft Ground. Journal of Geotechnical Engineering, American Society of Civil Engineers, GT4, pp. 307-325.

Attewell, P. B., and Farmer, I. W., (1974). Ground Disturbance Caused by Shield Tunneling in a Stiff, Overconsolidated Clay. Engineering Geology, Vol 8. pp. 361-381.

Bennett, R. D. (1998). Jacking Forces and Ground Deformations Associated with Microtunneling. Dissertation in Partial Fulfillment of the Requirements for the Degree of Doctor of Philosophy in Civil Engineering. University of Illinois at Urbana-Champaign, Illinois.

Bloodworth, A. (2002). Three-Dimensional Analysis of Tunnelling Effects on Structures to Develop Design Methods, Ph.D. Dissertation. University of Oxford.

Celestino, T. B., Gomes, R. A. M., and Bortolucci, A. A. (2000). Errors in Ground Distortions Due to Settlement Trough Adjustment. Tunn. Undergr. Space Technol., 15(1), 97–100.

Chaurasia, B., (2012). Identifying Issues Impacting Productivity of Box Jacking Projects. Arlington, TX. Master Thesis. The University of Texas at Arlington.

Cheng, C. Y., (2003). Finite Element Study of Tunnel-Soil-Pile Interaction. M Eng. thesis, National University of Singapore.

China National Complete Plant & Tools Co. Ltd. (2018). Earth Pressure Balance Rectangle Pipe Jacking Machine 6 m × 4.3 m Size CE, available at: < http://www.drillcuttingbit.com/sale-7711338-earth-pressure-balance-rectangle-pipe-jacking-machine-6-m-4-3-m-size-ce.html>.

Chu, V. (2010). A Self-Learning Manual, Mastering Different Fields of Civil Engineering Works (VC-Q & a Method), available at: <

https://www.scribd.com/document/52527588/Mastering-Civil Engineering-QA-Methods>.

Clarkson T. E. and Ropkins J.W.T. Pipe-Jacking Applied to Large Structures. Proc. Instn. Civ. Engnrs, Part I, 1977, 62, Nov. 539-561.

Cording, E. J. and Hansmire, W. H. (1975). Settlement around Soft Ground Tunnels, General Report: Session IV, Tunnels in Soil. Proc. 5th Pan-American Congress on Soil Mech. And Foundations Eng.

Craig, R. N., and Muir Wood, A. M., (1978). A Review of Tunnel Lining Practice in the United Kingdom. Supplementary Report. 335, Transport and Road Research Laboratory.

Deane, A. P., and Bassett, R. H., (1995). The Heathrow Trial Tunnel. Proceeding of Institution of Civil Engineering: Geotechnical Engineering, 113, pp.144-156.

Evans, C. (1983). An Examination of Arching in Granular Soils. Massachusetts. Master Thesis. Massachusetts Institute of Technology (MIT).

Fujita, K. (1981). On the surface settlements caused by various methods on shield tunneling. Proc. XIth Int. Conf. On Soil Mechanics and Foundations Engineering, Vol. 4, pp. 609-610.

Herrenknecht. (2018). Stability through Face Support Pressure, Available at: < https://www.herrenknecht.com/en/products/core-products/tunnelling/epb-shield.html>.

Hung, C. J., Monsees, J., Munfah, N., and Wisniewski, J. (2009). Technical manual for design and construction of road tunnels. Rep. FHWANHI- 09-010 prepared for U.S. Dept. of Transportation, Parsons Brinckerhoff. New York.

Iseley, T., & Gokhale, S. (1997). Trenchless Installation of conduits Beneath Roadways. Washington D.C.: National Academy Press.

Jacobsz, S. W. (2002). The Effects of Tunneling on Piled Foundations. Ph.D. Dissertation, University of Cambridge, Cambridge, U.K.

Lake, L. M., Rankin, W. J., and Hawley, J. (1992). Prediction and Effects of Ground Movements Caused by Tunneling In Soft Ground beneath Urban Areas. CIRIA Project Report 30, Construction Industry Research and Information Association, London.

Lee, K. M., Rowe, R. K., and Lo, K. Y., (1992). Subsidence Owing to Tunneling. I. Estimating the Gap Parameter, Canadian Geotechnical Journal, Vol. 29, pp. 929-940.

Lim K C (2003). Three-Dimensional Finite Element Analysis of Earth Pressure Balance Tunneling. Ph.D. thesis, National University of Singapore.

Liu, W.-T., & Lu, X.-Y. (2012). 3-D Numerical Analysis of Soil Structure Interaction Behaviors of Pipe Jacking Construction. Applied Mechanics and Materials, 534-538.

Loganathan, N., and Poulos. H. G., (1998). Analytical Prediction for Tunneling Induced Ground Movements in Clays. Journal of Geotechnical and Environmental Engineering, ASCE, 124(9), pp. 846-856.

Loganathan, N., Poulos, H. G., and Stewart, D. P., (2000). Centrifuge Model Testing of Tunneling Induced Ground and Pile Deformations. Geotechnique, Vol. 50, No. 3, pp. 283-294.

Mair, R. J. (1979). Centrifugal Modelling of Tunneling Construction in Soft Clay. Ph.D. Thesis, University of Cambridge.

Mair, R. J. and Taylor, R. N. (1997). Bored Tunneling in The Urban Environment. In 14th International Conference on Soil Mechanics and Foundation Engineering, pages 2353–2385, Hamburg, 1. Balkema: Rotterdam.

Mair. R. J. (1996). Settlement Effects of Bored Tunnels. In International Symposium on Geotechnical Aspects of Underground Construction in Soft Ground, pages 43–53, London, Balkema.

Mamaqani, B. (2014). Numerical Modeling of Ground Movements Associated with Trenchless Box Jacking Technique. Arlington, TX., Ph.D. Dissertation. The University of Texas at Arlington.

Marshall, A. M., Farrell, R., Klar, A., and Mair, R. J. (2012). Tunnels in Sands the Effect of Size, Depth, and Volume Loss on Greenfield Settlements. Geotechnique, 62(5), 385–399.

Marshall, M. (1998). Pipe-Jacked Tunnelling: Jacking Loads and Ground Movements. Ph.D. Dissertation. The University of Oxford.

Meissner, H., (1996). Tunnelbau unter Tage - Empfehlungen des Arbeitskreises 1.6 Numerik in der Geotechnik. Geotechnik, 19(2):99–108.

Möller, S. (2006). Tunnel Induced Settlements and Structural Forces in Lining. Ph.D. Thesis, University of Stuttgart.

Moradi, G, and Abbasnejad, A. (2013). The State of the Art Report on Arching Effect Journal of Civil Engineering Research, 3(5): 148-161.

Moser, A. P. and Folkman, S. (2008). Buried Pipe Design, 3d ed., McGraw-Hill, New York.

Najafi, M. (2010). Trenchless Technology Piping: Installation and Inspection. New York: McGraw-Hill Companies.

Najafi, M. (2013). Trenchless Technology; Planning, Equipment, and Methods. New York: McGraw-Hill Companies.

Najafi, M. and Gokhale, S. (2004). Trenchless Technology, Pipeline and Utility Design, Construction, and Renewal, McGraw-Hill, New York, NY.

Najafi, M. and Gunnink, B. and Davis, G. (2005). Preparation of Construction Specifications, Contract Documents, Field Testing, Educational Materials, and Course Offerings for Trenchless Construction, available at: <https://library.modot.mo.gov/rdt/reports/ri02003/or06007.pdf>.

Najafi, M., Ardekani, S. and Shahandashti, M., (2016). Integrating Underground Freight Transportation into Existing Intermodal Systems. Final Report, Texas Department of Transportation, Austin, Texas. Available at: <http://library.ctr.utexas.edu/Presto/content/Detail.aspx?q=MC02ODcw&ctID=M2UxNzg5YmEtYzMyZS00ZjBlLWIyODctYzljMzQ3ZmVmOWFl&rID=MzU1&qcf=&ph=VHJ1ZQ==&bckToL=VHJ1ZQ==&> (Accessed on Jan. 2017).

O'Reilly, M. P. and New, B. M. (1982). Settlements above Tunnels in the United Kingdom –Their Magnitude and Prediction. Tunneling 82, London, IMM, pp. 173-181.

Ong, C. W., Leung, C. F., Yong, K. Y., and Chow, Y. K., (2007). Performance of Pile Due To Tunneling-Induced Soil Movements. Underground Space- the 4th Dimension of Metropolises- Bartak, Hrdina, Romancov & Ziamal (eds), pp. 619-624.

Open Face Shield. (2018). Available at: <https://www.trenchlesspedia.com/definition/2932/open-face-shield>.

Open Face TBM. (2018). Available at: < http://www.tunnel-online.info/en/index.html >.

Panet, M. and Guenot, A., (1982). Analysis of Convergence behind the Face of a Tunnel. Proc. Tunneling, 82, London, The Institution of Mining & Metallurgy, pp.197-204.

Peck, R. (1969). Deep Excavations and Tunneling in Soft Ground. State of the Art Report. (pp. 225-290). Mecico City: 7th International Conference on Soil Mechanics and Foundation Engineering.

Pipe Jacking Association. (2017). An Introduction to Pipe Jacking and Microtunnelling, available at: < http://www.pipejacking.org/assets/pj/static/PJA intro.pdf>.

Planning Engineer. (2018). Tunnel Boring Machine (TBM) Method, Available at: <http://www.p3planningengineer.com/productivity/tunneling/tunneling.htm>.

Potts, D. M. and Addenbrooke, T. I., (1997). A Structure's Influence on Tunneling Induced Ground Movements. Proceedings of the Institution of Civil Engineers: Geotechnical Engineering. Vol.125, No. 2, pp. 109-125.

Ropkins, J. (1998). Jacked Box Tunnel Design. Proc., Geo-Congress 98 October 18-21, 1998 Boston, Massachusetts, United States.

Rowe, R. K. and Lee, K. M., (1991). Subsidence Owing to Tunneling. II. Evaluation of a Prediction Technique, Canadian Geotechnical Journal, Vol. 29, pp. 941-954.

Schmidt, B. (1969). Settlements and Ground Movements Associated with Tunneling in Soil. Urbana, IL: Ph.D. Dissertation, University of Illinois.

Spangler, M. G. and R. L. Handy (1982), Loads on Underground Conduits, Soil Engineering, 4th Edition, Harper Collins, New York, pp. 727-763.

Spangler, M.G. and R.L. Handy (1973) Loads on Underground Conduits, Soil Engineering, 3rd Edition, Harper Collins, New York, pp. 658-686.

Staheli, K. (2006). Jacking Force Prediction: An Interface Friction Approach Based on Pipe Surface Roughness, Ph.D. Dissertation in civil and environmental engineering, Georgia Institute of Technology.

Su, T. (2015). Study on Ground Behavior Associated with Tunnelling in Mixed Face Soil Condition. Singapore., Ph.D. Dissertation. National University of Singapore.

Swoboda G (1979). Finite Element Analysis of the New Austrian Tunneling Method (NATM), Proc. 3rd International Conference on Numerical Method in Geomechanics, Aachen, Vol. 2, pp. 581-586.

Tavakoli, H., (2012). Productivity Analysis of Box Jacking. Master Thesis. The University of Texas at Arlington, Arlington, TX.

Terzaghi, K. (1943) Theoretical Soil Mechanics, John Wiley and Sons, New York, pp. 66-76.

Verruijt, A. and Booker, J. R. (1996). Surface Settlements Due to Deformation of A Tunnel in an Elastic Half Plane, Geotechnique, Vol. 46, No. 4, pp. 753- 756.

Vorster, T. E. B., Mair, R. J., Soga, K., and Klar, A. (2005). Centrifuge modeling of the effect of tunneling on buried pipelines: Mechanisms observed. Proc., 5th Int. Symp. TC28 Geotechnical Aspects of Underground Construction in Soft Ground, Amsterdam, the Netherlands, 131–136.

Wallin, M., Wallin, K., & Bennett, D., (2008). Analysis and Mitigation of Settlement Risks in New Trenchless Installations. No-Dig Conference and Exhibition.

Wongsaroj, J., (2005). Three-Dimensional Finite Element Analysis of Short and Long-Term Ground Response to Open-Face Tunneling in Stiff Clay. Ph. D. thesis, University of Cambridge.

Yih, C. (2003). Finite Element Study of Tunnel-Soil-Pile Interaction. Master Thesis. National University of Singapore.

Zymnis, M., (2009). Evaluation of Analytical Methods to Interpret Ground Deformations due to Soft Ground Tunneling. Master Thesis. Massachusetts Institute of Technology.

BIOGRAPHICAL INFORMATION

Taha Ashoori graduated with a Bachelor of Science in Civil Engineering from University of Tehran, Iran, in 2008. He then managed a family-owned construction company in Tehran until 2012. He graduated with his Master of Science in Geotechnical Engineering at Sharif University of Technology, Tehran, Iran, in 2012. Taha started his Ph.D. in Geotechnical Engineering at Iran University of Science and Technology (IUST) as soon as he graduated from Sharif University. Meanwhile, Taha worked as a Field and Quality Control Engineer for Perlite Construction Company in Tehran, Iran. In 2013, he joined Kayson Inc., in Tehran, at the water and wastewater department as a Project Engineer. He was responsible for design and construction of North Tehran's Sewer Pipeline Project using Trenchless Technology method with Pipe Jacking with Microtunneling. This project motivated Taha to follow his interest in this field so he decided to join the Center for Underground Infrastructure Research and Education (CUIRE) at University of Texas at Arlington (UTA) to work on his Doctoral studies under supervision of Dr. Mohammad Najafi in 2015. During his time at UTA/CUIRE, Taha was a Teaching Assistant for various graduate courses such as Construction Planning and Scheduling, Construction Field Operations, Construction Law and Contracts and Construction Management. Also during this time, he was appointed as the construction method analyst for a research project on underground freight transportation granted to CUIRE by the Texas Department of Transportation. In summer 2017, Taha joined Staheli Trenchless Consultants and had an opportunity to work closely with Dr. Kimberlie Staheli in Seattle, working in design and construction of major horizontal directional drilling (HDD) projects. A great enthusiasm to both fields of geotechnical engineering and trenchless technology led Taha to complete his dissertation in comparison of ground movements during trenchless technology operations for pipe and box installations by numerical analysis.